

Course B: rf technology
Normal conducting rf
Part 6: High-Gradient Acceleration

Walter Wuensch, CERN
Eighth International Accelerator School for Linear Colliders
Antalya, Turkey
7 to 10 December 2013



Now – acceleration
with high gradient!



We are now going to look at what happens when you operate an rf structure at high-gradient and high-power.

To remind you of the CLIC parameters: the accelerating gradient is 100 MV/m, an input power of around 64 MW and a pulse length of around 180 ns giving a pulse energy of 12 J.

PETS feed two accelerating structures so need to produce 130 MW.

High-power behavior is not described by a nice, clear theory, with proofs and theorems.

Instead what we have is picture emerging from the fog. I will describe the current understanding of how rf structures behave at high-power:

- How achievable gradient and power level depend on rf geometry.
- The physics of high-power phenomenon.
- Technology and why we think it works.

To do this I will cover:

1. Experiments and results.
2. Scaling laws
3. Physics of breakdown

A few more words of background.

A number of effects which emerge at high-power and high-gradient.

These include:

1. Breakdown – This is essentially the same phenomenon you all know from daily life, sparking and arcing. This is the main effect limiting gradient in CLIC.
2. Pulsed surface heating – Surface currents cause pulsed temperature rises, consequently cyclical stress which breaks up the surface and induces breakdown.
3. Electromigration – This is a new area of investigation in which rf currents directly affect the crystal structure of the copper surface.
4. Dark currents – Field emission currents are captured by the rf and can be accelerated over longer distances.
5. Dynamic vacuum – Field emission currents desorbs gasses which cause pressure rises during the rf pulse.
6. Multipactor – not really a problem at the highest gradients.

- What does a high-power rf test look like?
- What happens when an rf structure breaks down?

The basic layout of an rf test

klystron



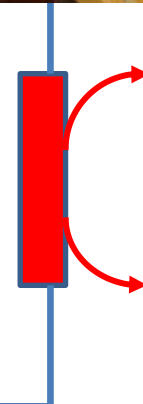
directional coupler



load



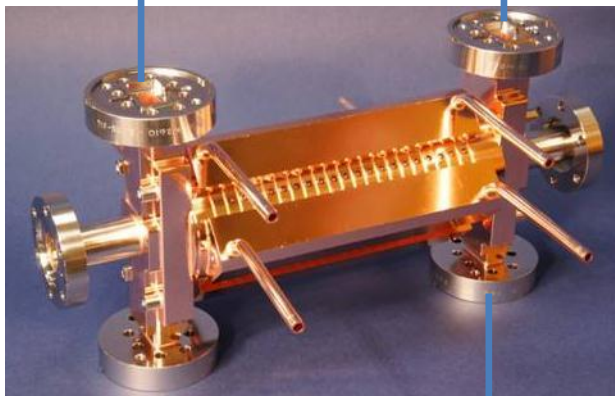
Transmitted



splitter

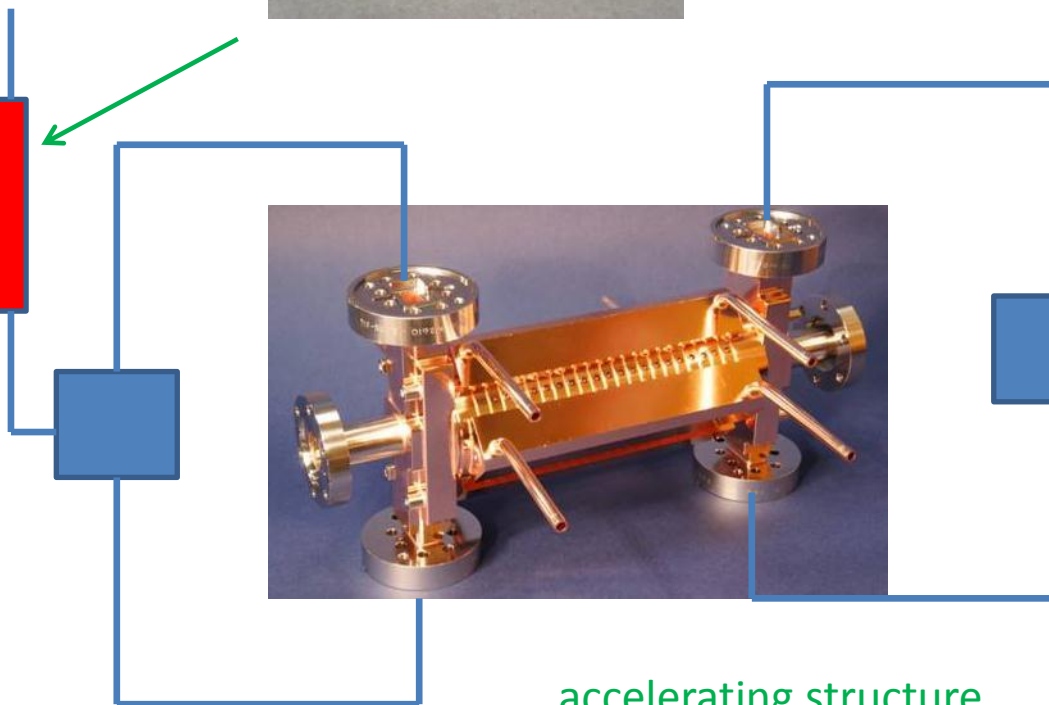


accelerating structure



Reflected

Incident



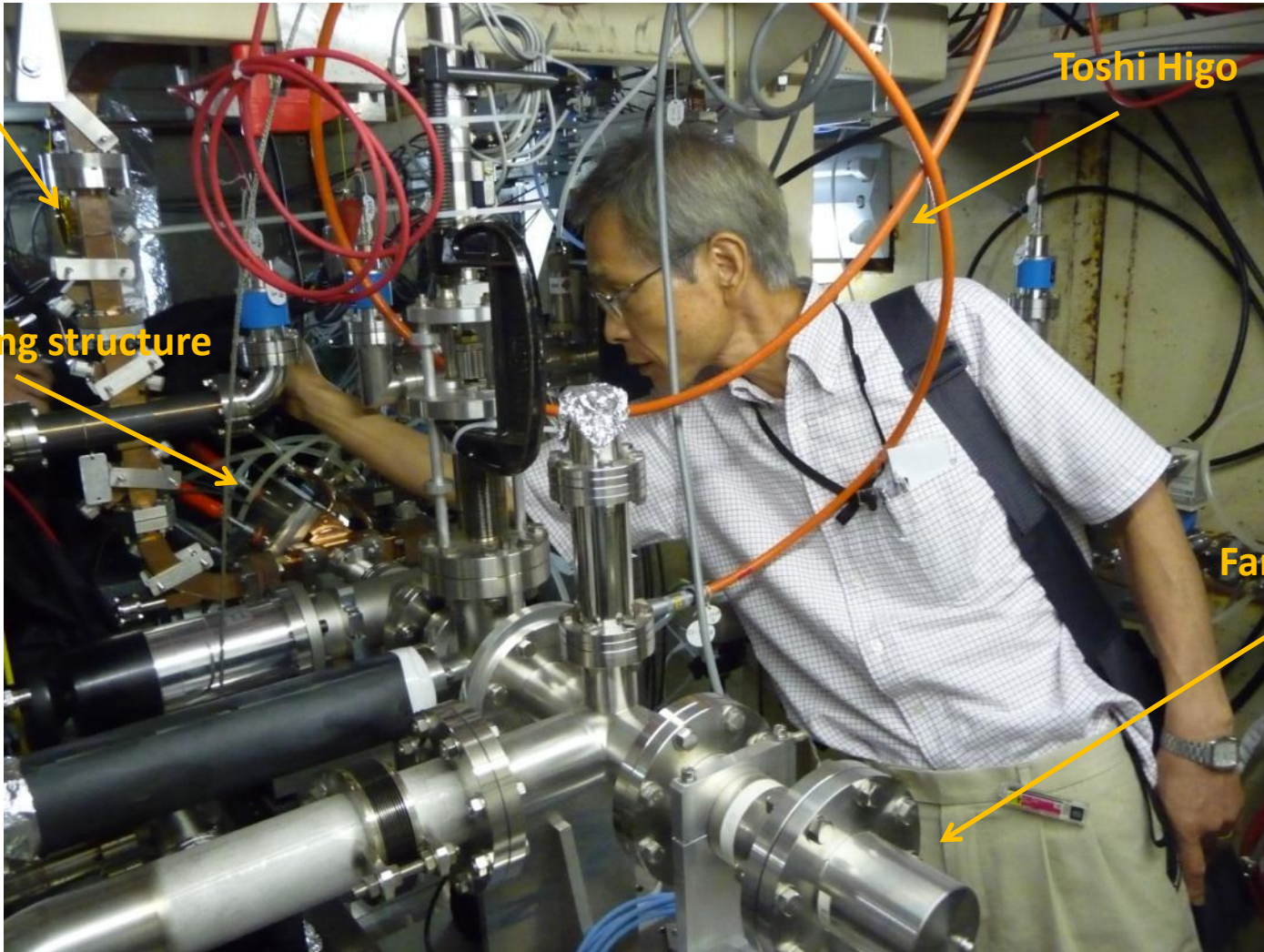
The basic layout of an rf test

Waveguide

Accelerating structure

Toshi Higo

Faraday cup





Prototype accelerating structure test areas



NLCTA at SLAC



Nextef at KEK



New klystron at CERN



ASTA at SLAC

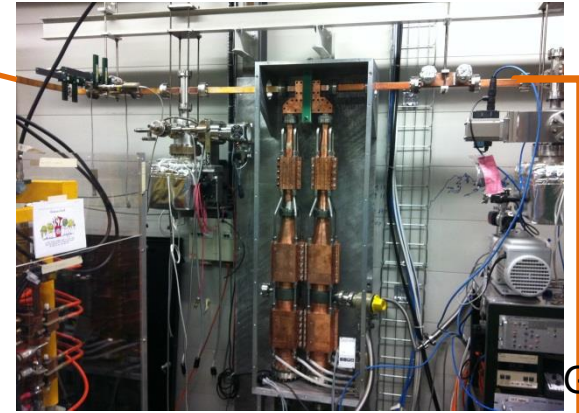


Two-beam test stand at CERN

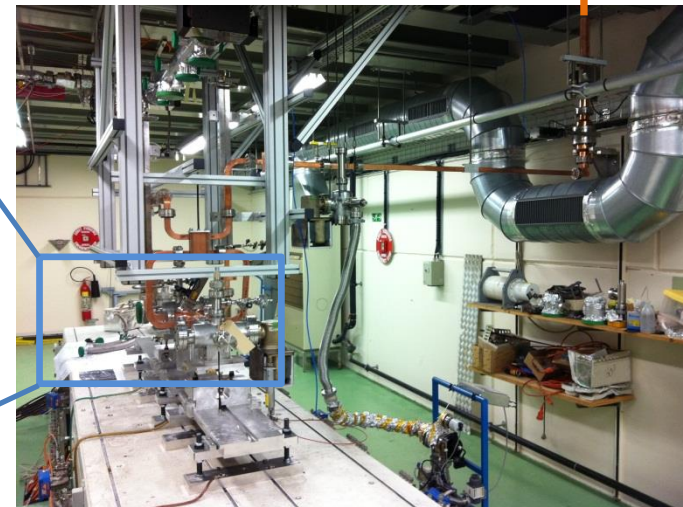
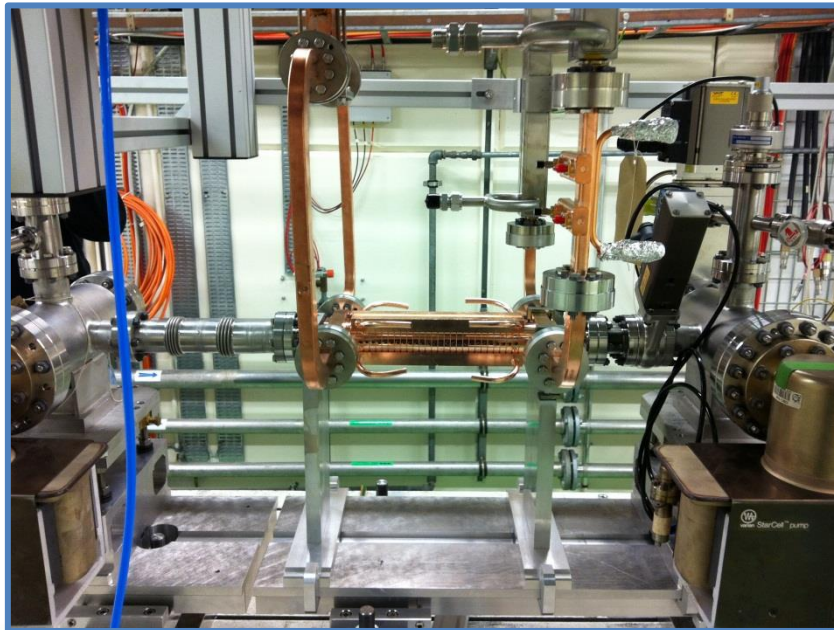
Xbox-1 Layout

Clockwise from top-left:

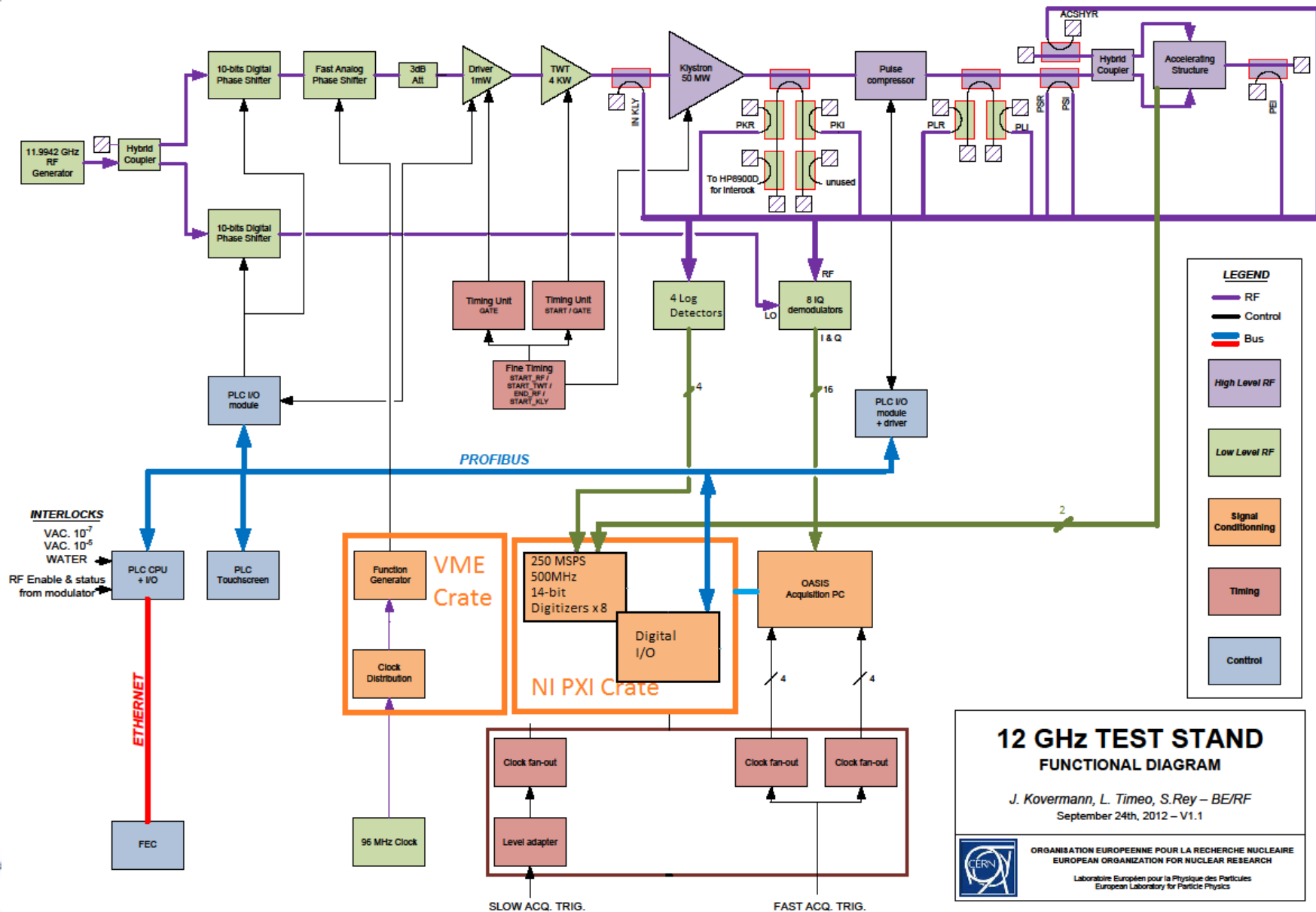
- Modulator/klystron (50MW, 1.5us pulse)
- Pulse compressor (250ns, ratio 2.8)
- DUT + connections
- Acc. structure (TD26CC)



Gallery
Bunker



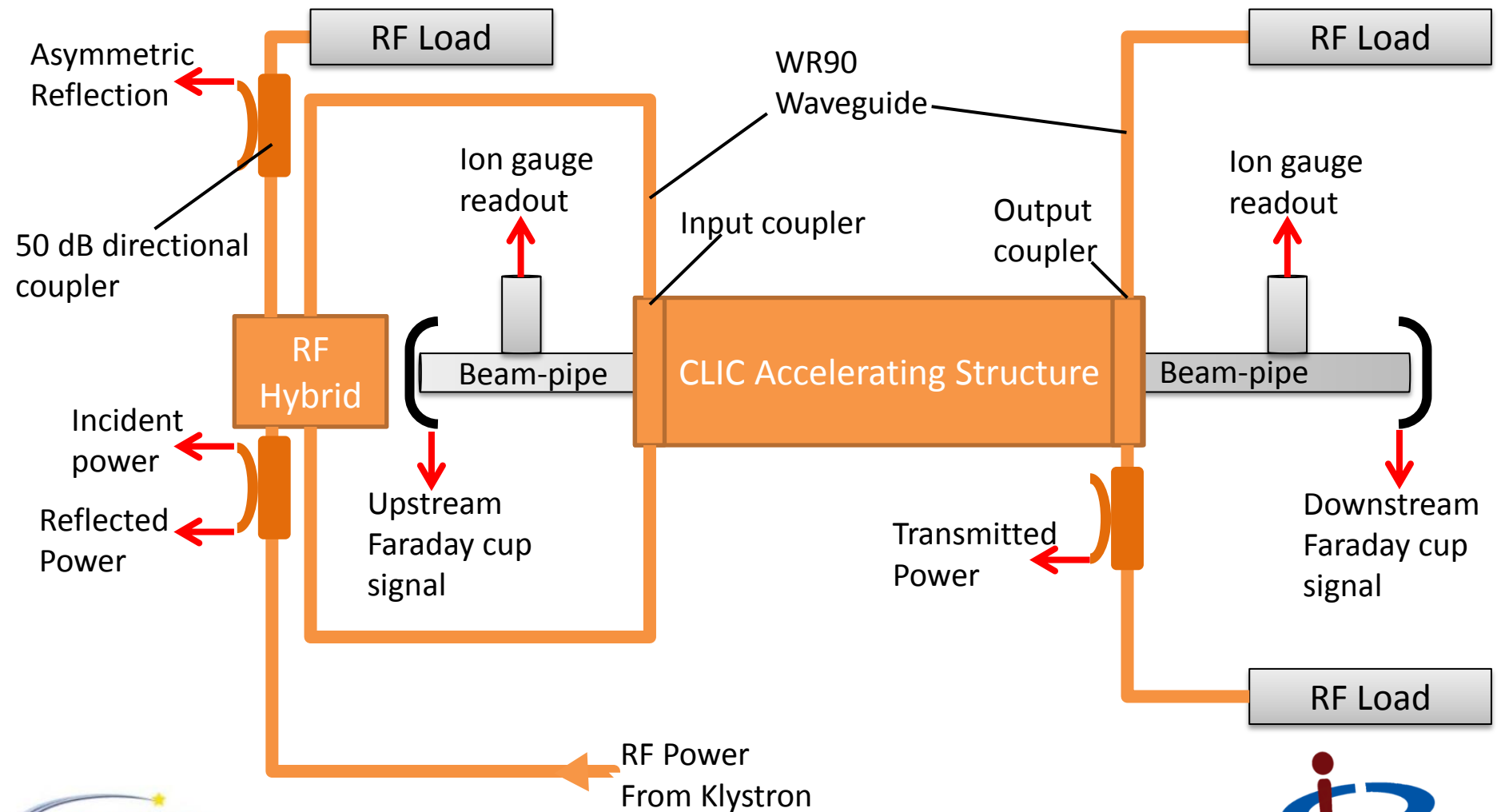
System Layout and diagnostics

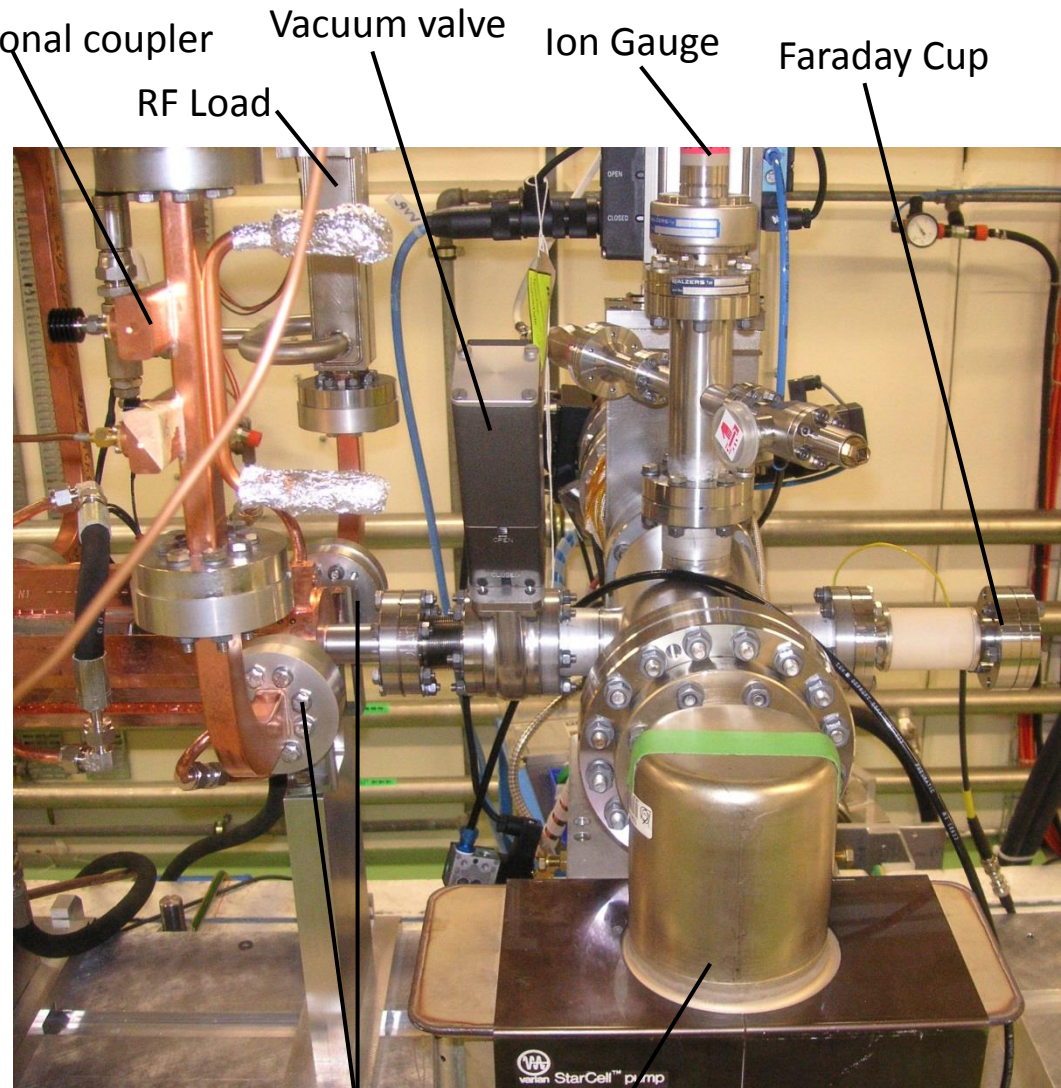
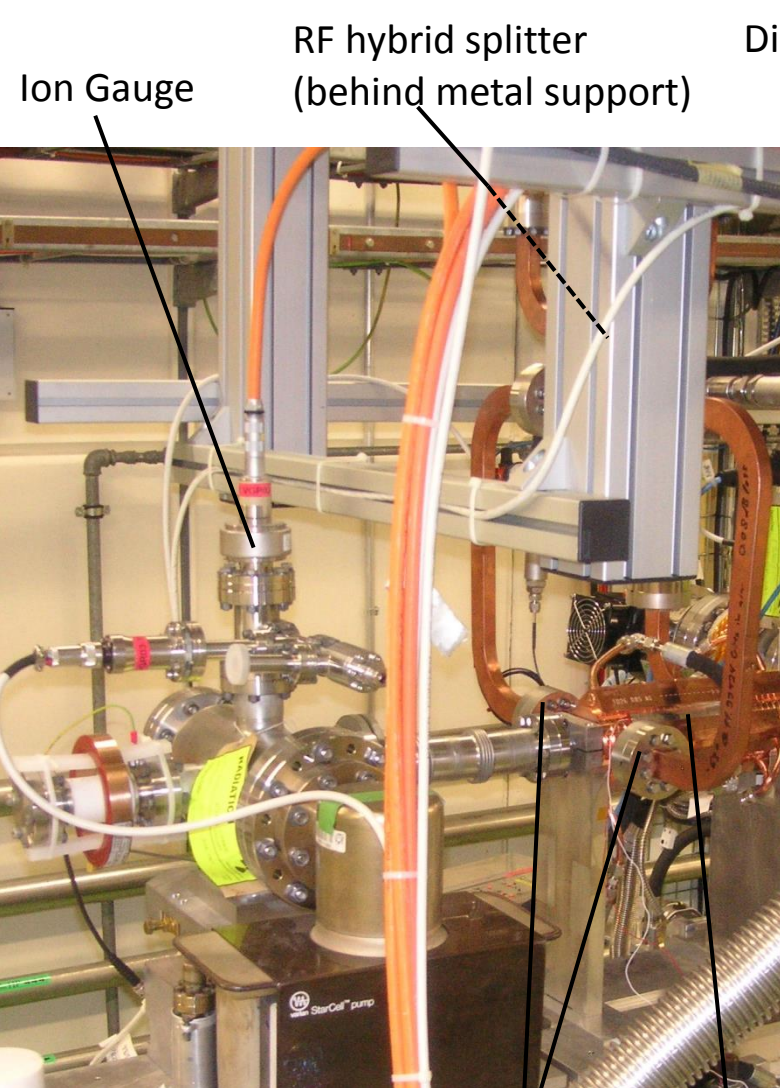


**12 GHz TEST STAND
FUNCTIONAL DIAGRAM**

J. Kovermann, L. Timeo, S. Rey – BE/RF
September 24th, 2012 – V1.1

ORGANISATION EUROPEENNE POUR LA RECHERCHE NUCLEAIRE
EUROPEAN ORGANIZATION FOR NUCLEAR RESEARCH
Laboratoire Européen pour la Physique des Particules
European Laboratory for Particle Physics





Ion Gauge

RF hybrid splitter
(behind metal support)

Directional coupler

Vacuum valve

Ion Gauge

Faraday Cup

RF Load

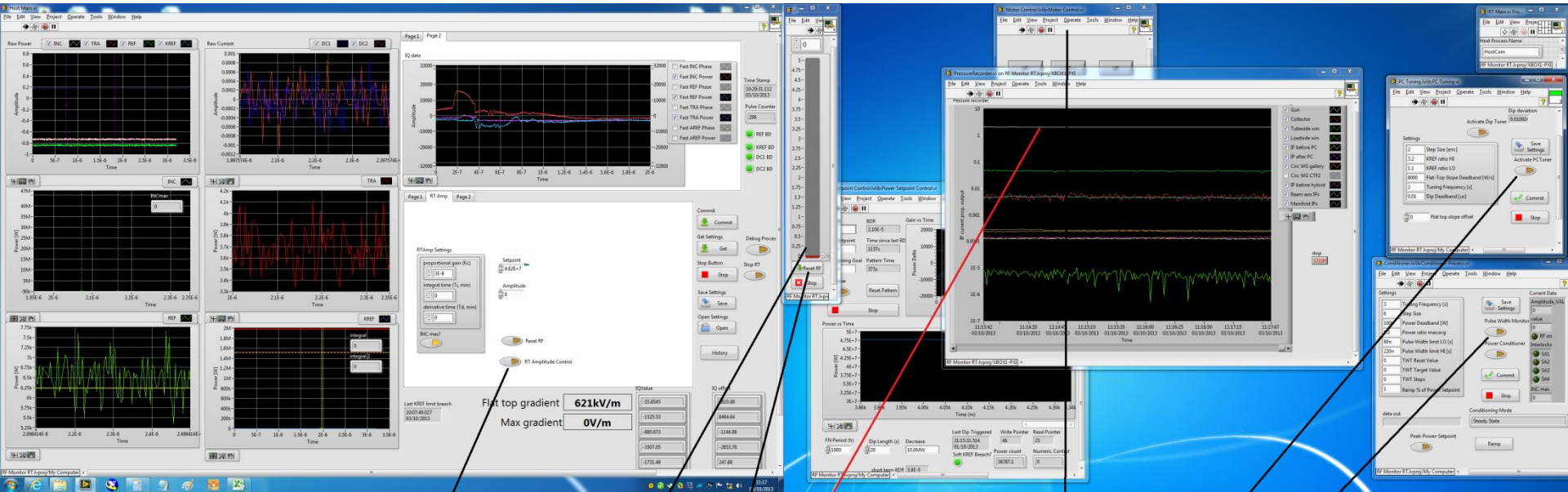
Structure input
couplers

Temperature
probe

Structure output
couplers

Ion Pump

Operator display



2. Toggle and then turn OFF RT amplitude control

3. press Reset RF

1. Turn OFF Pulse Width Monitor

8. Increase voltage of attenuation in Amplitude Control.vi

4. Reset and Trig the modulator at 250 V

5. Deactivate PC tuner

6. Tune pulse compressor to cold state (step 1000 then back to 20)

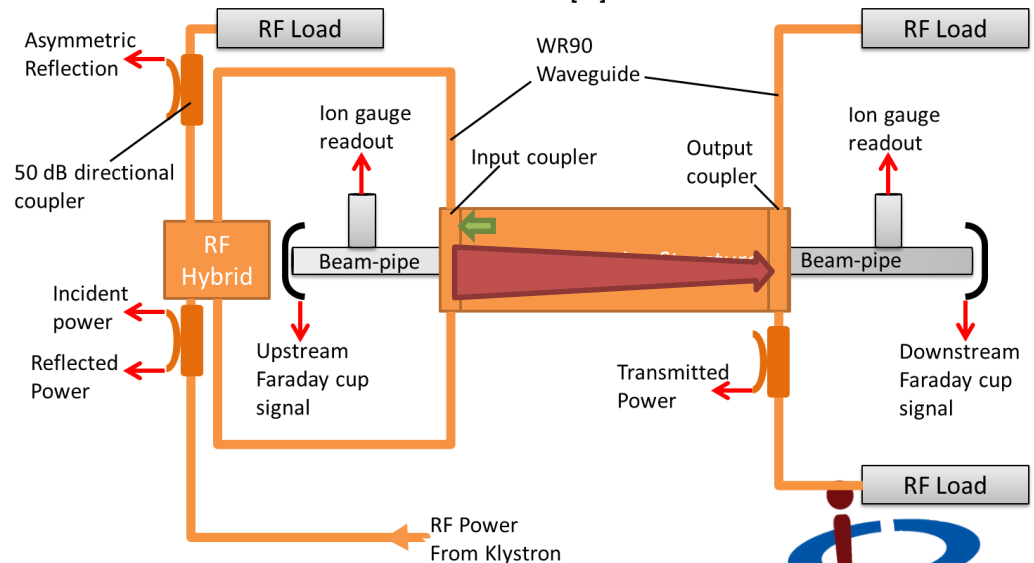
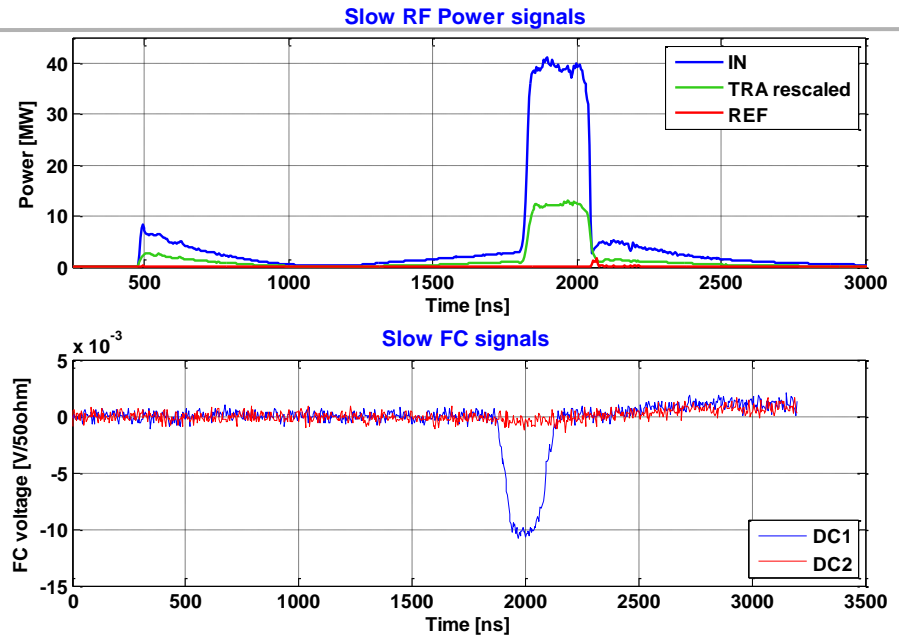
7. Ramp modulator voltage while checking gun vacuum level

9. If tuning is good activate PC tuner (press Set Zero position when dip is good)

10. Switch ON pulse width monitor(1) and RT amplitude control(2)

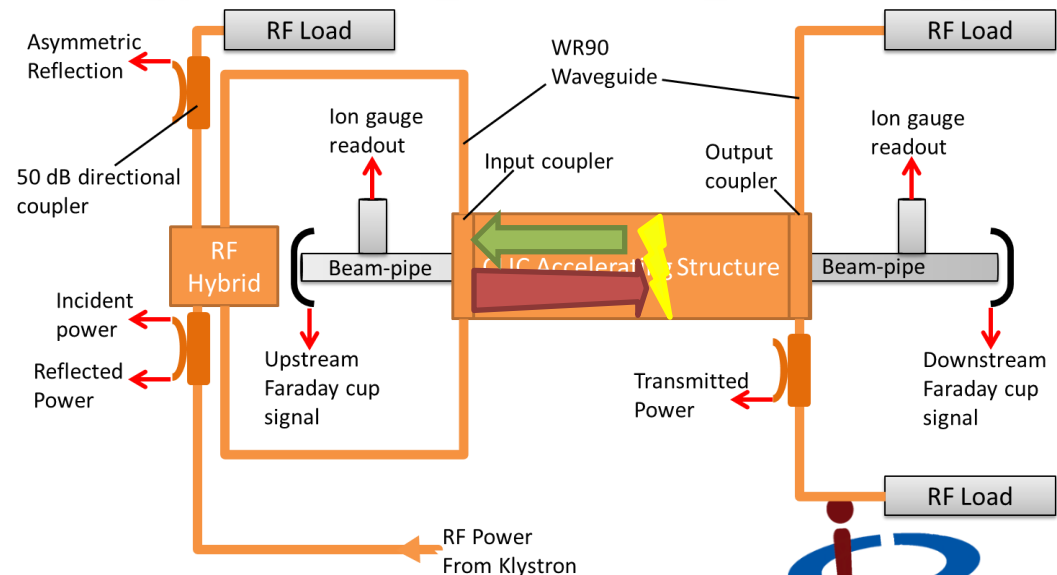
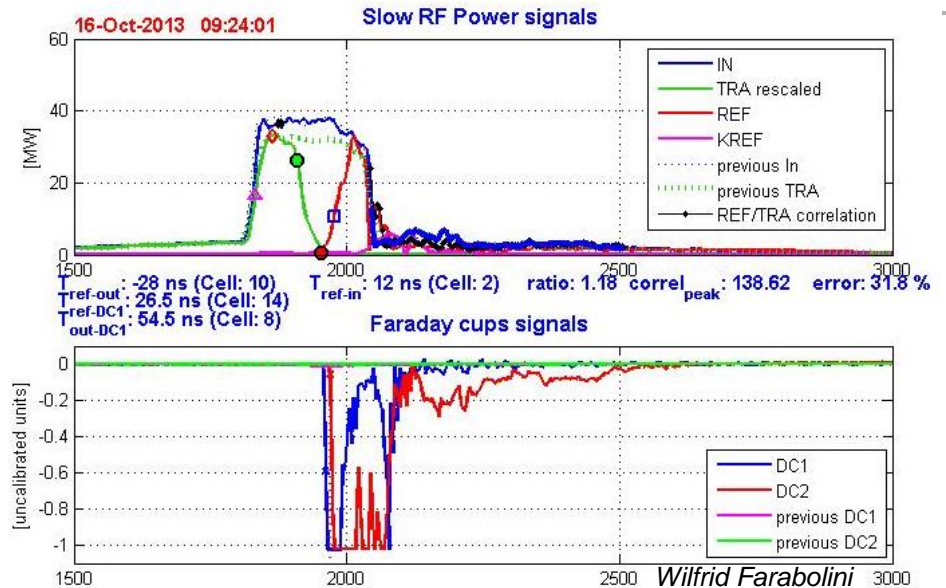
BD Detection: Normal Pulse

- Transmitted pulse follows the incident pulse but with $\sim 4\text{dB}$ of attenuation.
- Reflected signal is $\sim 20\text{dB}$ lower than incident pulse.
- Only a few mV seen on the faraday cups. DC2- Upstream sees 1/10 of the signal compared to downstream.



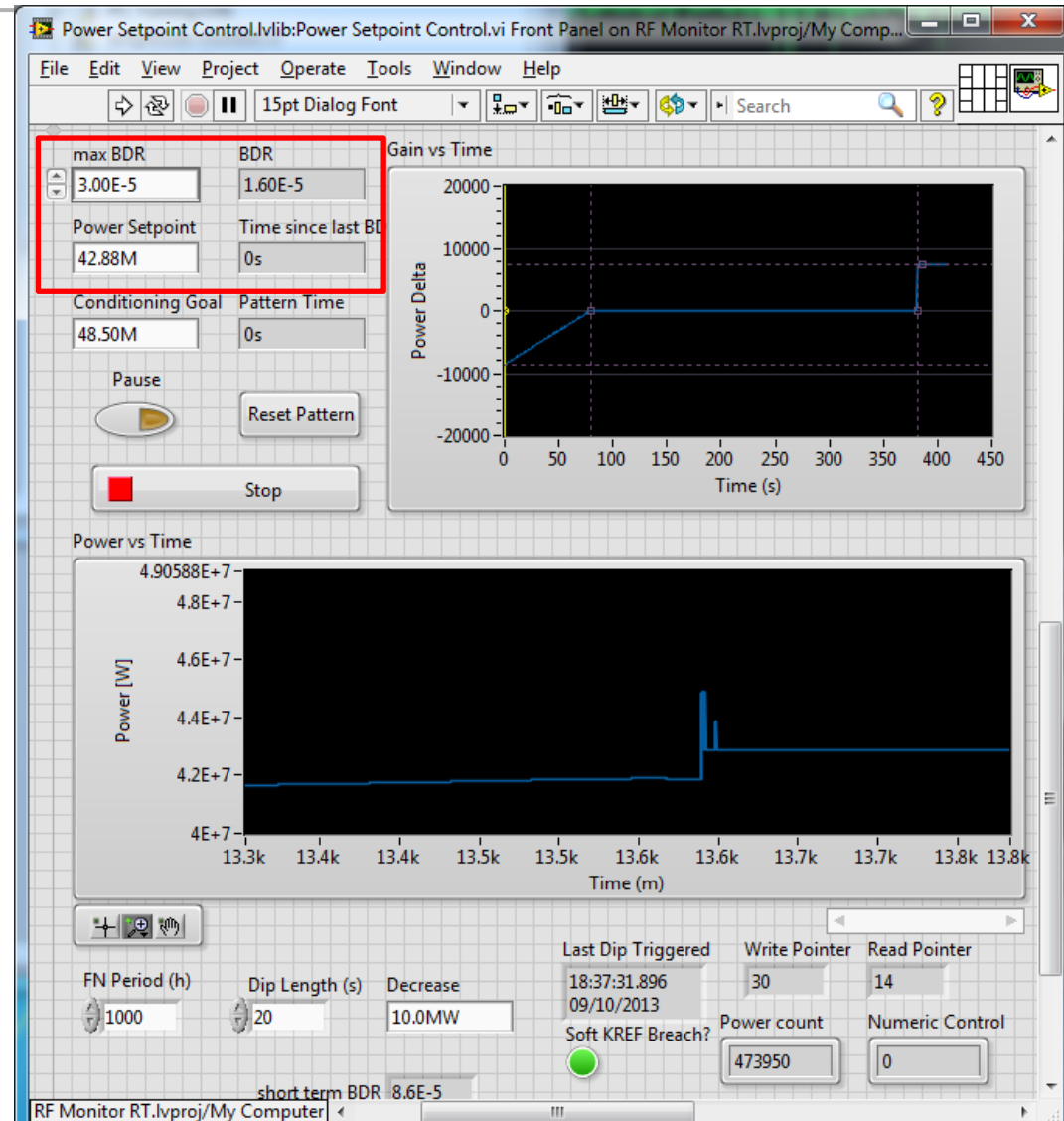
BD Detection: Breakdown

- Transmitted pulse drops as the arc is established.
- Reflected power increases to the same order as the incident pulse.
- Faraday cup voltages are saturated: 100-1000x increase in charge emitted.
- We can use the difference in time between the transmitted power falling and the reflected power increasing to find the BD cell location.
- The phase of the reflected signal is used to pinpoint cell location.



Cavity Conditioning Algorithm

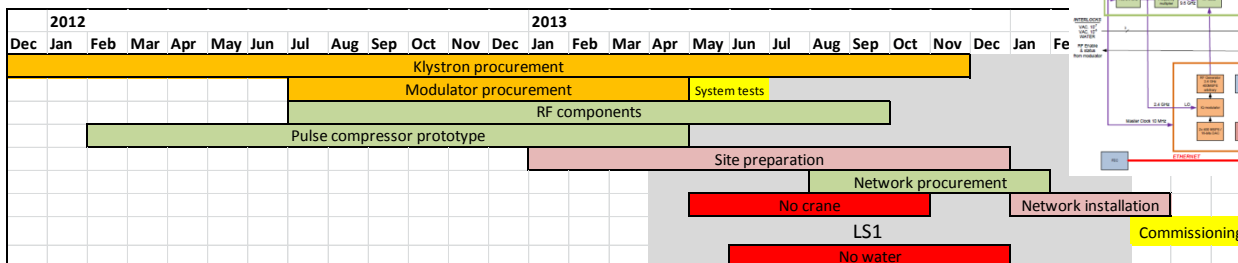
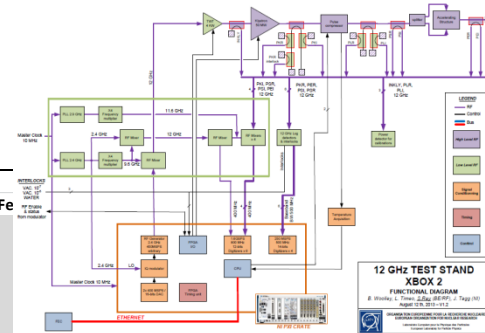
- Automatically controls incident power to structure.
- Short term: +10kW steps every 6 min and -10kW per BD event.
- **Long Term:** Measures BDR (1MPulse moving avg.) and will stop power increase if BDR too high.



Xbox2 in building 150



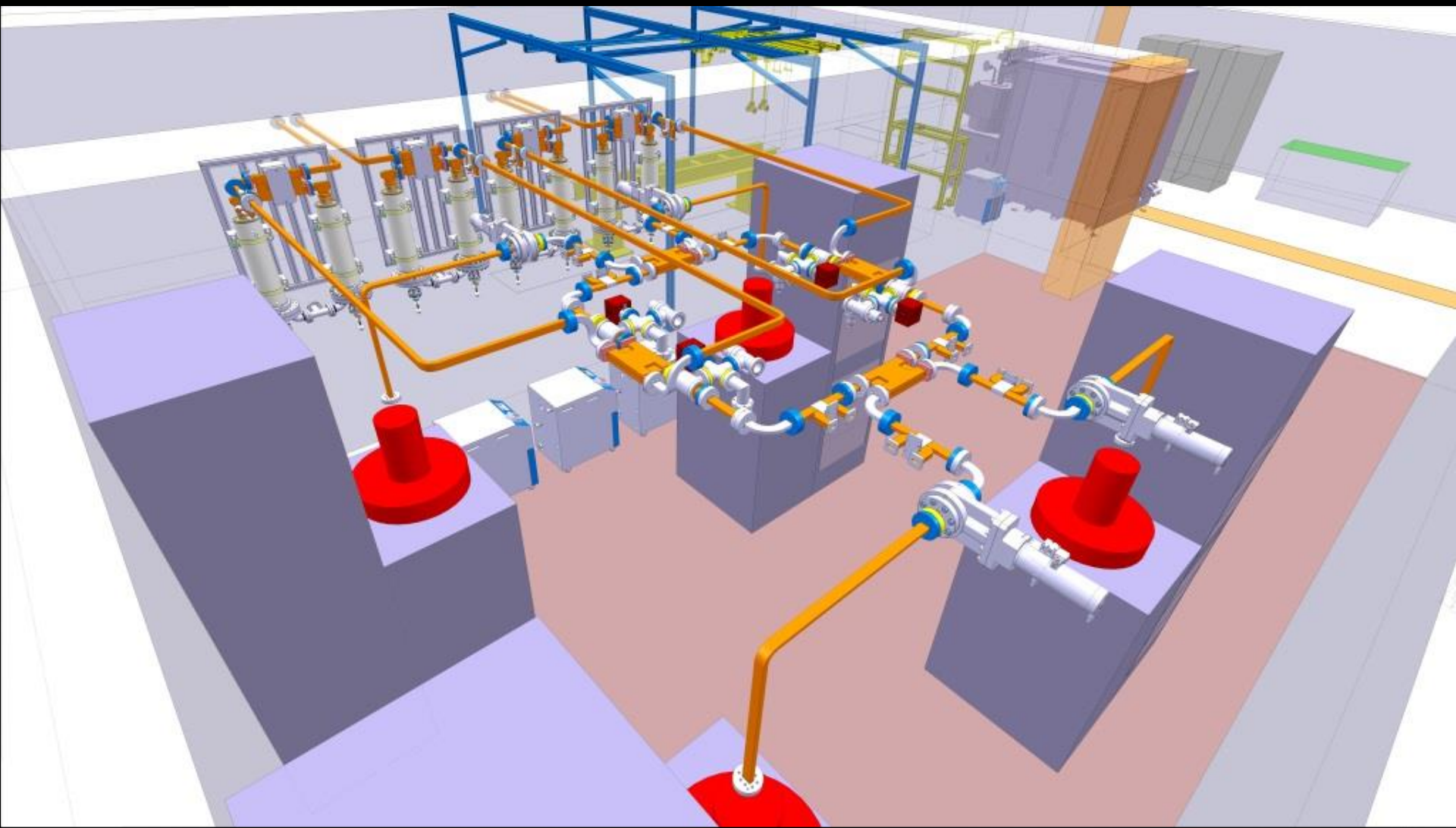
- New X-band test bench in building 150 next to cafeteria
- Modulator arrived in May. Acceptance tests ok.
- Not as fast as we would have liked due to cohabitation with LS1 works. Five months break for water distribution consolidation
- Waiting now for the Klystron being tested in SLAC
- Components available. Waveguides in fabrication.



- Modulator arrived, installed and tested successfully to the require voltag, pluse length and stability
- Klystron being currently tested in SLAC
 - Some problems with testing network solved.
 - Testing now at 25MW at 1.5 us
 - Expected delivery in November

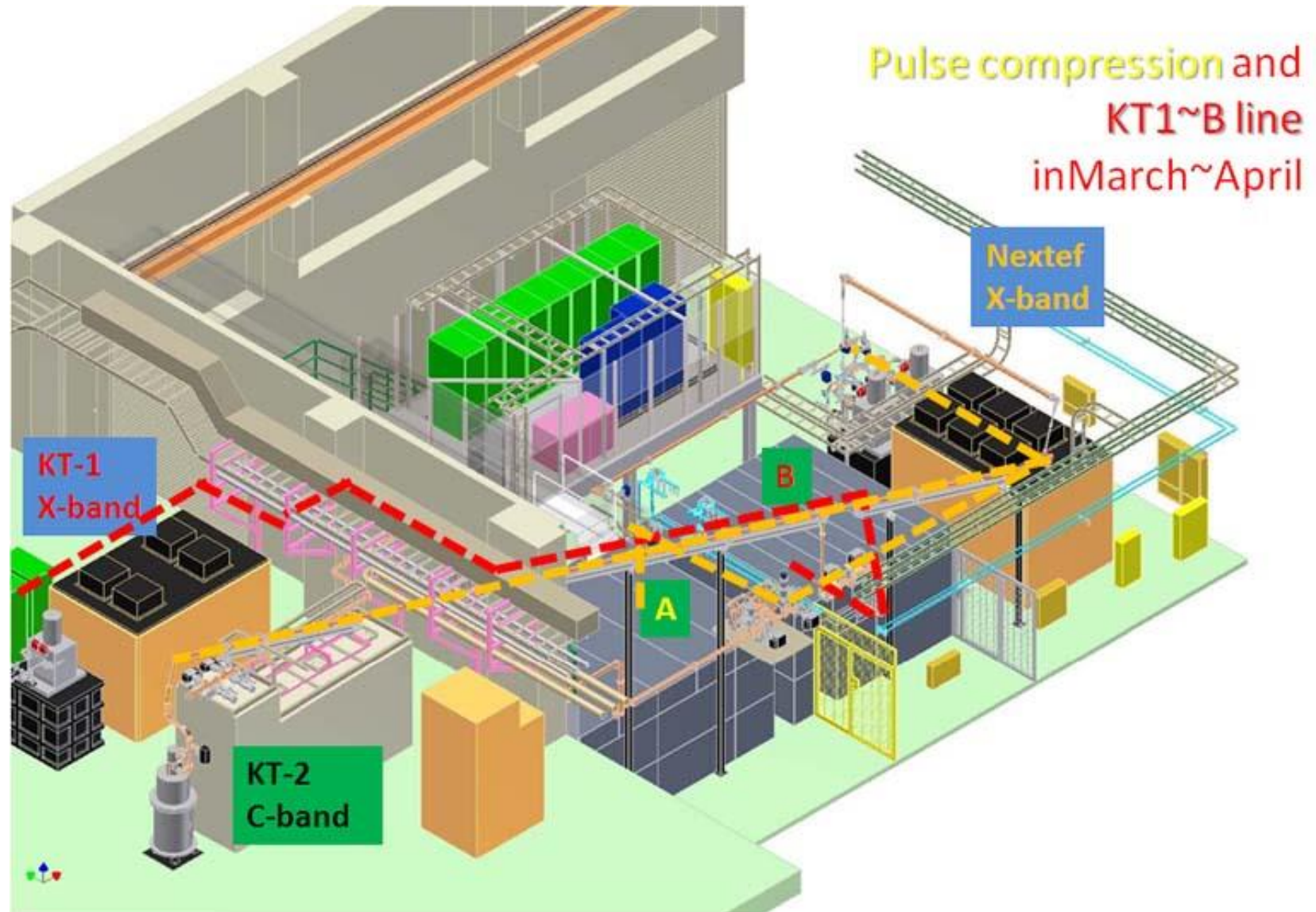


Preparation now underway at CERN for Xbox-3

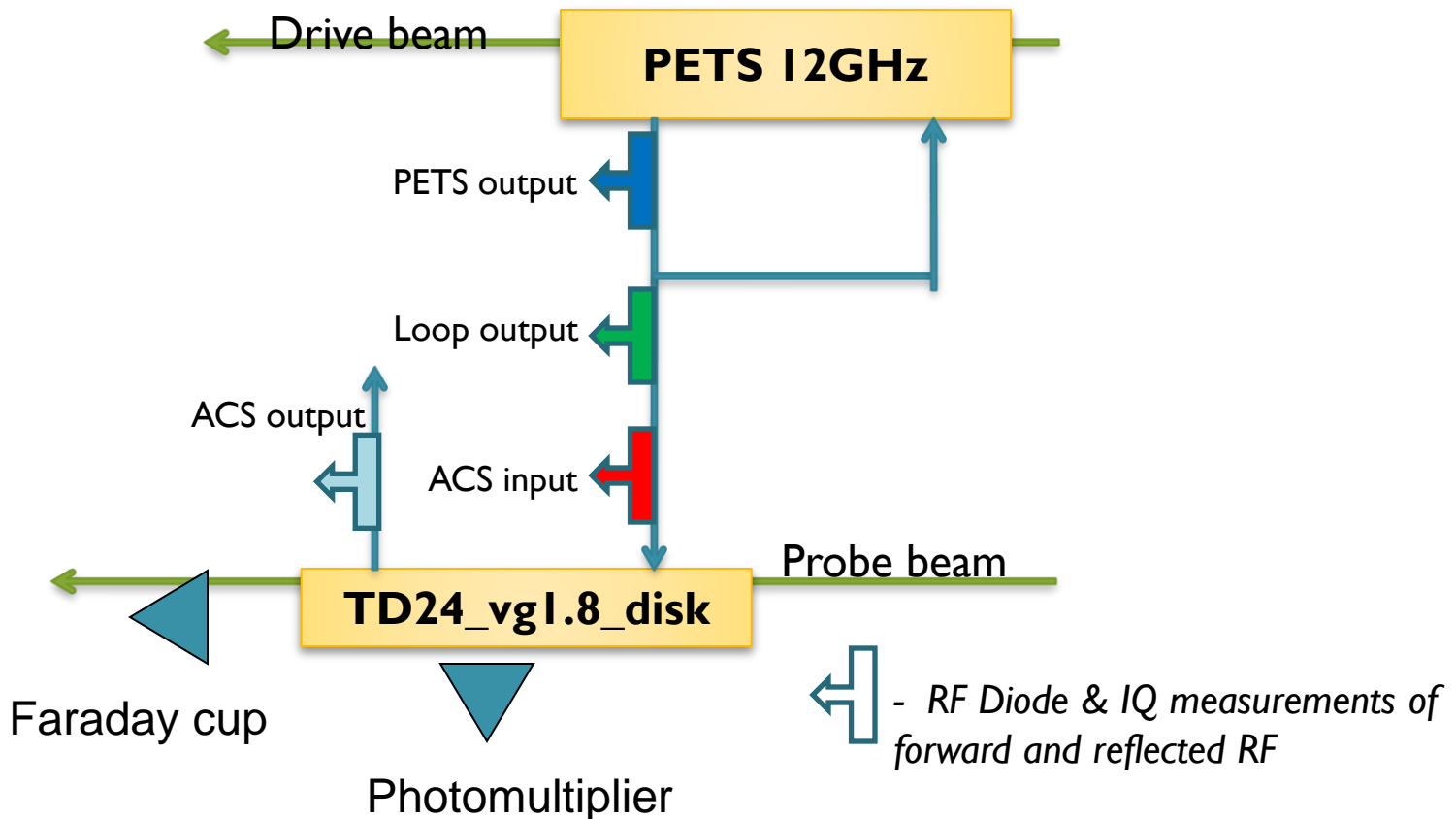


Based on combining four 6 MW Toshiba klystrons

Nextef expansion is being proceeded



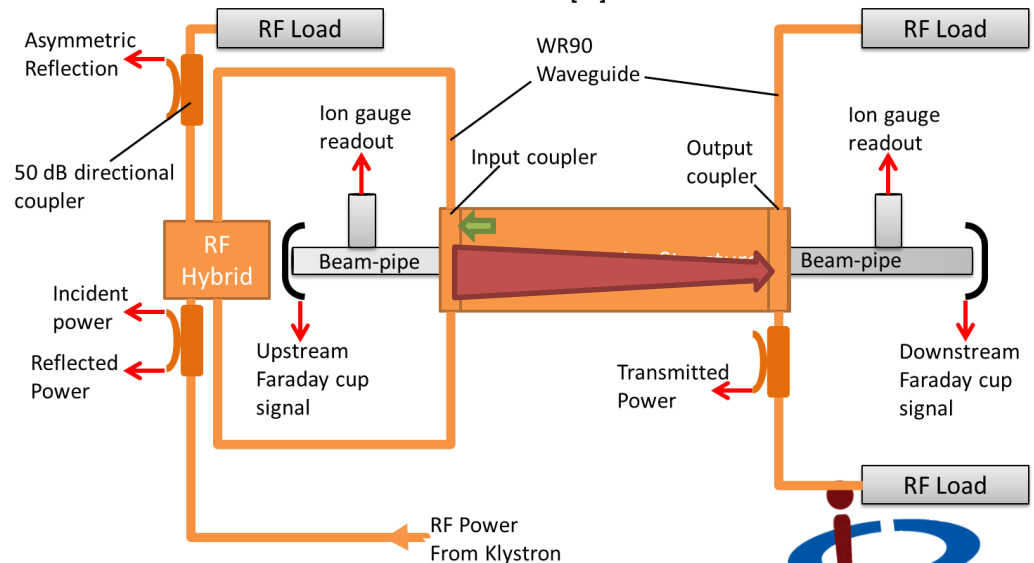
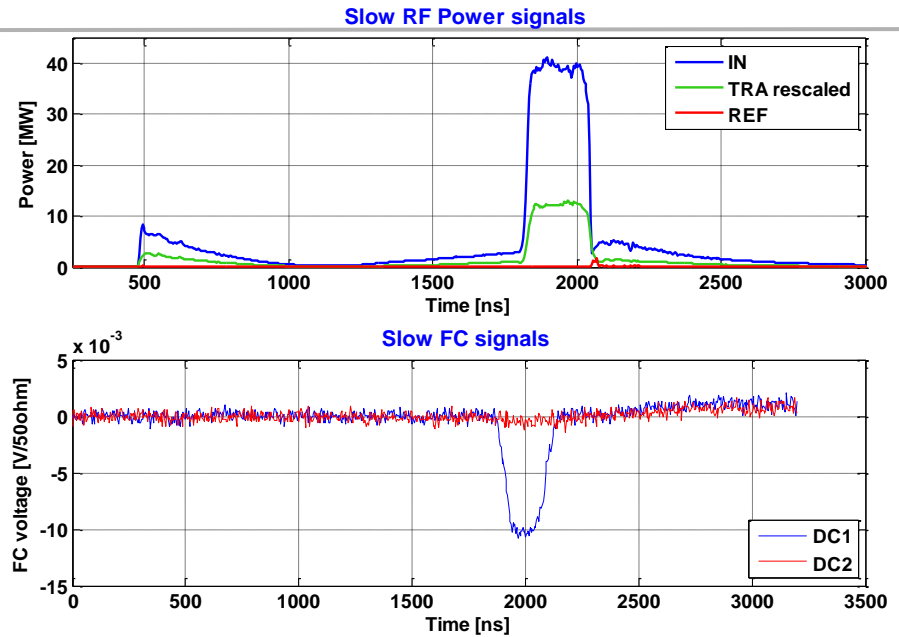
BD detection



- Breakdowns in the recirculation loop are detected only from the reflected power ($P_{ref} / P_{fwd} > \sim 15\%$).
- Breakdowns in attenuator and the waveguide are detected from the missing energy ($U_{tran} / (U_{fwd} * \text{transmission factor}) > 15\%$)
- Breakdowns in the ACS are detected from the reflected power, the missing energy, the Faraday cup and the photomultiplier.

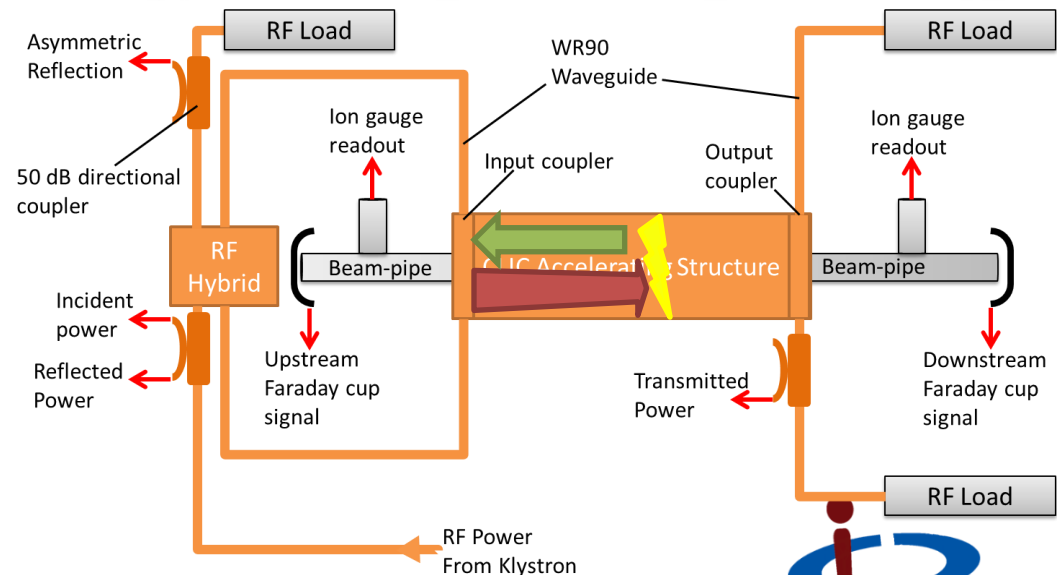
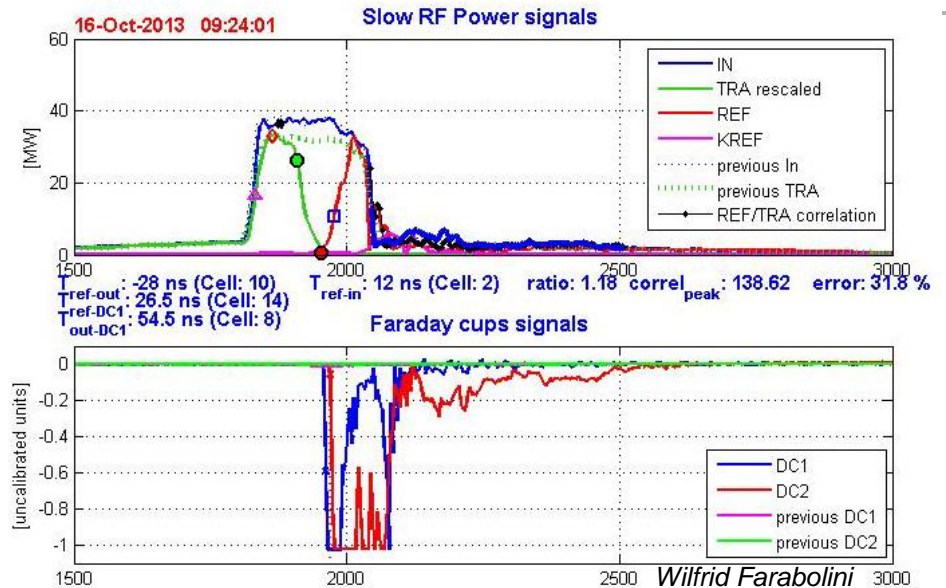
BD Detection: Normal Pulse

- Transmitted pulse follows the incident pulse but with $\sim 4\text{dB}$ of attenuation.
- Reflected signal is $\sim 20\text{dB}$ lower than incident pulse.
- Only a few mV seen on the faraday cups. DC2- Upstream sees 1/10 of the signal compared to downstream.



BD Detection: Breakdown

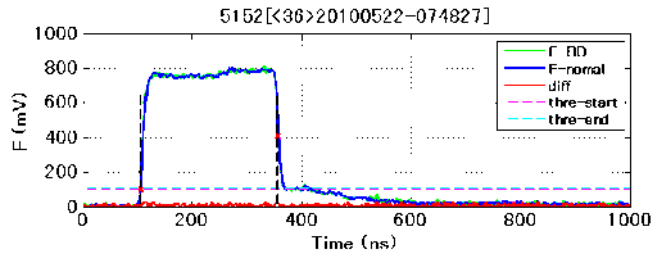
- Transmitted pulse drops as the arc is established.
- Reflected power increases to the same order as the incident pulse.
- Faraday cup voltages are saturated: 100-1000x increase in charge emitted.
- We can use the difference in time between the transmitted power falling and the reflected power increasing to find the BD cell location.
- The phase of the reflected signal is used to pinpoint cell location.



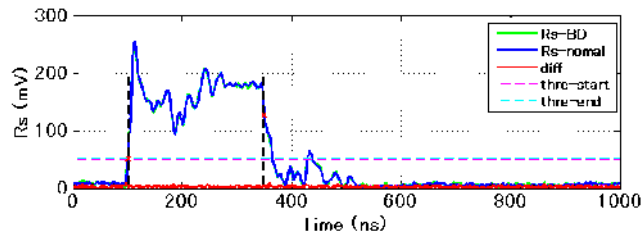
51+52 Normal pulse #36

F RsX10 Tr

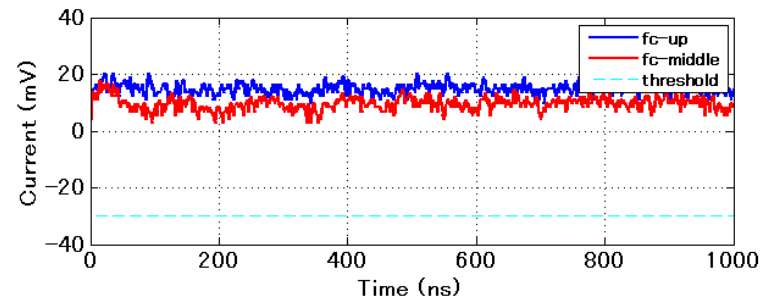
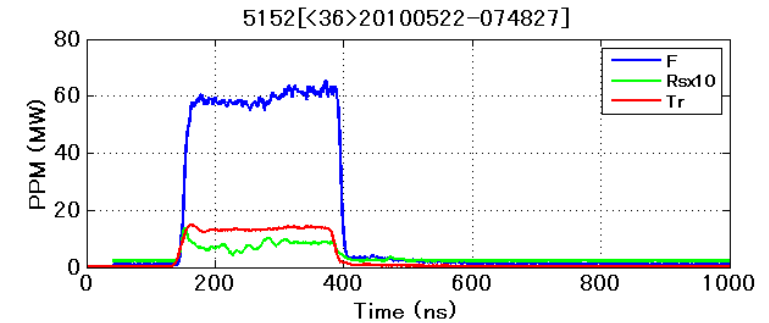
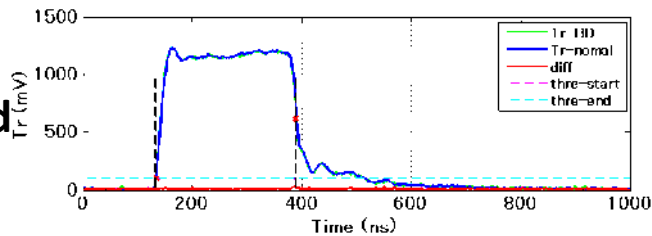
Incident
(F)



Reflected
(Rs)



Transmitted
(Tr)



FC-UP FC-Mid Threshold

Last pulse

Last pulse but one

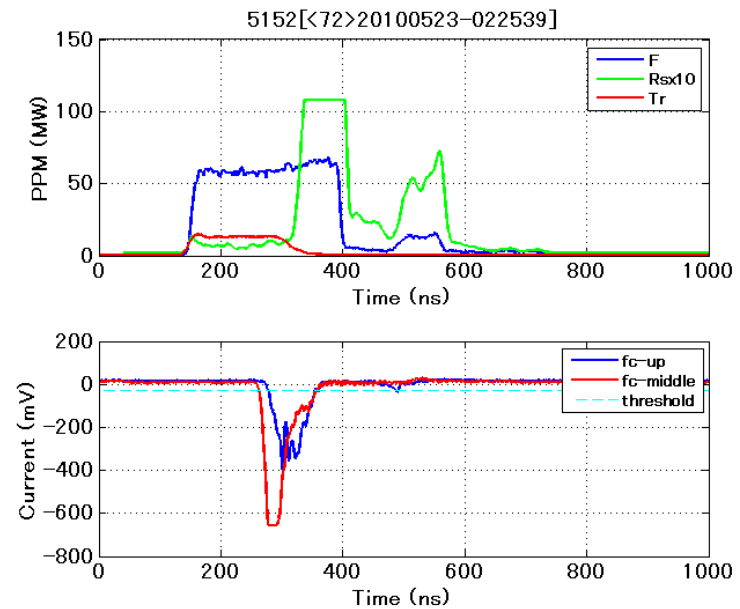
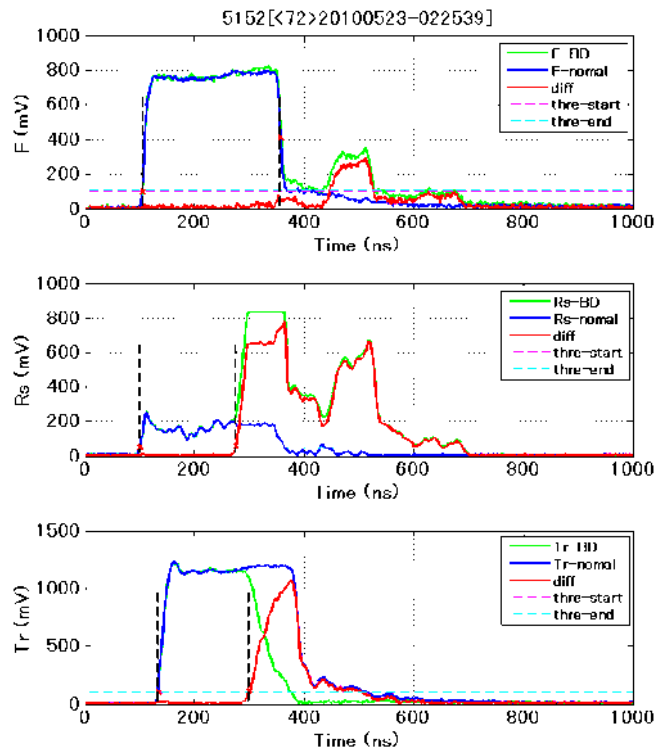
Difference between the two

Dashed lines = Analysis threshold

T. Higo, KEK
Test of TD18 structure

51+52 typical BD pulses

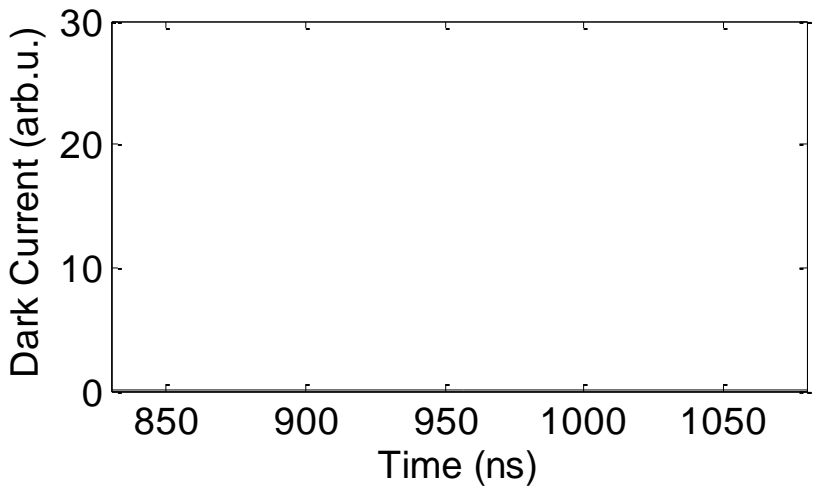
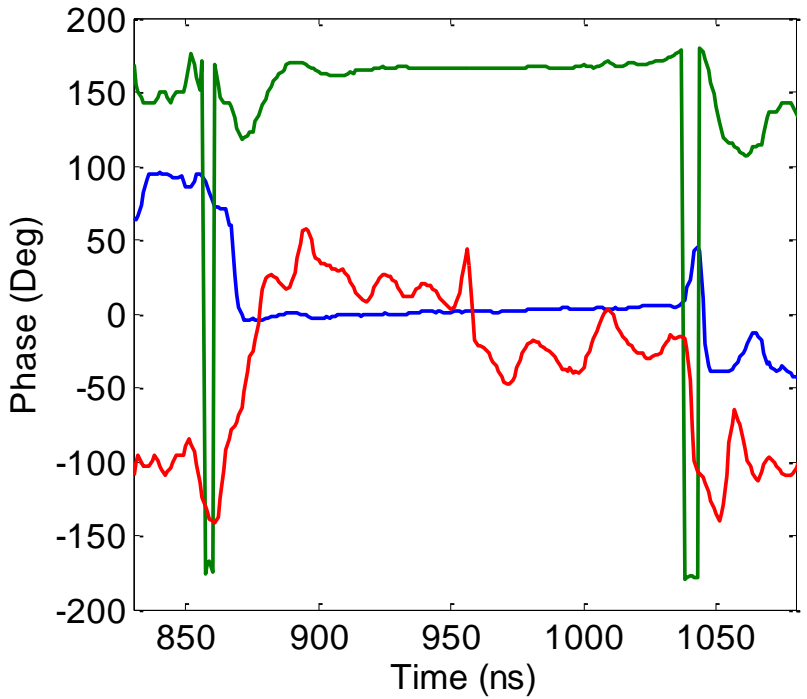
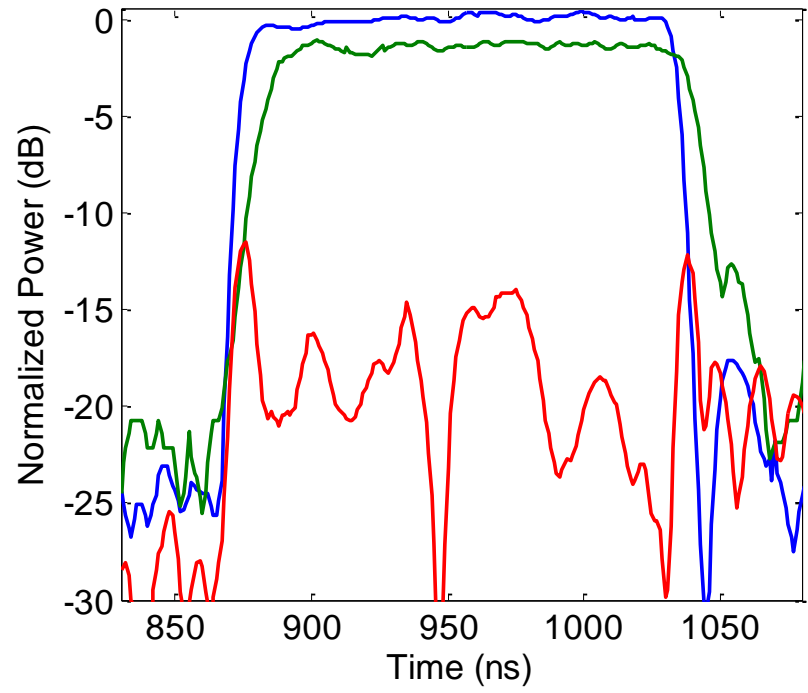
#72 Reflected RF back from klystron again



T. Higo, KEK
Test of TD18 structure

Normal Waveforms of TD18

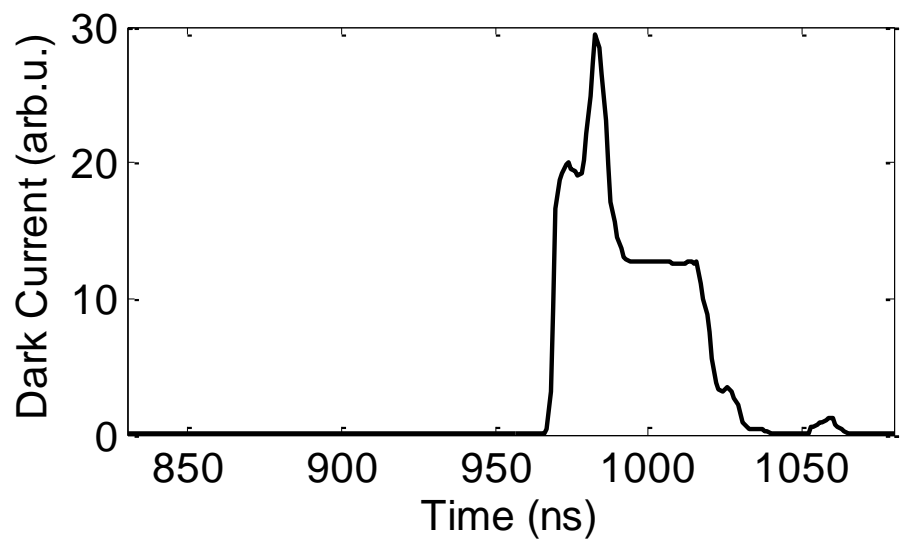
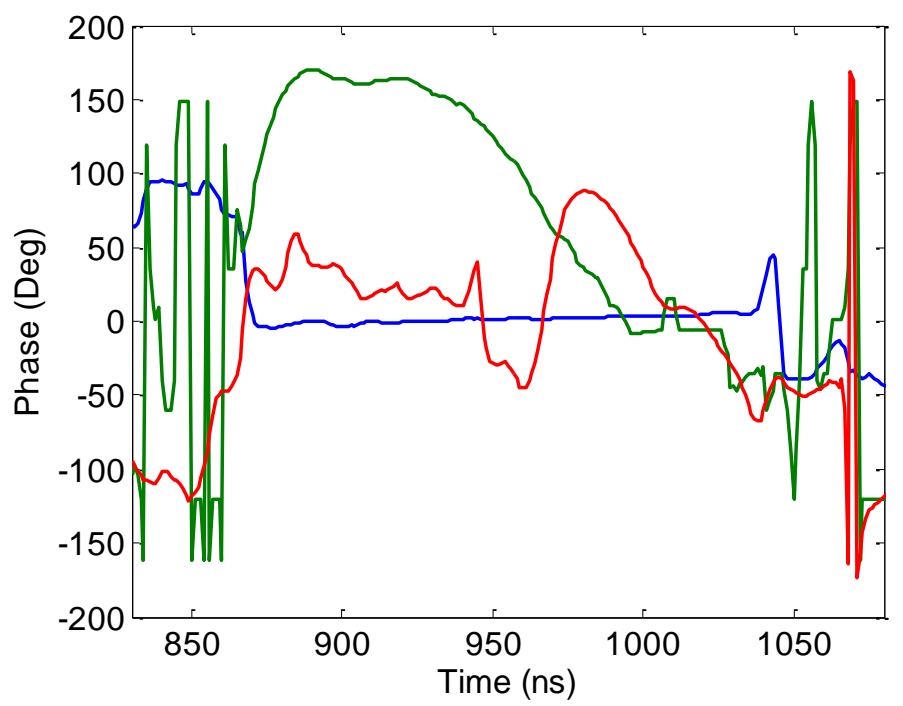
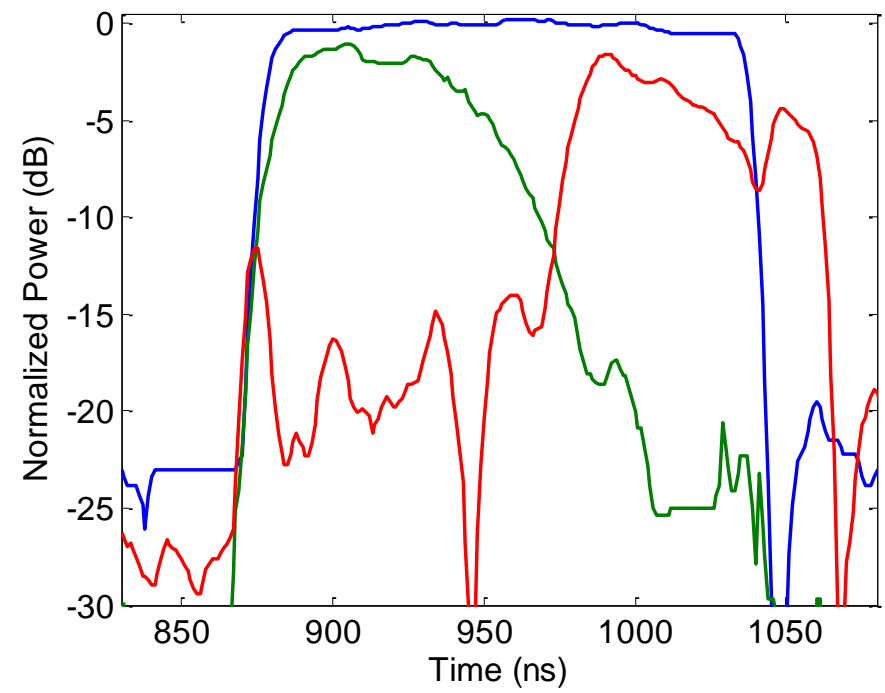
(s11 = -26.55 dB, s21 = -1.37 dB)



Blue – Input Forward, Green – Output Forward, Red – Input Reflected, Black – dark current.

F. Wang, SLAC
Test of TD18 structure

Breakdown Waveforms of TD18

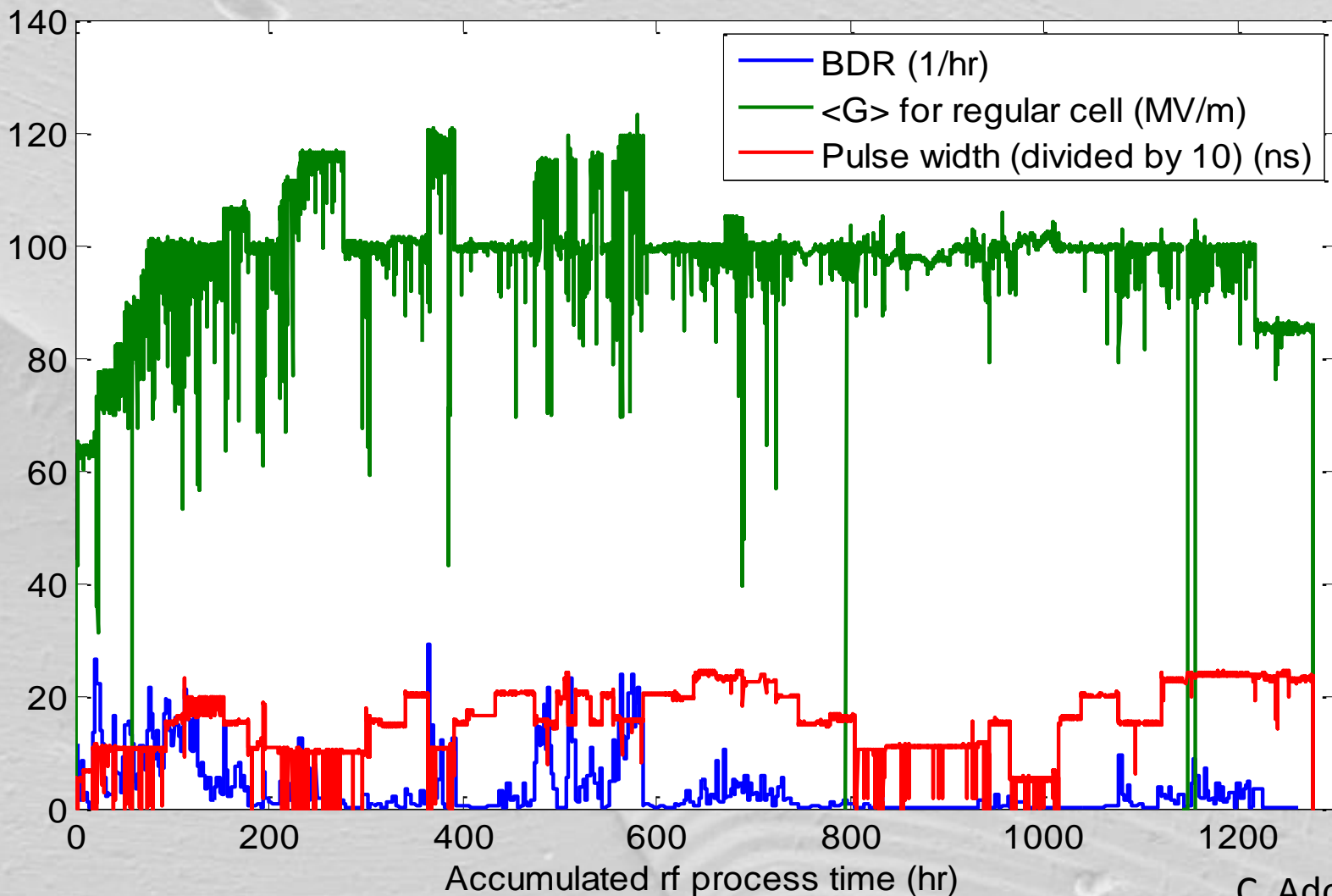


Blue – Input Forward, Green – Output Forward, Red – Input Reflected, Black – dark current.

F. Wang, SLAC
Test of TD18 structure



High Power Operation History



Final Run at 230 ns: 94 hrs at 100 MV/m w BDR = 7.6×10^{-5}
 60 hrs at 85 MV/m w BDR = 2.4×10^{-6}
 Walter Wuensch

C. Adolphsen
 F. Wang
 SLAC

10 October 2011

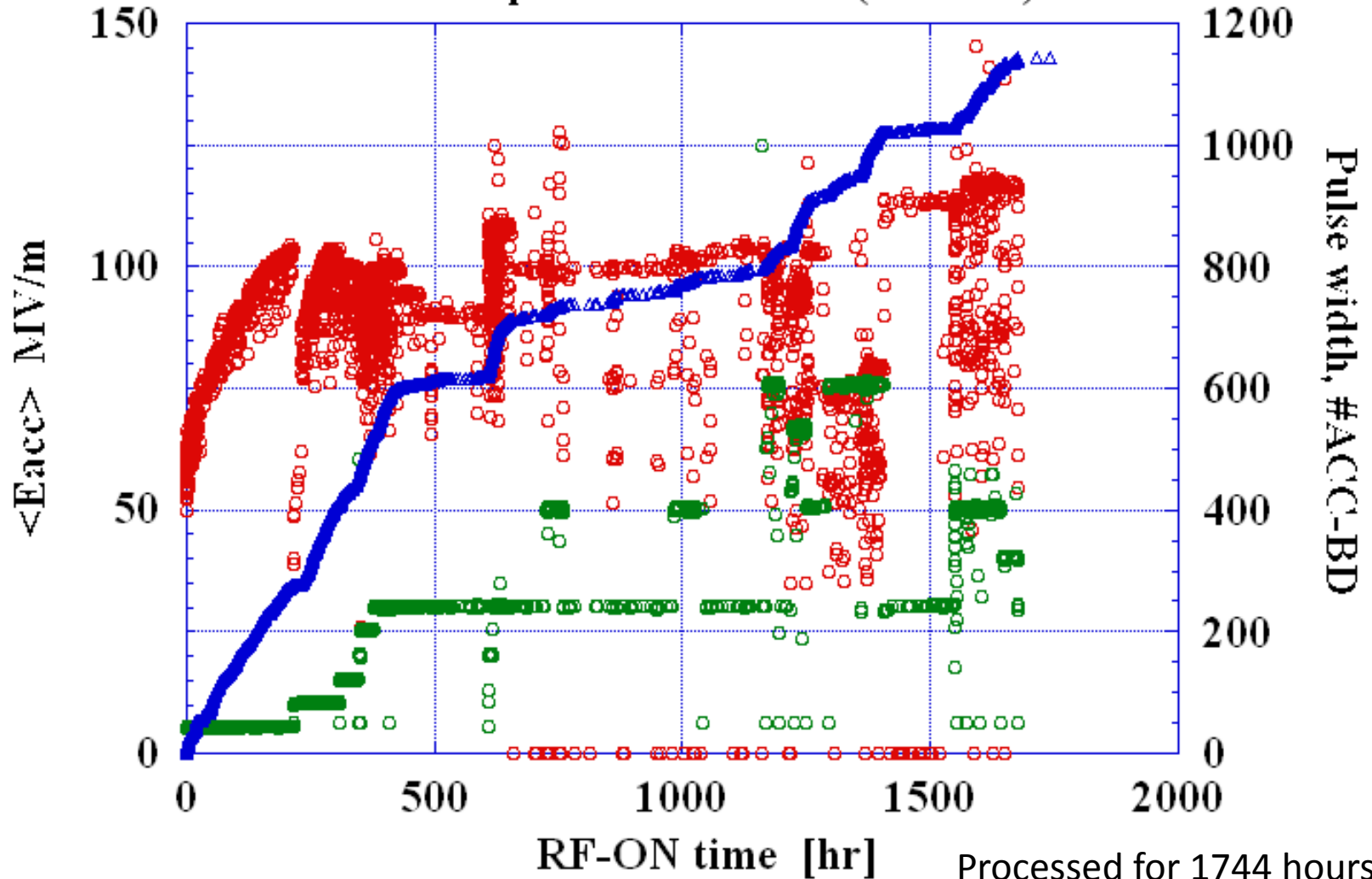
TD18

EPFL presentation

○ $\langle E_{acc} \rangle$ MV/m

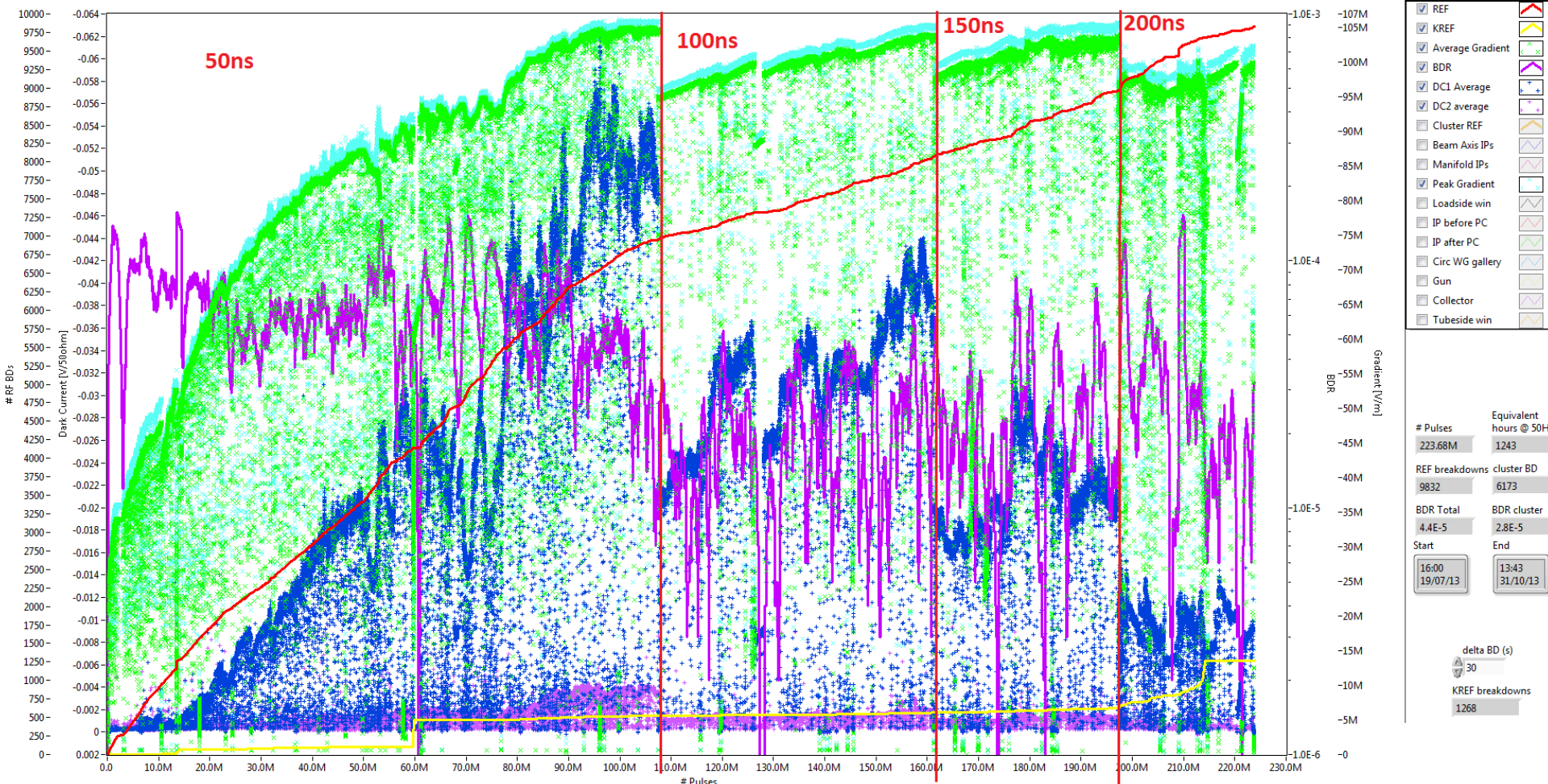
T24#3 History run1-36 till earthquake on Mar. 11 (1744hrs)

○ F50 width[ns]
△ #ACC-BD

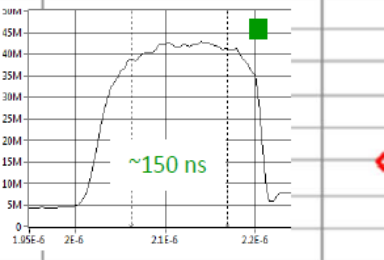
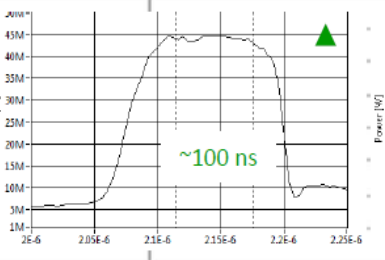
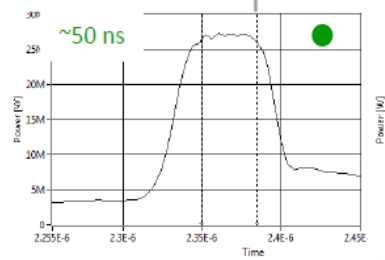
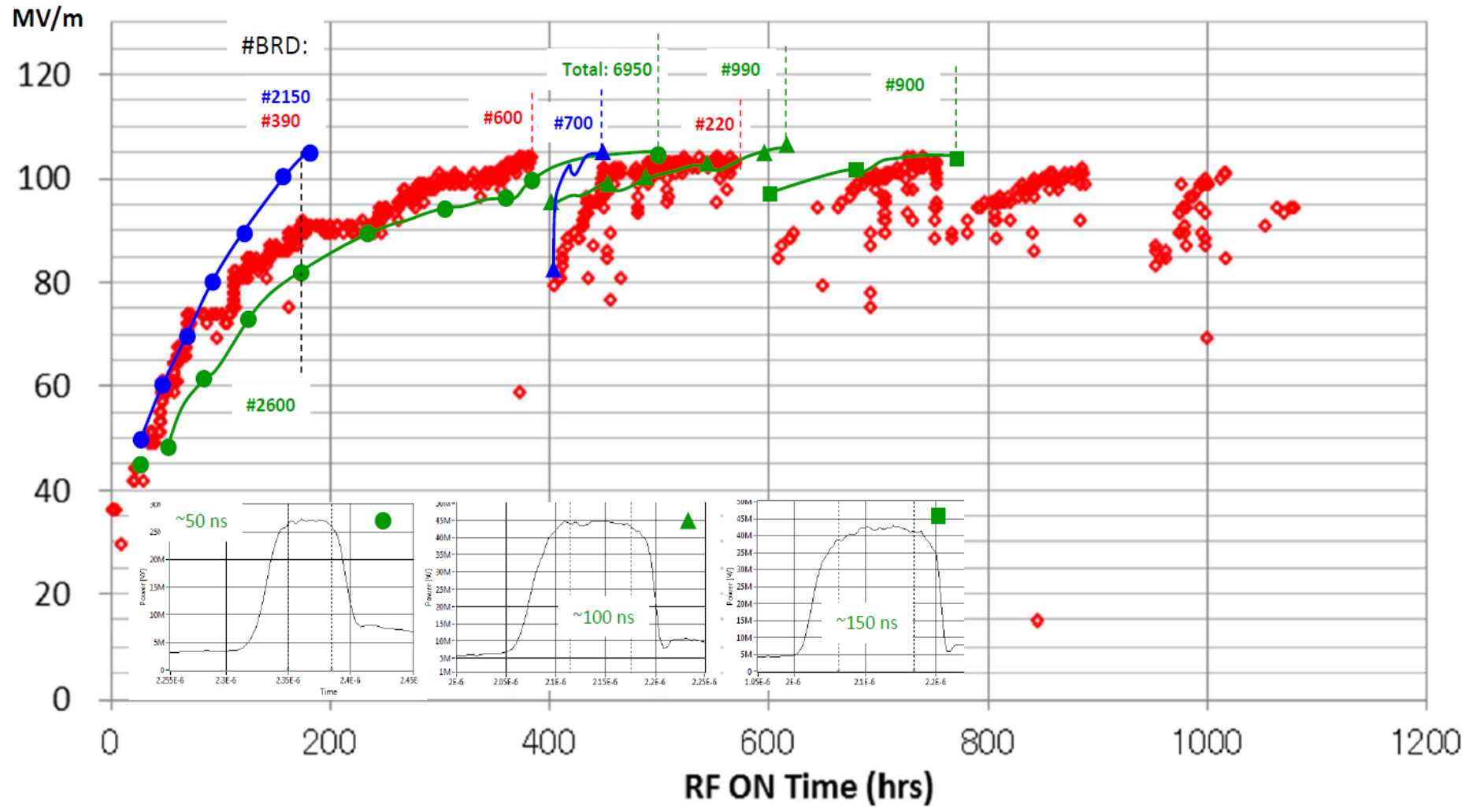


KEK

Results: TD26CC

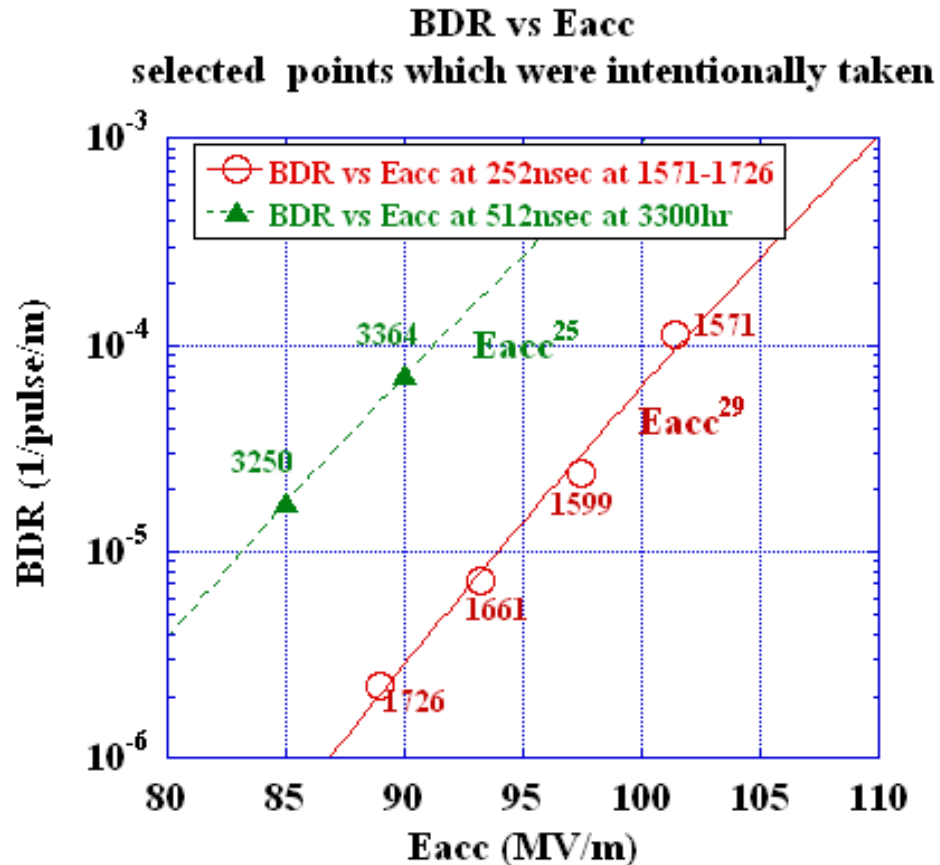


Comparison of the TD24R05(KEK); TD24R05(CERN) and TD26R05CC (CERN) processing histories.



Relevant data points of BDR vs Eacc

101017



TD18

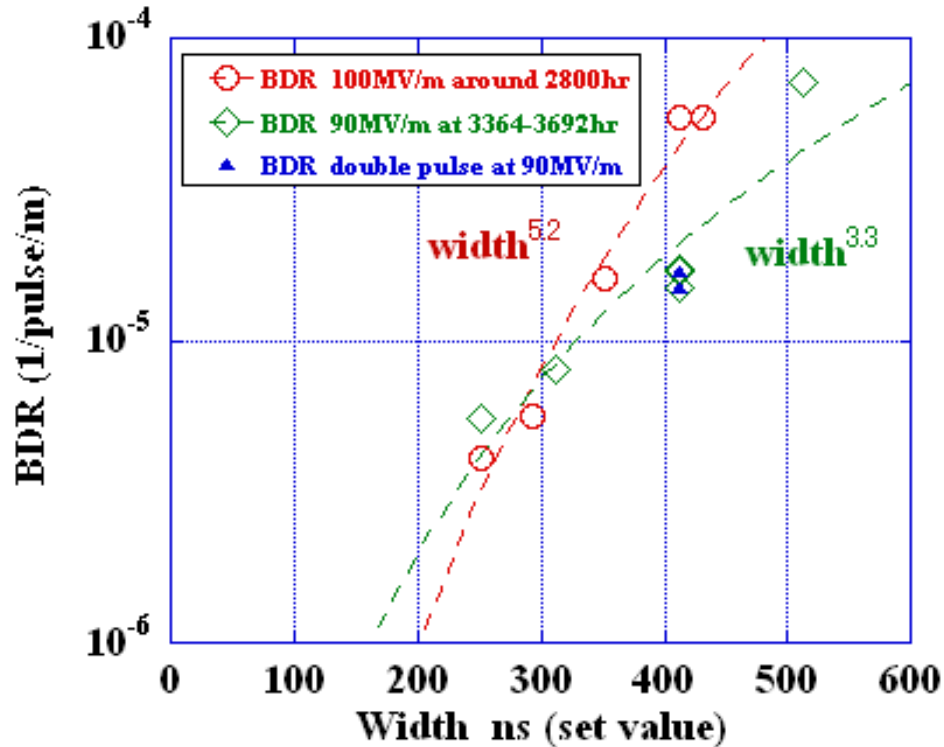
Step rise as Eacc, 10 times per 10 MV/m, less steep than T18

TD18_#2 BDR versus width

at 100MV/m around 2800hr and at 90MV/m around 3500hr

101017

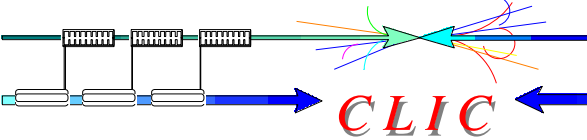
TD18_Disk_#2 BDR vs Width



TD18

Similar dependence at 90 and 100 if take usual single pulse?

Summary on gradient scaling



For a fixed pulse length

$$BDR \sim E_a^{30}$$

For a fixed BDR

$$E_a \cdot t_p^{1/6} = const$$

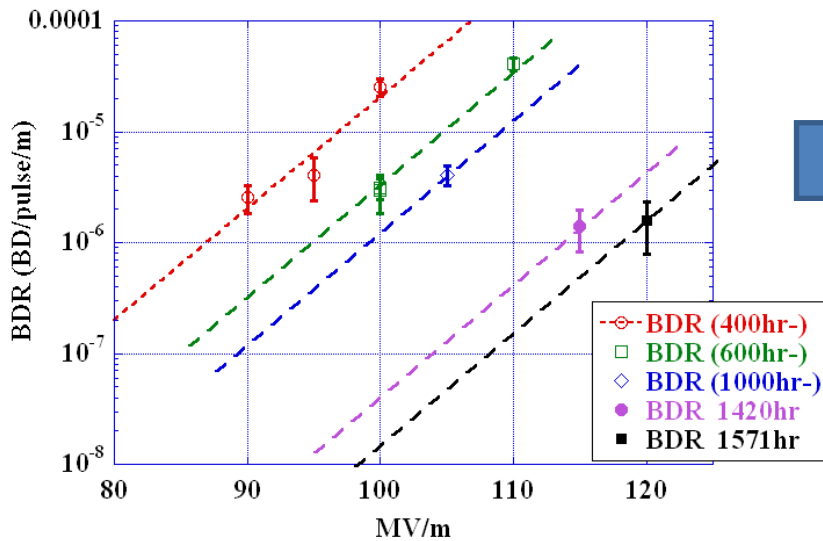
$$\frac{E_a^{30} \cdot t_p^5}{BDR} = const$$

- In a Cu structure, ultimate gradient E_a can be scaled to certain BDR and pulse length using above power law. It has been used in the following analysis of the data.
- The aim of this analysis is to find a field quantity X which is geometry independent and can be scaled among **all** Cu structures.

T24#3

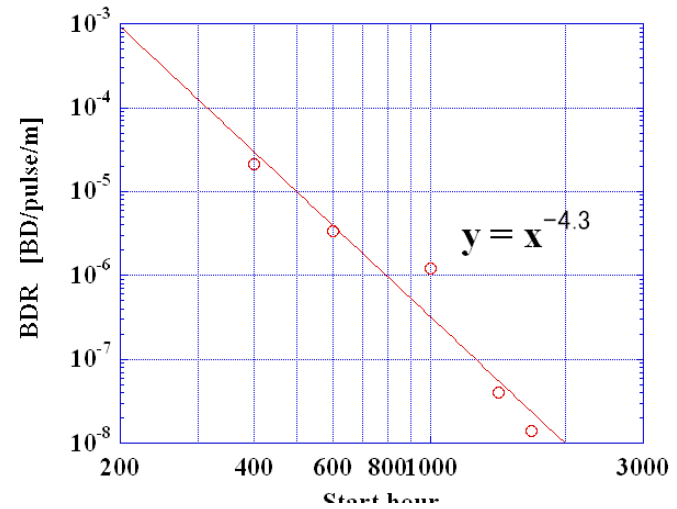
BDR evolution at 252ns normalized 100MV/m

T24#3 Breakdown rate at 252nsec

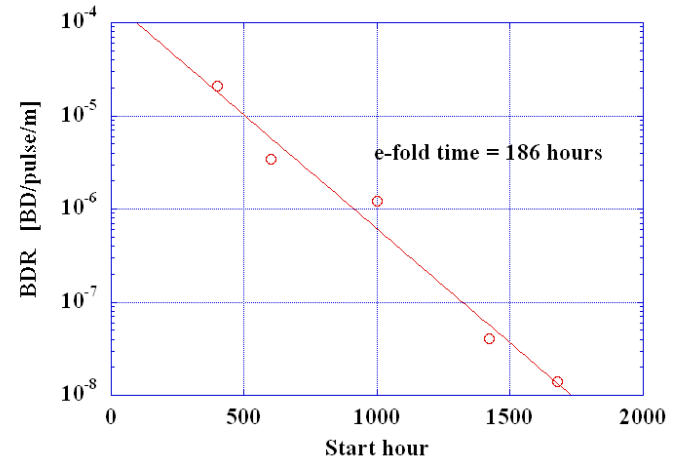


Assuming the same exponential slope as that at 400hr

T24#3 BDS vs time at 252ns 100MVm



T24#3 BDS vs time normalized at 252ns 100MVm



We understand the BDR has been kept decreasing.

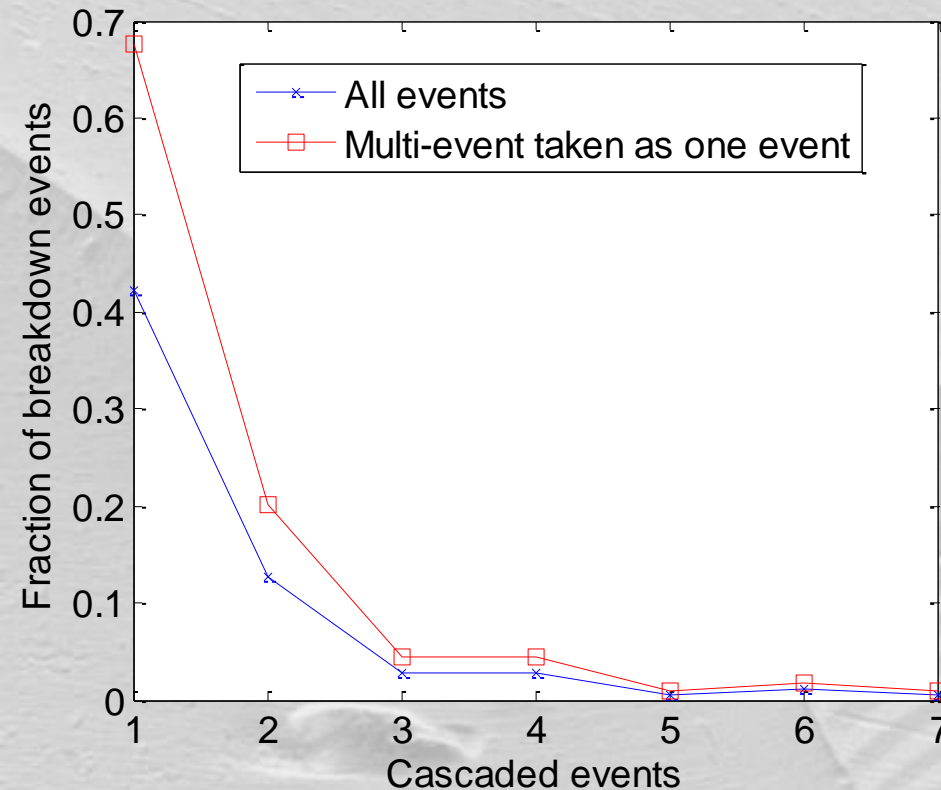


Breakdown sequence statistics

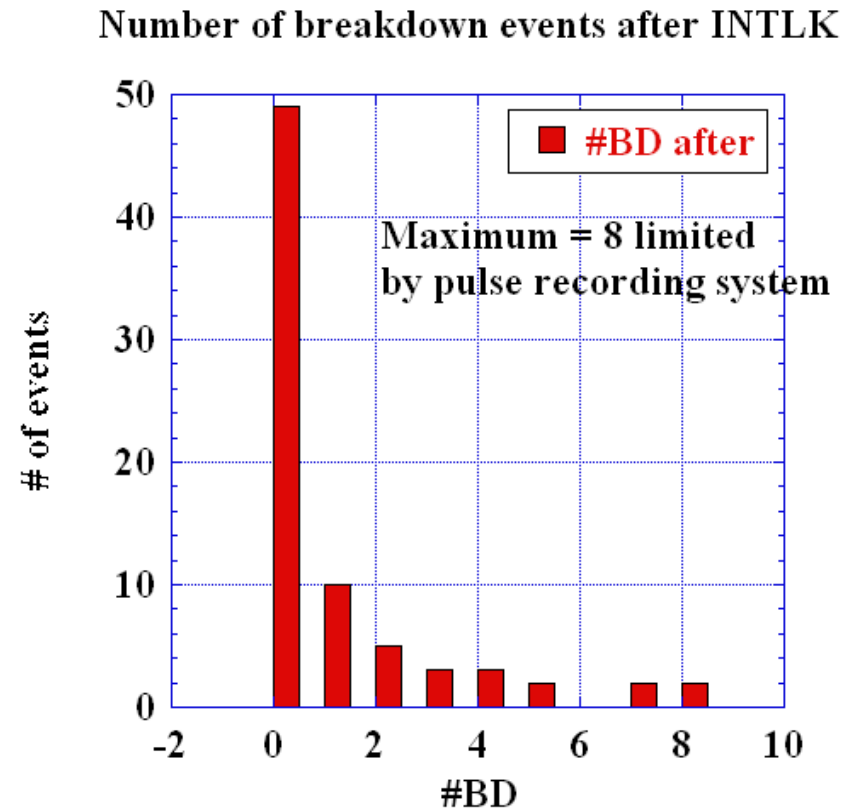


Both sets of measurements were made on TD18s

101028



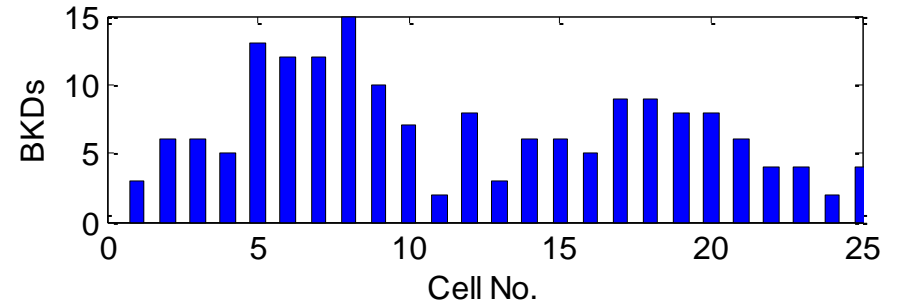
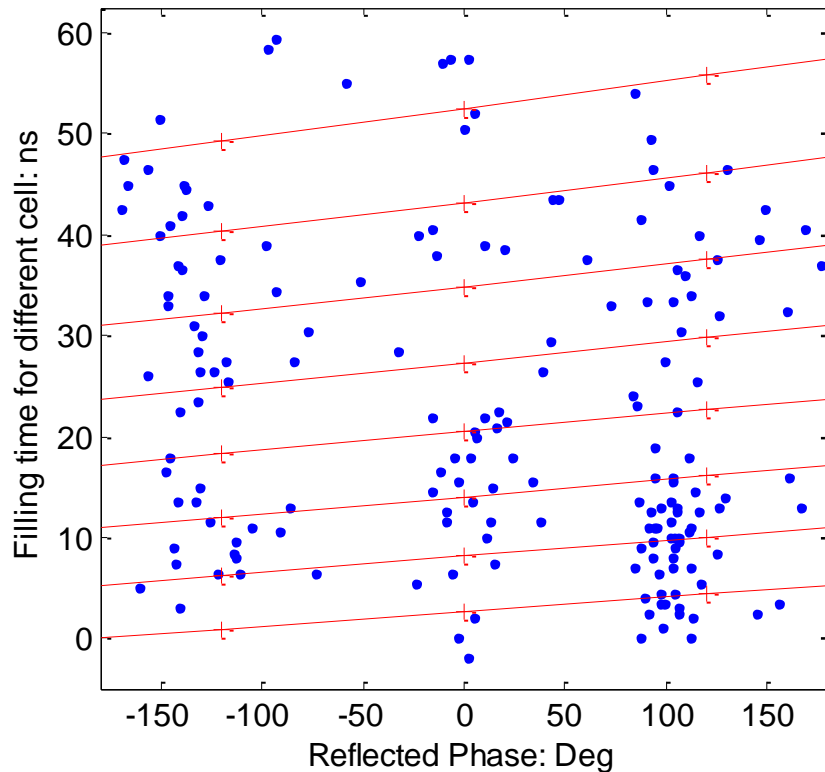
SLAC



KEK

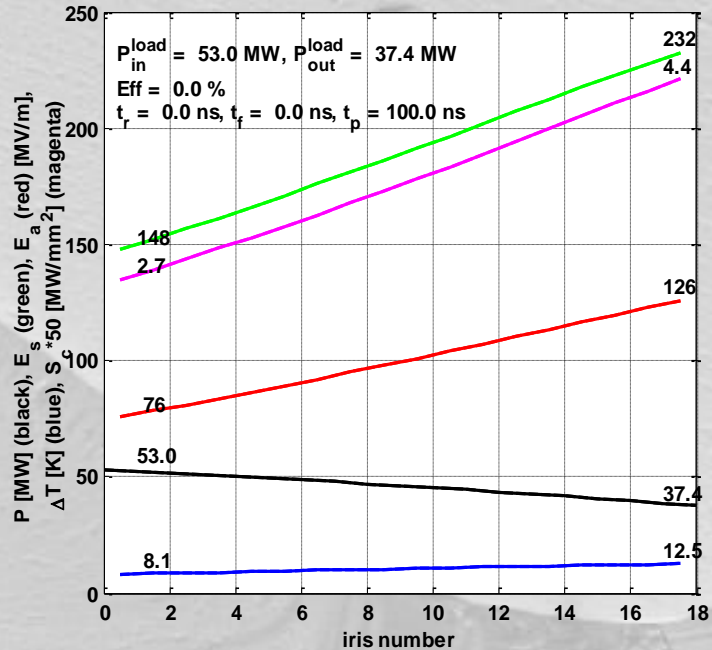
This kind of data is essential for determining rf hardware – on/off/ramp? – and establishing credible operational scenarios.

Breakdown Distribution for T24_SLAC_Disk1 of Last 50 Hours

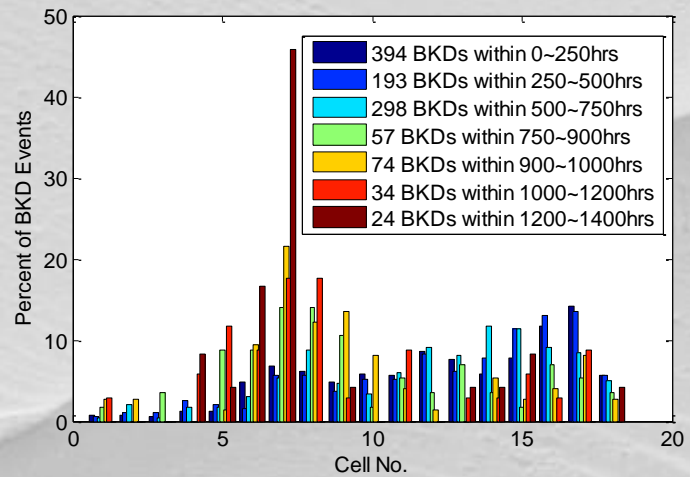




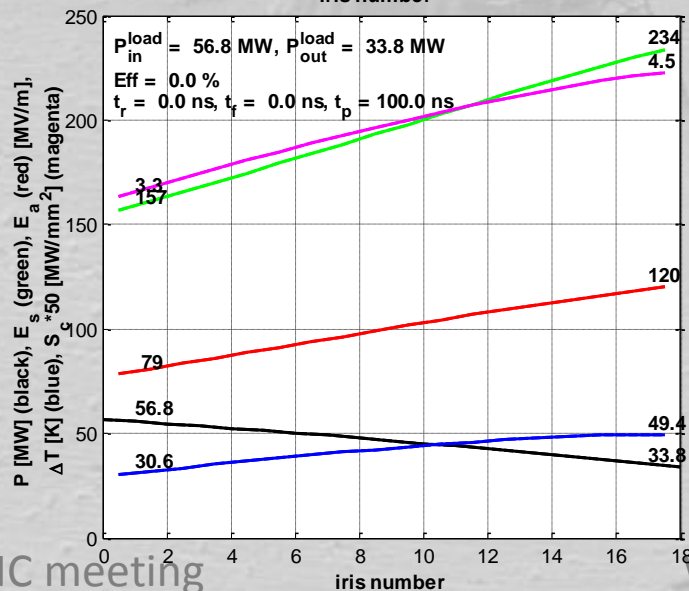
18 series breakdown rate distributions



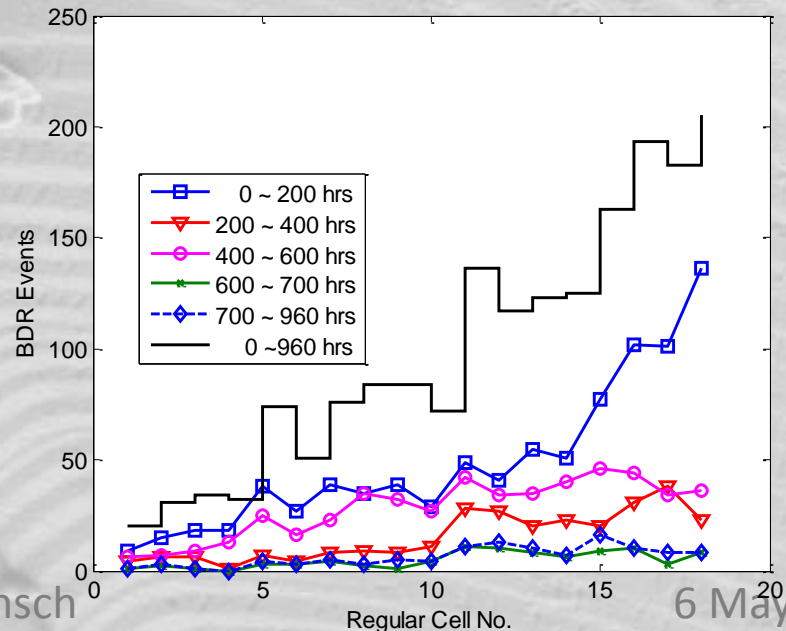
T18



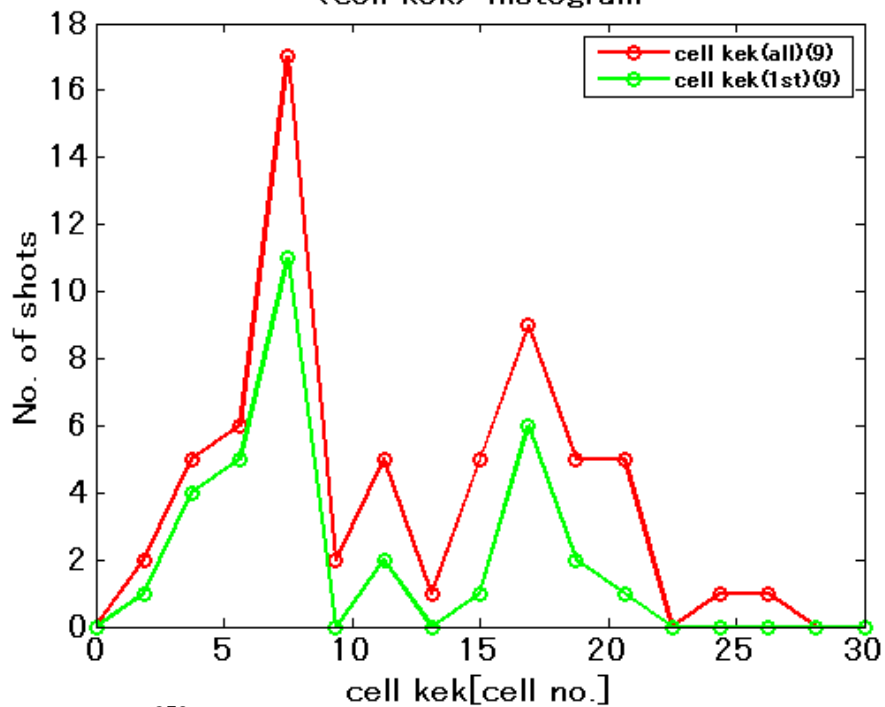
SLAC



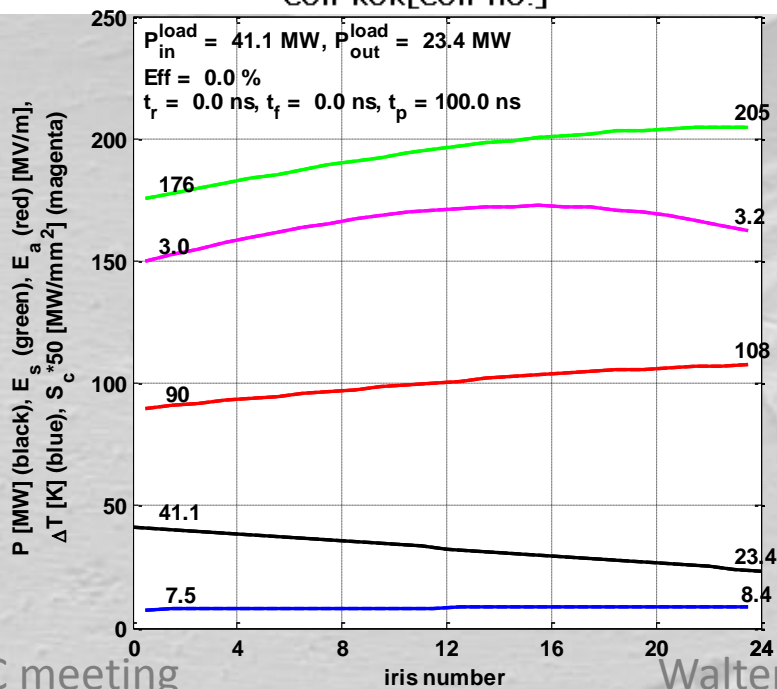
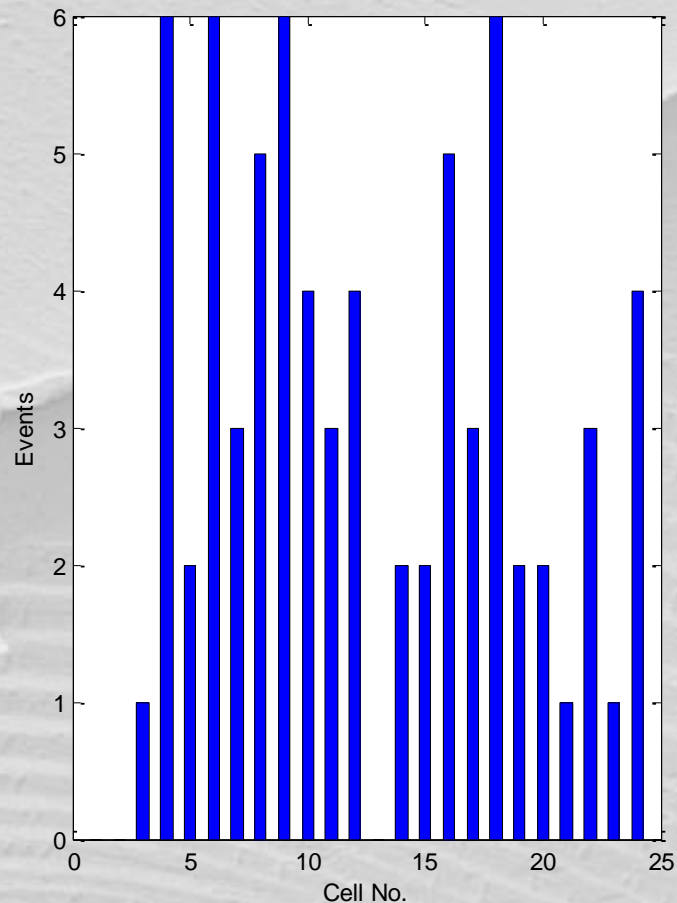
TD18



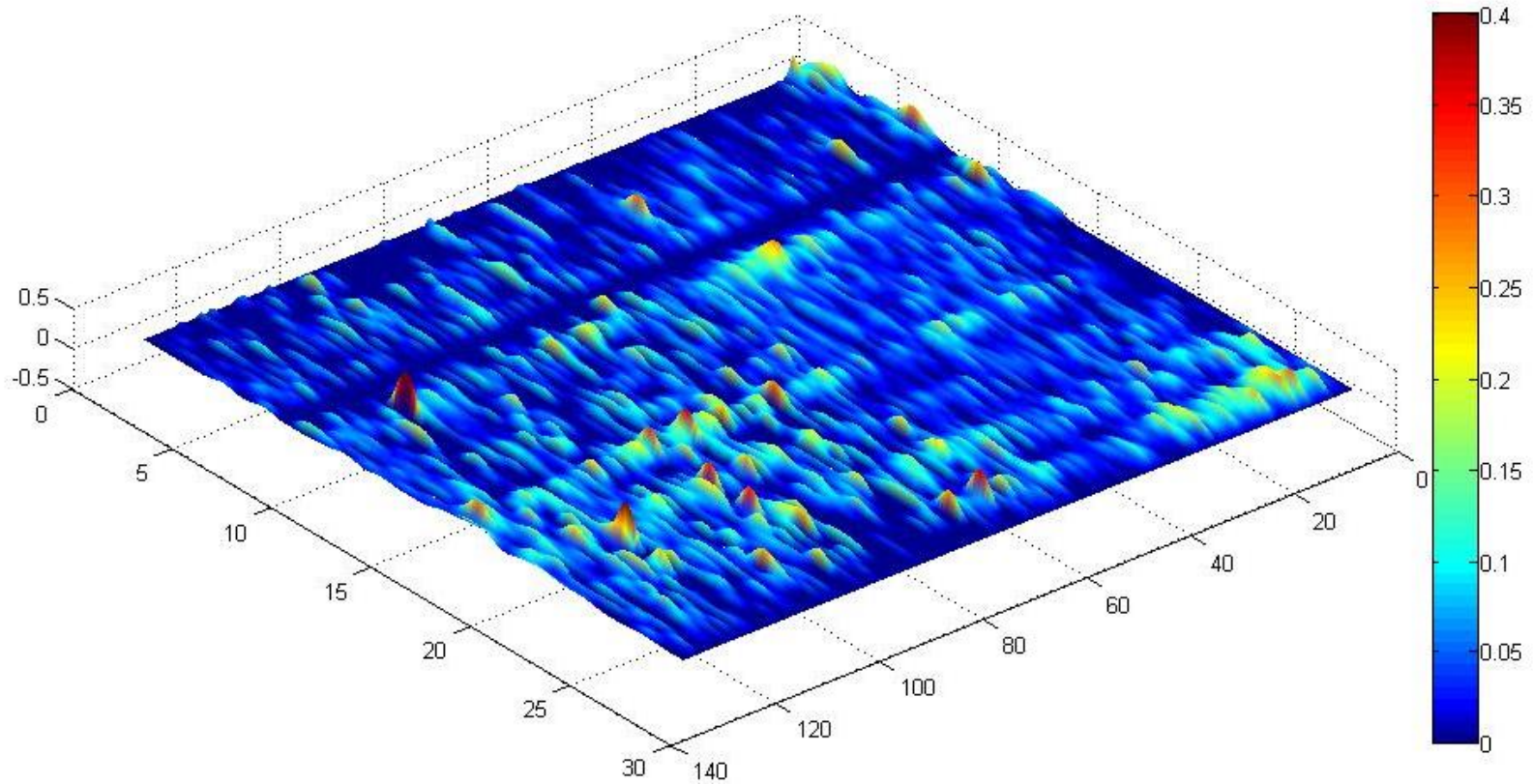
<cell kek> histogram



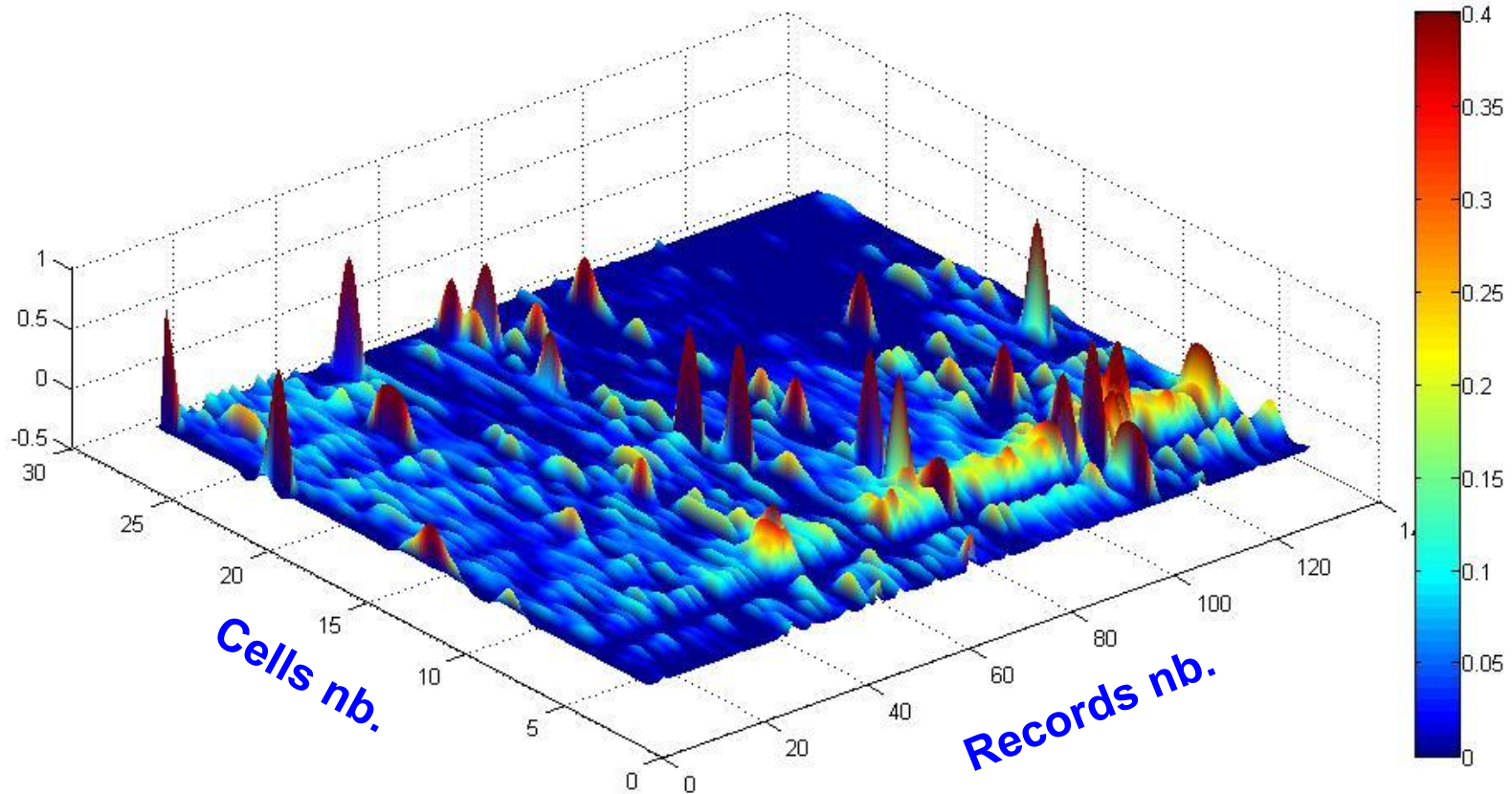
T24 breakdown location distributions



SLAC



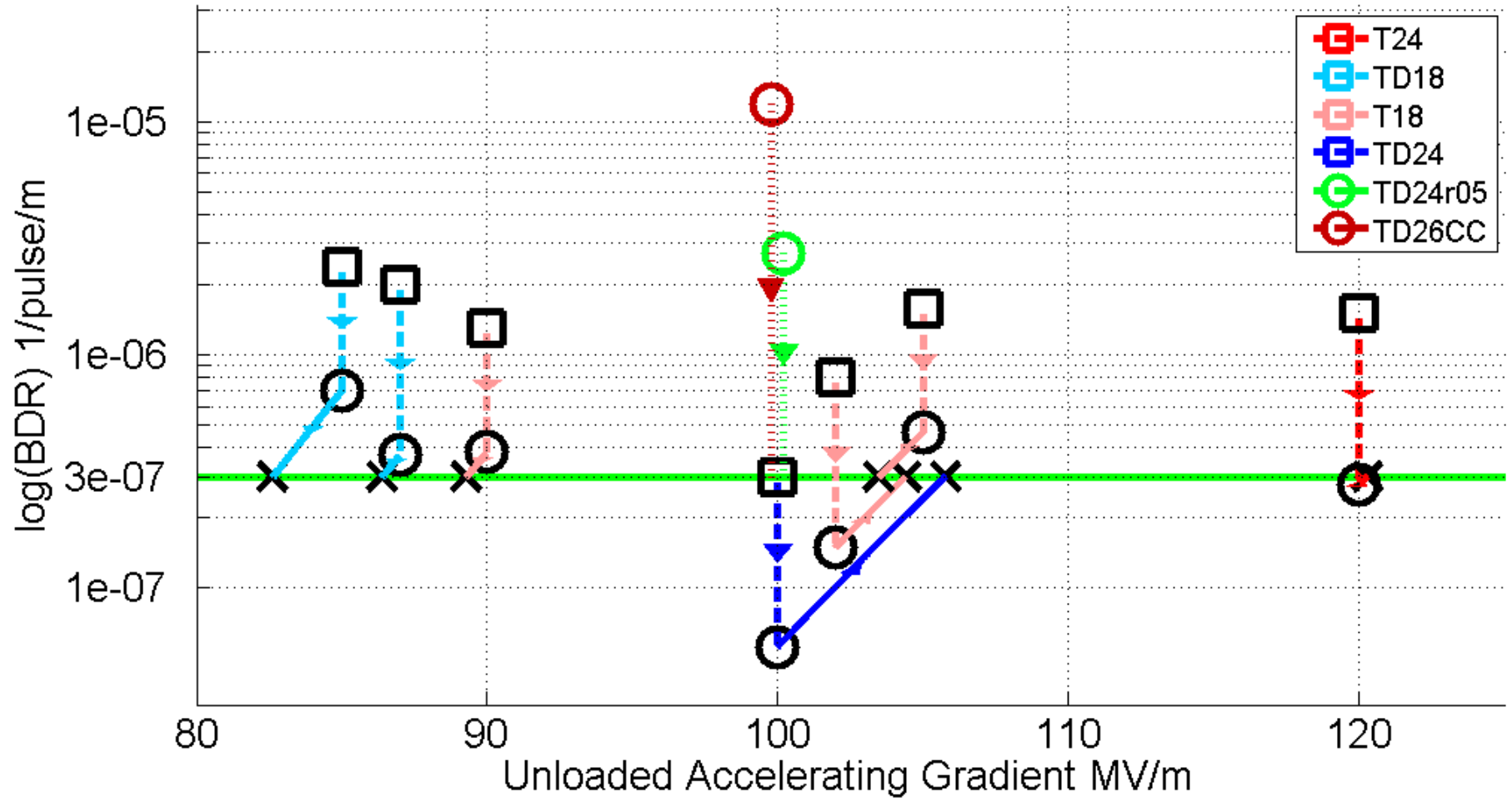
Corrupted files and no powered periods have been removed from the record



Hot cells (5 and 6) have appeared from record #50

The very high peak values are an artifact of the normalization (if only 2 BDs during a record these cells will result very active)

CLIC structure performance summary



Quantifying geometrical dependence of high-power performance

Importance of geometric dependence - motivation

As you have seen in other presentations, there is a strong interplay between the rf design of accelerating structures and the overall performance of the collider.

One of the strongest dependencies is emittance growth as function of the average iris aperture which acts through transverse wakefields.

The iris aperture also influences required peak power and efficiency through its effect on group velocity.

But crucially, the iris aperture has an extremely strong influence on achievable accelerating gradient.

Very generally, we expect that the gradient of an rf structure should be calculable from its geometry if material and preparation are specified.

The big questions

Where does such a geometrical dependency come from?

Can we quantify the dependence of achievable accelerating gradient on the geometry?

Trying to understand, derive and quantify geometrical dependence has been a significant effort because an essential element of the overall design and optimization of the collider.

The basic approach

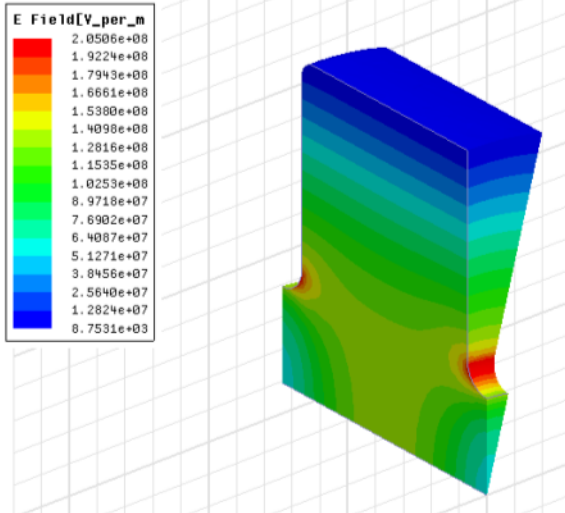
The basic element is to express our high-power limits as a function of the unperturbed fields inside our structures – like the electric field limit in dc spark.

So first we are going to make sure that we have a feel for how those fields vary as a function of geometry.

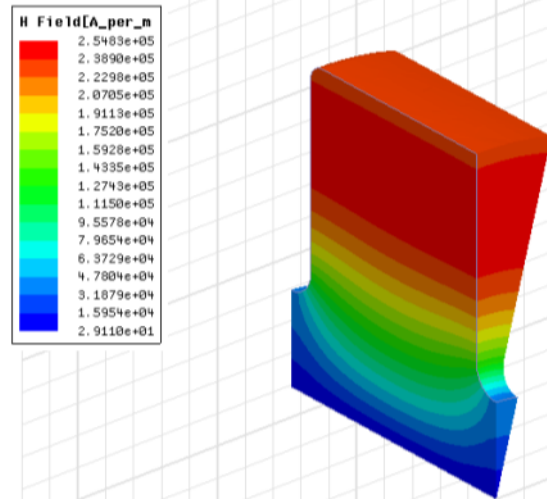
We use a specific example of iris variation for a fixed phase advance in a travelling wave structure.

Field distribution

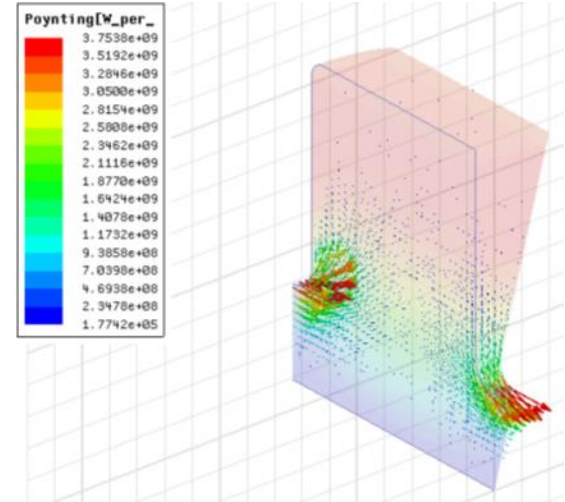
Electric field (V/m)



Magnetic field (A/m)

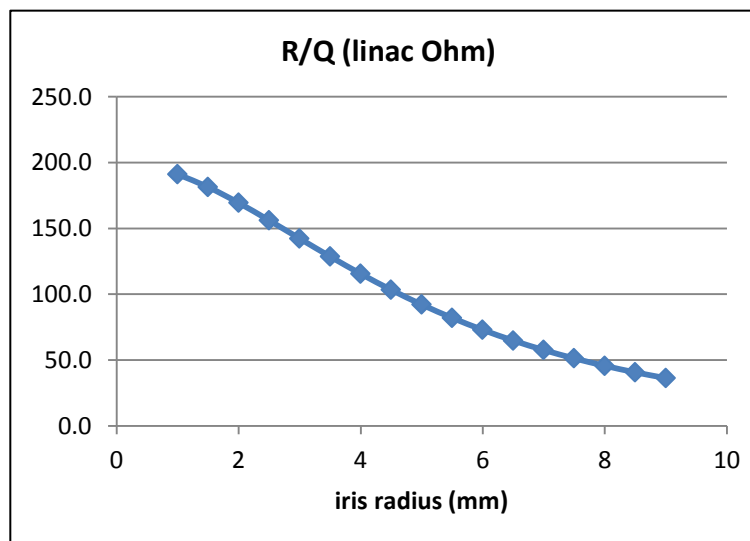
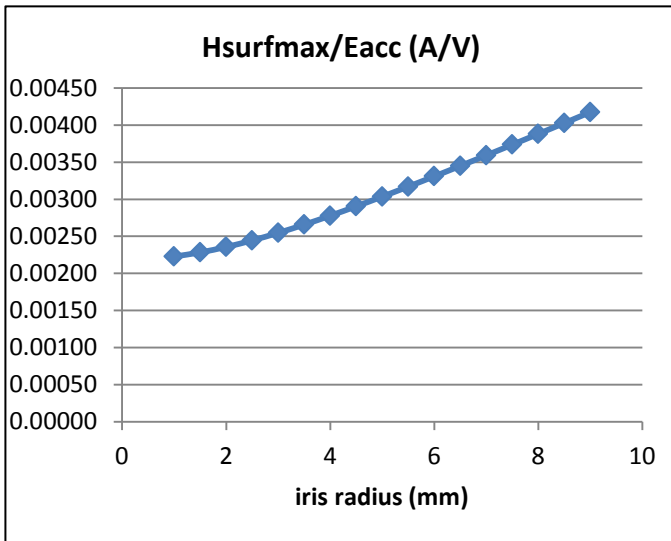
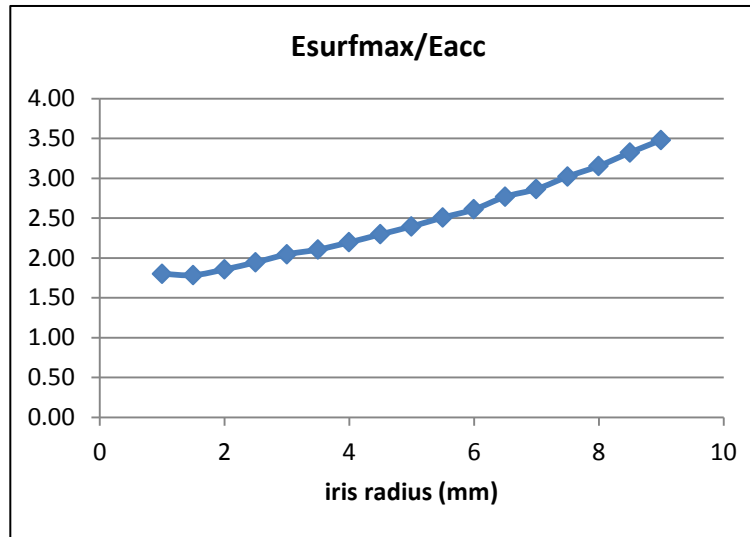
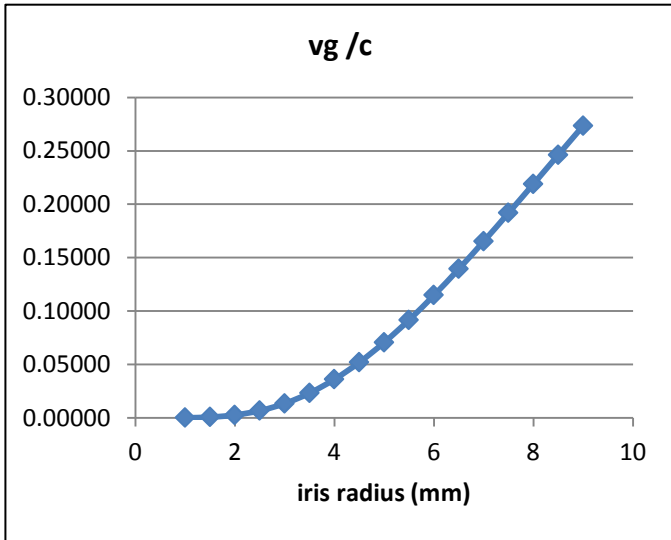


Poynting vector (W/m²)



- Simulation in HFSS12
- Field values are normalized to accelerating gradient, $E_{acc}=100\text{MV/m}$
- Frequency: 11.424GHz
- Phase advance per cell: 120 degree
- *Iris radius*: 3mm
- $v_g/c= 1.35\%$

Parameters v.s. iris



Simulation in HFSS12
Iris thickness: 1.66mm
Frequency: 11.424GHz
Phase_adv/cell: 120 degree

$$R/Q = V_{acc}^2 / (\omega U)$$

Overview of how different types of structures actually behave – results of high-power tests of accelerating structures to PETS

Achieving high gradients has been a high profile concern for CLIC and NLC/JLC since roughly 2000. Here are the target specifications we have had:

	frequency [GHz]	Average loaded gradient [MV/m]	Input (output for PETS) power [MW]	Full pulse length [ns]
NLC/JLC	11.424	50	55	400
CLIC pre-2007				
Accelerating	29.928	150	150	70
PETS	29.985	-5.7	642	70
CLIC post 2007				
Accelerating	11.994	100	64	240
PETS	11.994	-6.3	136	240

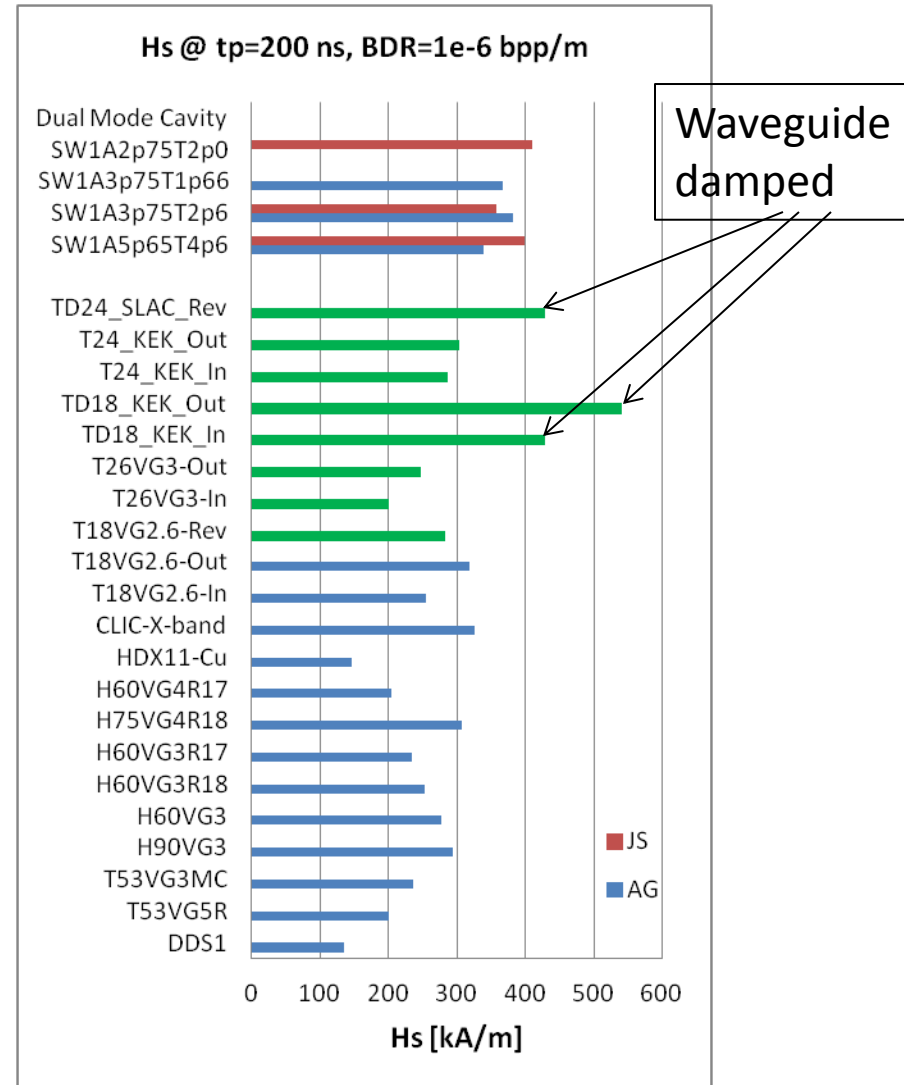
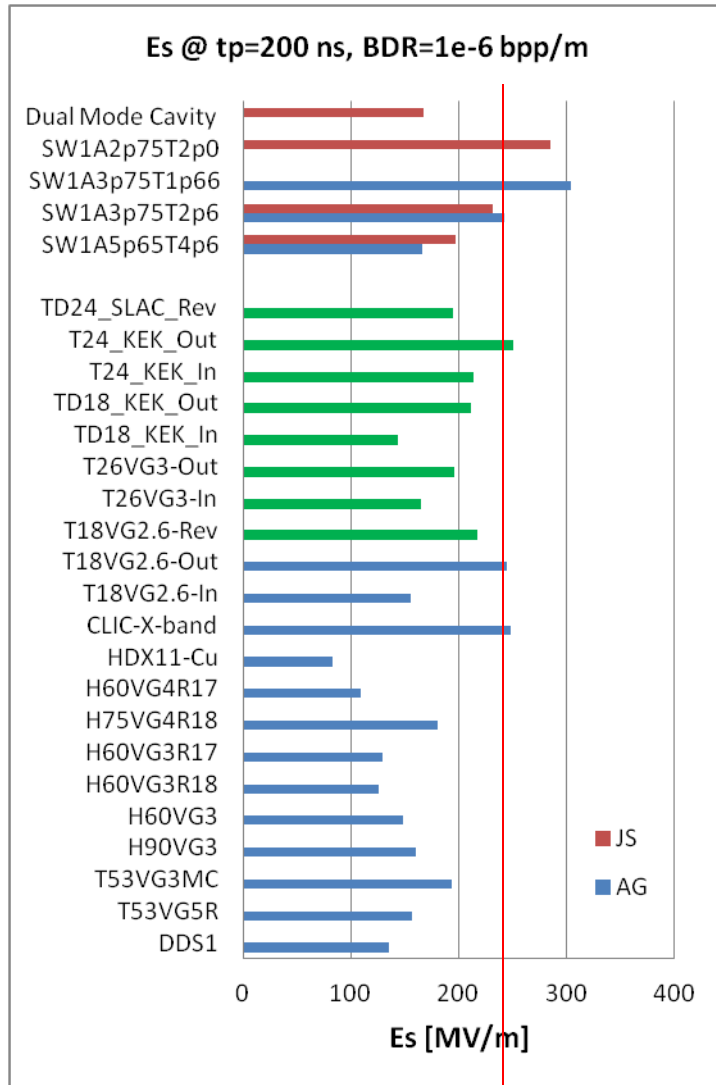
Trying to achieve these specifications has resulted over the years in the test of many structures of diverse rf design.

The preparation and testing conditions of the test structures which were built were not always the same – these processes also evolved over the period the structures were being developed.

But the wide variety of structure geometries were tested under reasonably similar conditions.

So we have used this unique set of data to try to understand and then quantify the geometrical dependency of gradient.

Maximum surface electric and magnetic fields



Es = 250 MV/m or higher has been achieved in several cases: very low or zero group velocity

What do can make out of this mess?

My personal conclusion from looking at data like this, was that a something else is important, beyond E and B surface fields.

This something felt like it had to be related to the power flowing through the structure. In particular some kind of power density, since larger apertures generally support larger powers.

This is reasonable when you think about what we know about breakdown.

Field emission is pico or nano amps. Breakdowns in rf and dc produce 10's, 100's even kA of current.

A lot of power is needed to accelerate so much current. The breakdown must need to be “fed” with the necessary power so power density is crucial.

This has resulted in the development of two power-density based design criteria:

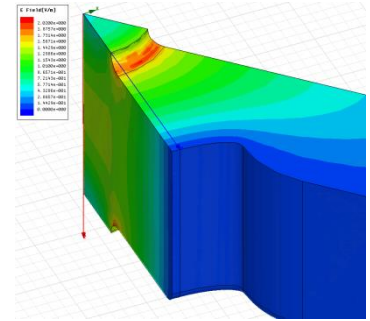
$$\frac{P}{\lambda C} = \text{const}$$

global power flow

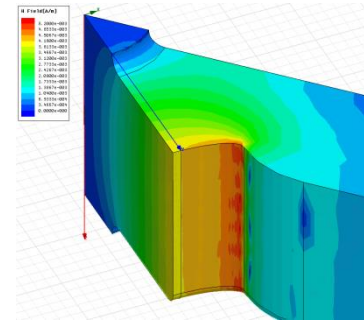
$$S_c = \text{Re}(\mathbf{S}) + \frac{1}{6} \text{Im}(\mathbf{S})$$

local complex power flow

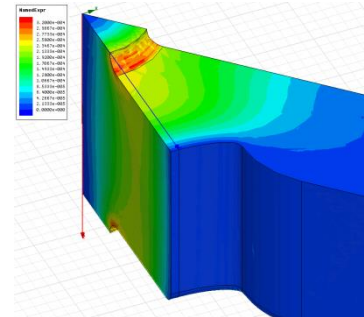
$$E_s/E_a$$



$$H_s/E_a$$



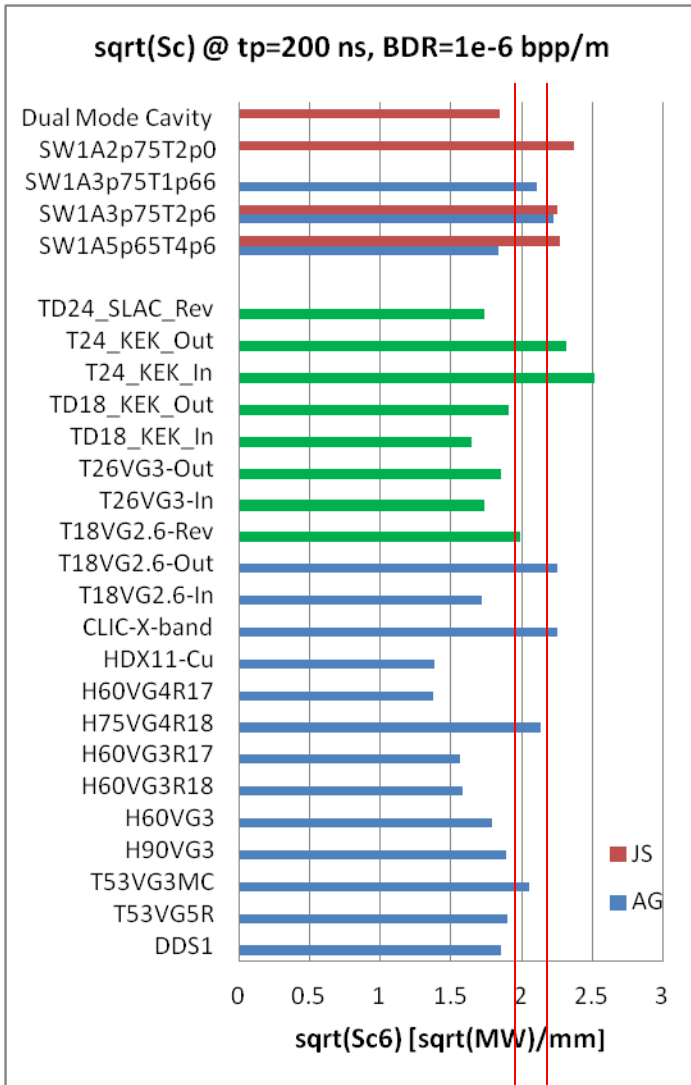
$$S_c/E_a^2$$



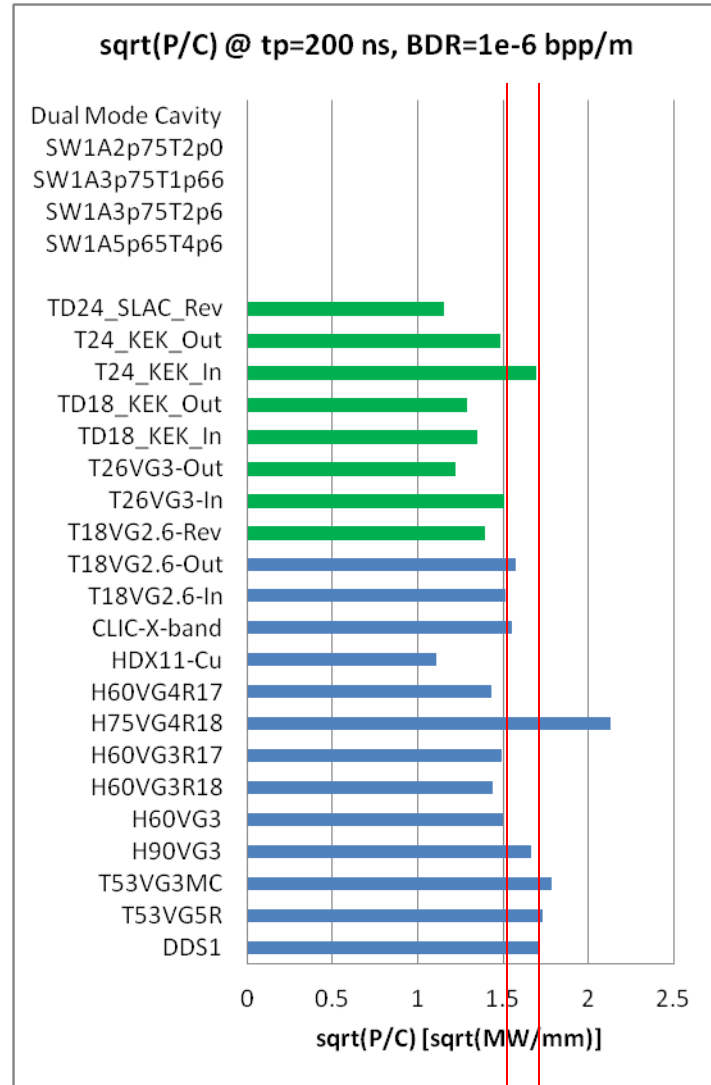
New local field quantity describing the high gradient limit of accelerating structures.
 A. Grudiev, S. Calatroni, W. Wuensch (CERN).
 2009. 9 pp.
 Published in Phys.Rev.ST Accel.Beams 12
 (2009) 102001

There is no proof (yet) but rather the general set of physical arguments plus reasonably good consistency with measurements.

Power flow related quantities: Sc and P/C



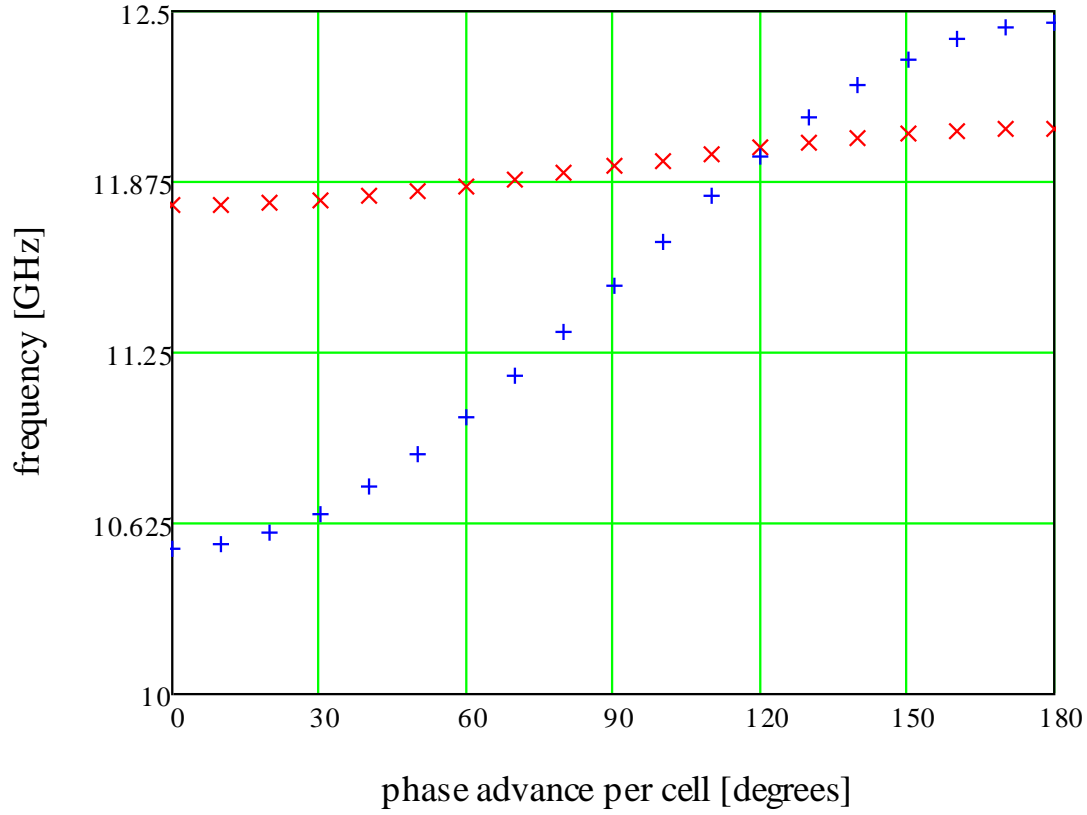
Sc = 4 - 5 MW/mm²



P/C = 2.3 - 2.9 MW/mm

Another aspect of geometrical dependence – bandwidth.

Lower group velocity structures support larger surface fields. Lower group velocity is lower bandwidth – think of the dispersion curves – which could make it harder to feed the breakdown transient, when currents shoot from nano to kA.



Summary of turn on times

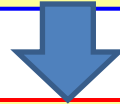
Test	Frequency	Measurement	Result
Simulation dc spark			5-10 ns
New DC System	DC	Voltage Fall Time	12-13ns
Swiss FEL (C-Band)	5.7GHz	Transmitted Power Fall Time	110 - 140ns
KEK T24 (X-Band)	12GHz	Transmitted Power Fall Time	20-40ns
CTF/TBTS TD24 (X-Band)	12GHz	Transmitted Power Fall Time	20-40ns
CTF SICA (S-Band)	3GHz	Transmitted Power	60-140ns

The turn on time could be related to the bandwidth of the structures or possibly the intrinsic size.

Summary on the high-power RF constraints

RF breakdown and pulsed surface heating constraints used for CLIC_G design (2007):

- $E_s^{\max} < 250 \text{ MV/m}$
- $P_{\text{in}}/C_{\text{in}} \cdot (t_p^{\text{P}})^{1/3} = 18 \text{ MW} \cdot \text{ns}^{1/3}/\text{mm}$
- $\Delta T^{\max}(H_s^{\max}, t_p) < 56 \text{ K}$

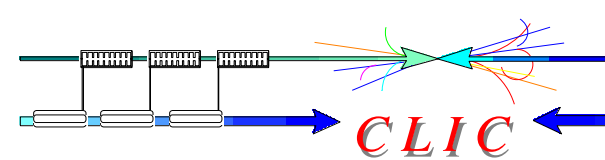


Optimistic RF breakdown and pulsed surface heating constraints for BDR= 10^{-6} bpp/m:

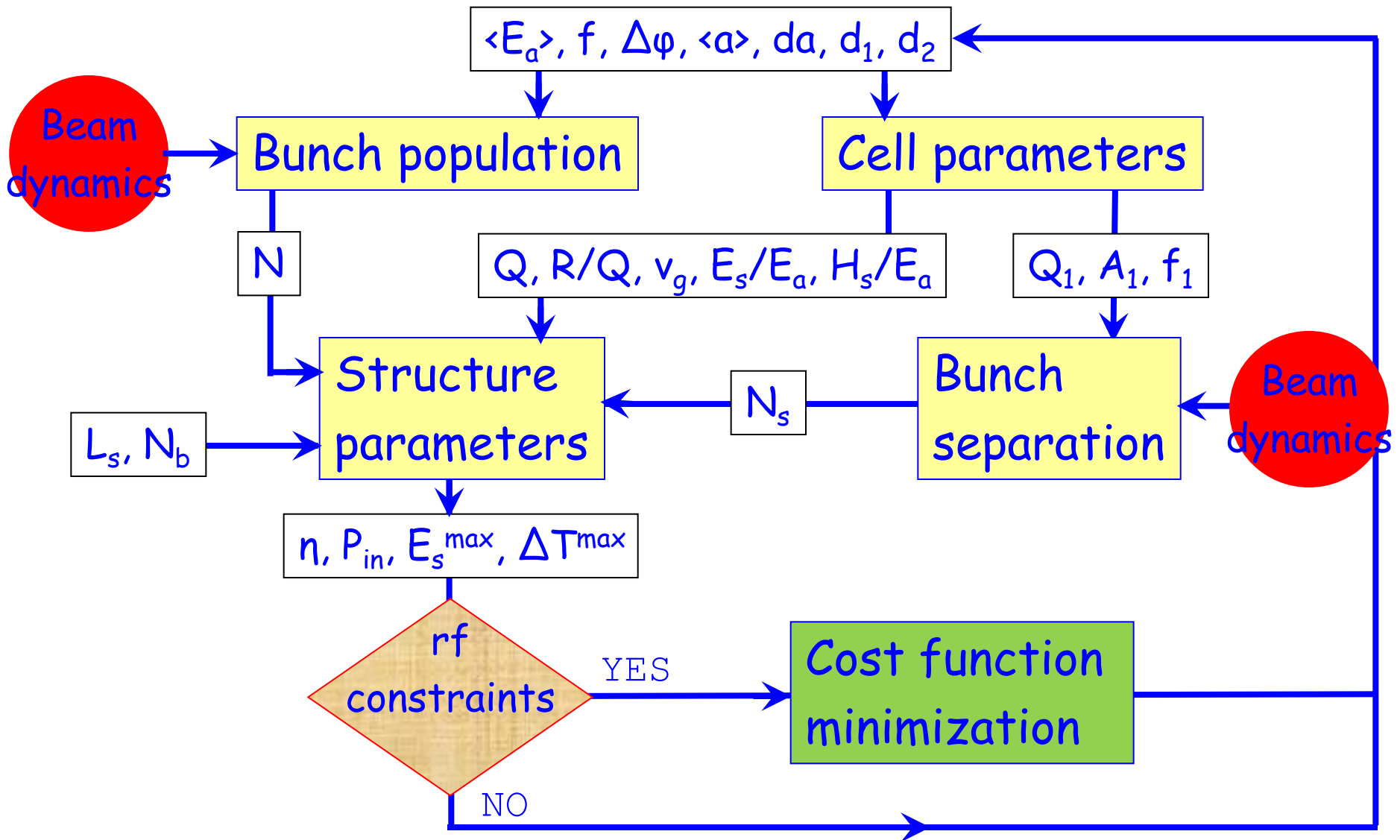
- $E_s^{\max} \cdot (t_p^{\text{P}})^{1/6} < 250 \text{ MV/m} \cdot (200\text{ns})^{1/6}$
 - $P_{\text{in}}/C_{\text{in}} \cdot (t_p^{\text{P}})^{1/3} < 2.8 \text{ MW/mm} \cdot (200\text{ns})^{1/3} = 17 \text{ [Wu]}$
 - $S_c^{\max} \cdot (t_p^{\text{P}})^{1/3} < 5 \text{ MW/mm}^2 \cdot (200\text{ns})^{1/3}$
- and
- $\Delta T^{\max}(H_s^{\max}, t_p) < 50 \text{ K}$

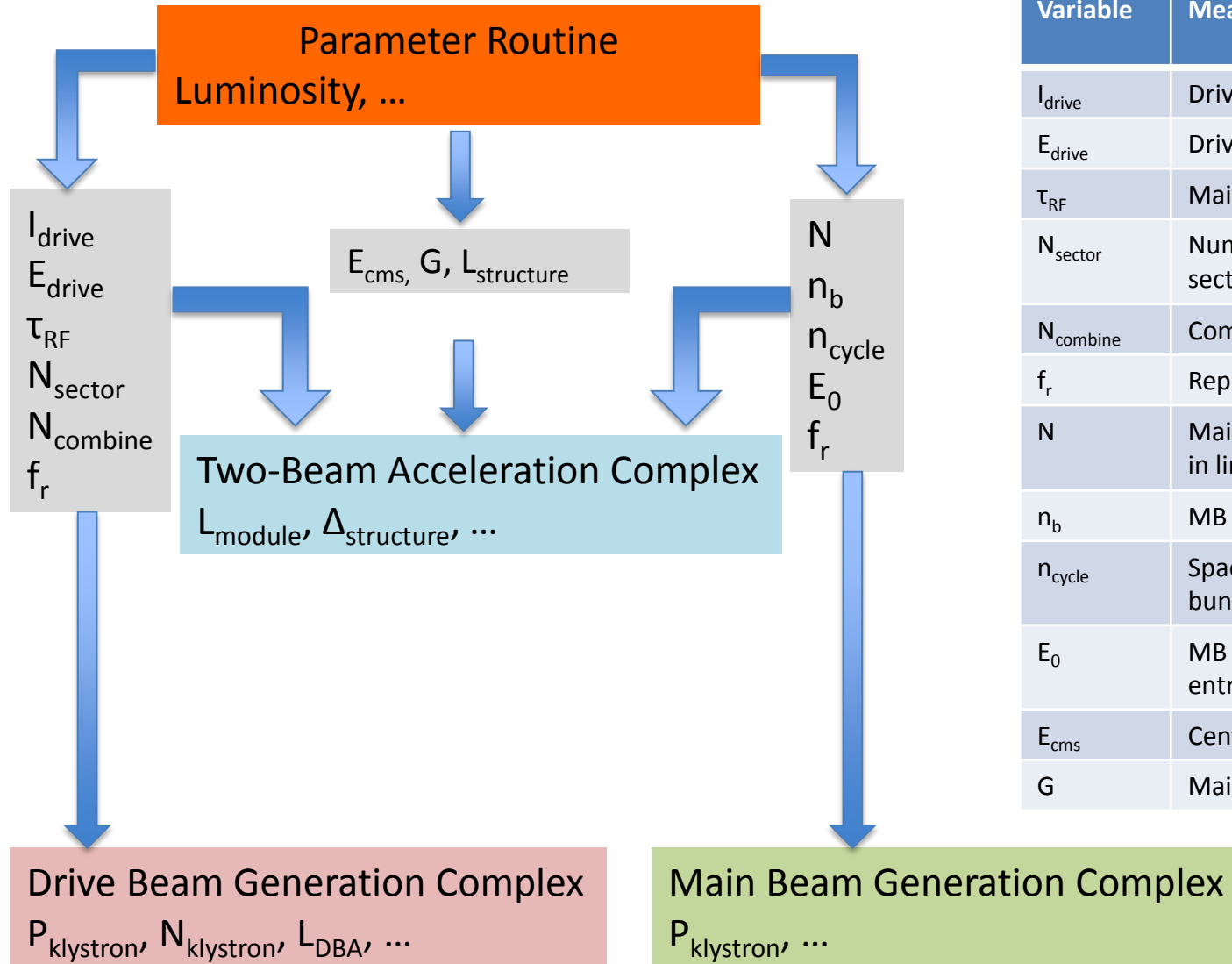
- Depending on degree of our optimism a safety margin has to be applied.
- Varying RF constraints in the optimization how much money one can save by being optimistic.

Optimization procedure



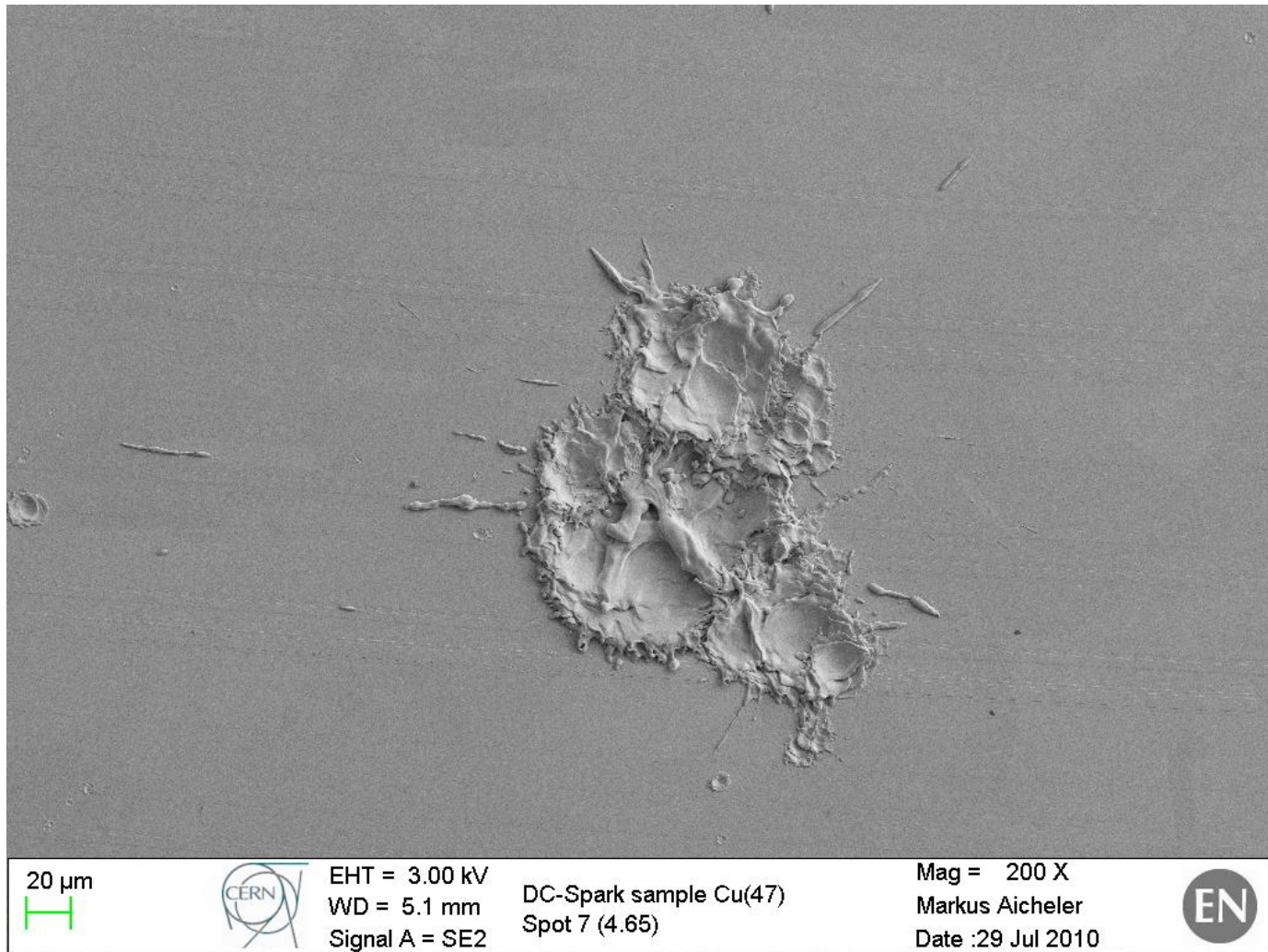
CLIC





Variable	Meaning	Current value
I_{drive}	Drive beam current	101A
E_{drive}	Drive beam energy	2.37GeV
τ_{RF}	Main linac RF pulse length	244ns
N_{sector}	Number of drive beam sectors per linac	4
$N_{combine}$	Combination number	24
f_r	Repetition rate	50Hz
N	Main beam bunch charge in linac	3.72e9
n_b	MB bunches per pulse	312
n_{cycle}	Spacing between MB bunches	6 cycles
E_0	MB energy at linac entrance	9GeV
E_{cms}	Centre-of-mass energy	500GeV
G	Main linac gradient	100MV/m

Breakdown!



From pA to kA and from Angstroms to 100s of μm to mms.

An overview of the breakdown process

Vacuum



Copper

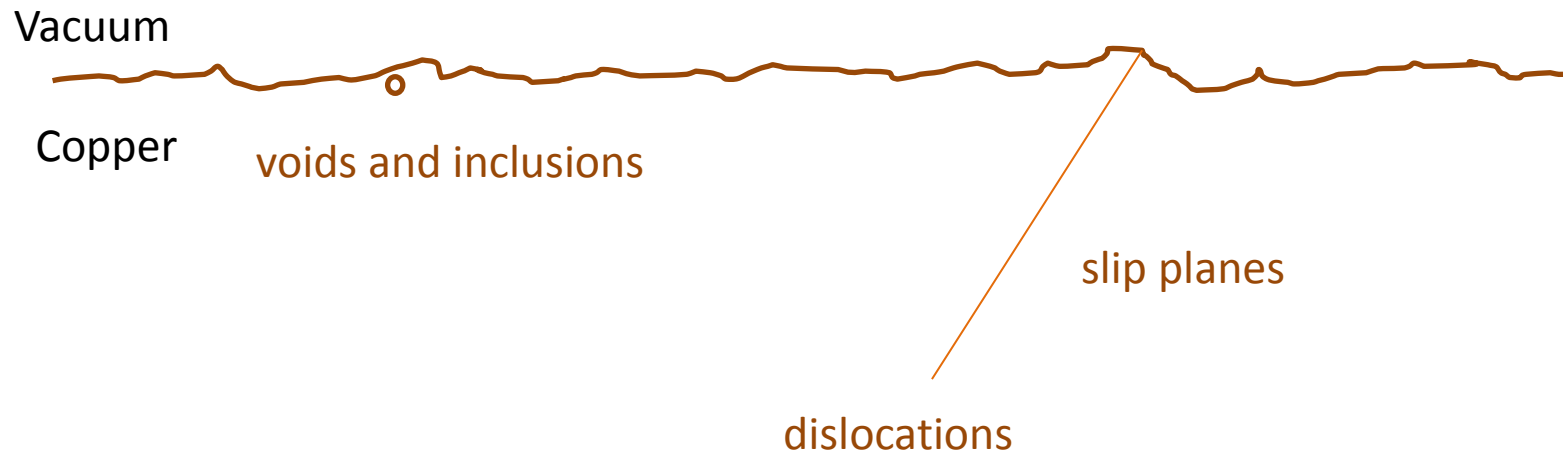
Actually real surfaces are imperfect

Vacuum

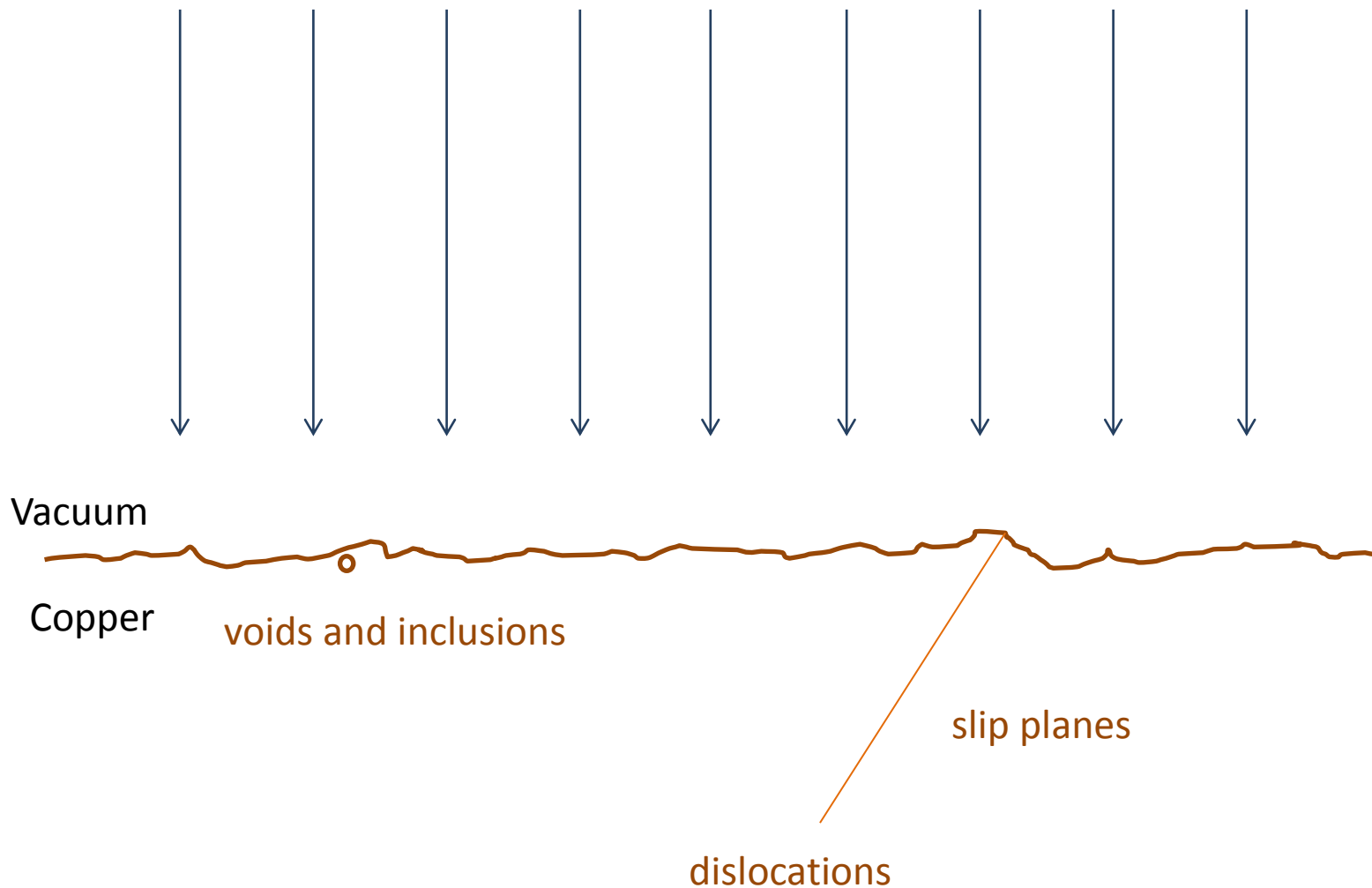
Copper



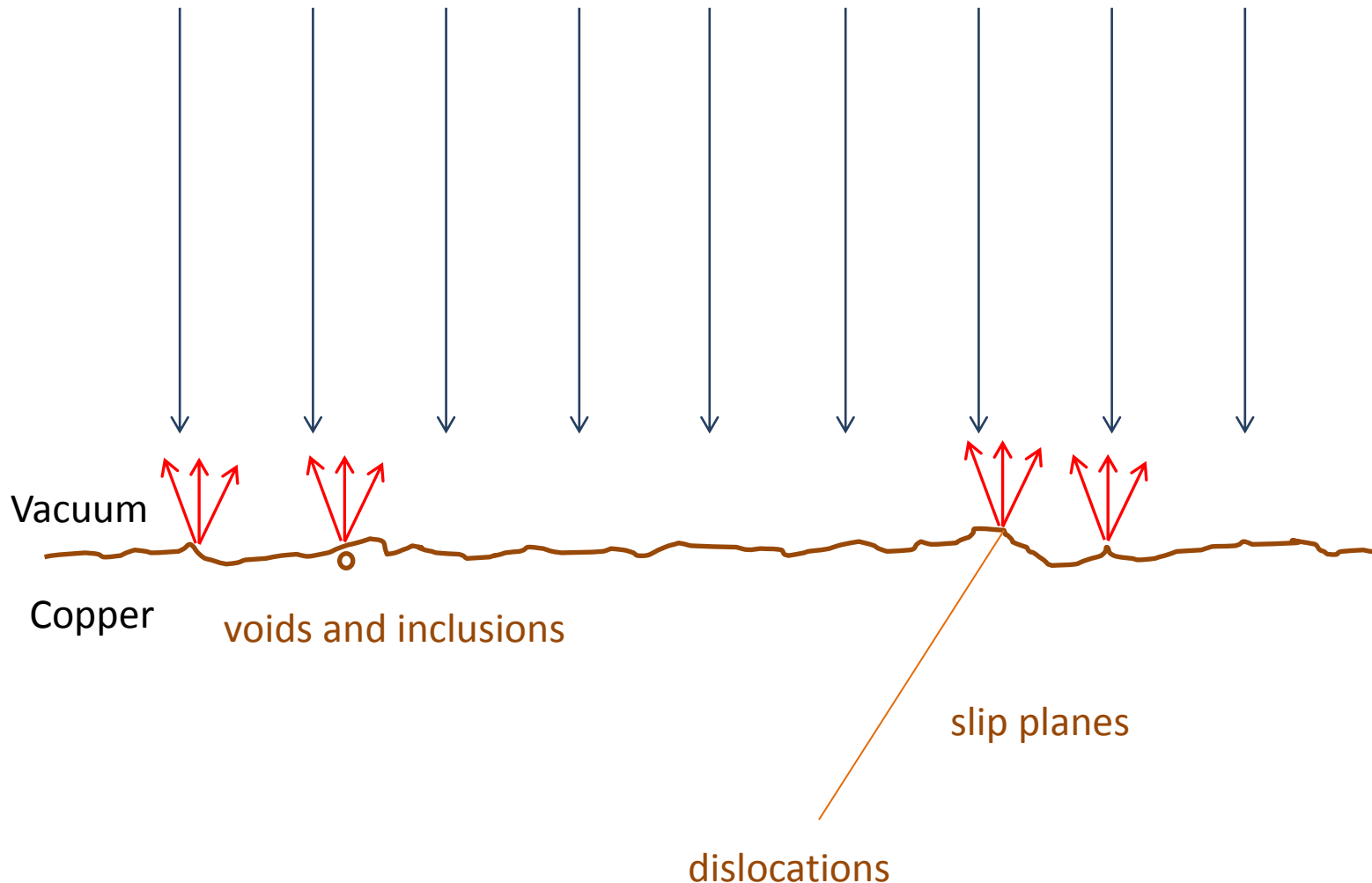
And the material below the surface isn't perfect either



Add an external electric field, around 200 MV/m. Surface charges re-arrange themselves in fs.

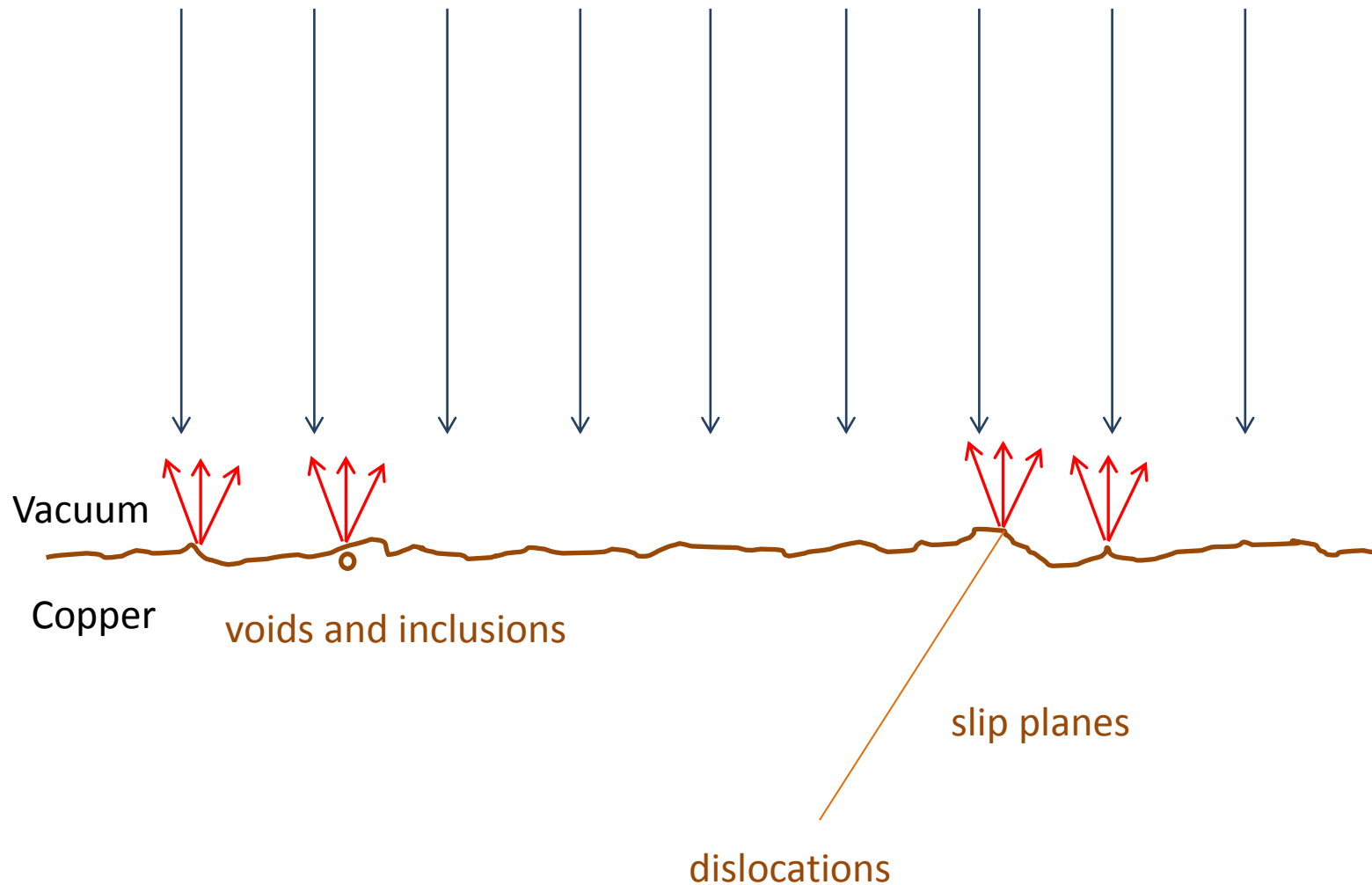


Field emission current flows from metal into vacuum (Fowler-Nordheim) from local areas ($O[10 \text{ nm}]$) of geometrical field enhancement and low local work function. There is a local field enhancement β of around 50-100. The total current from something like 0.1 mm^2 is a nanoAmp.

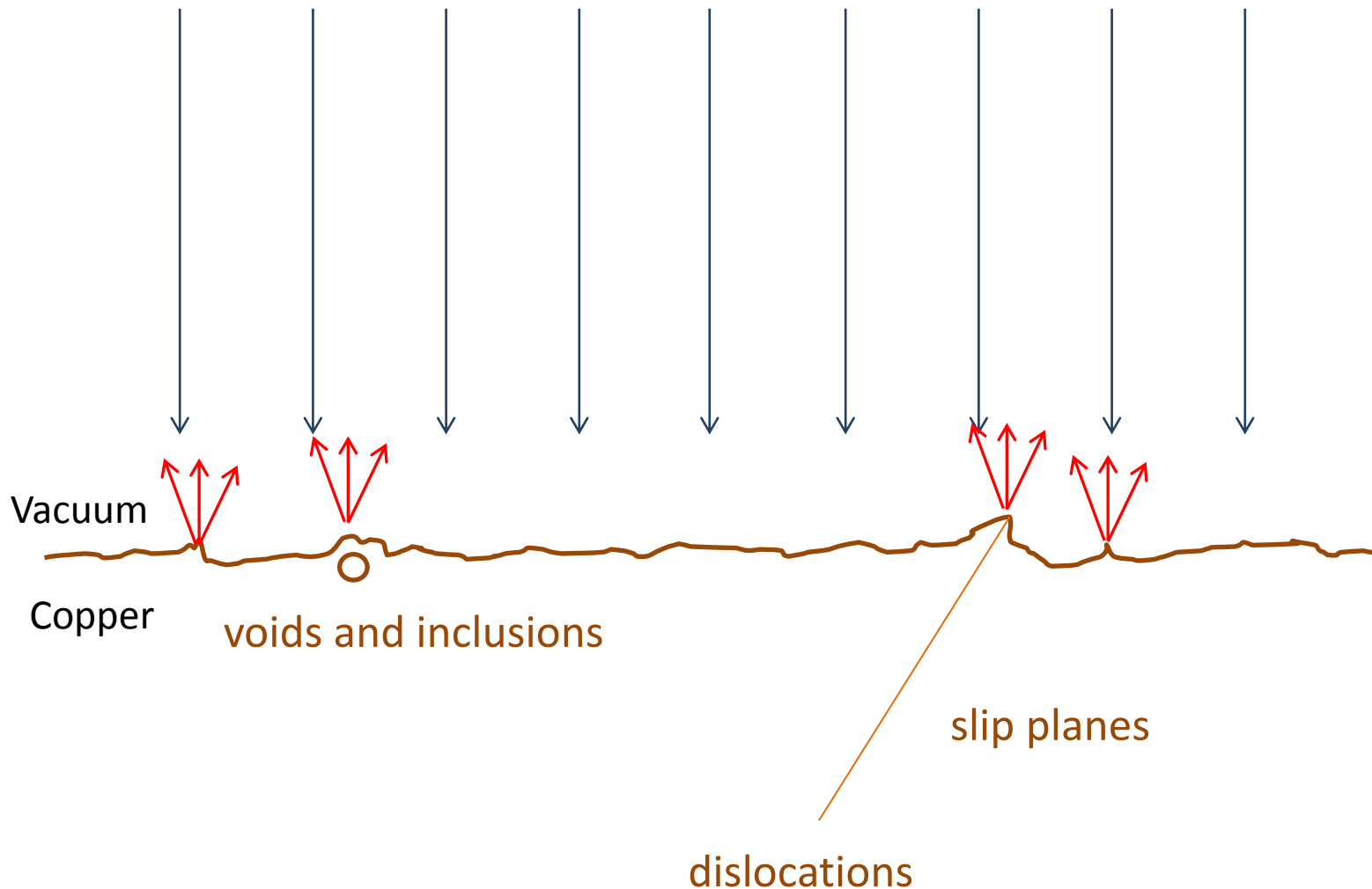


Note: Identifying the weak points is a crucial, unresolved research issue.

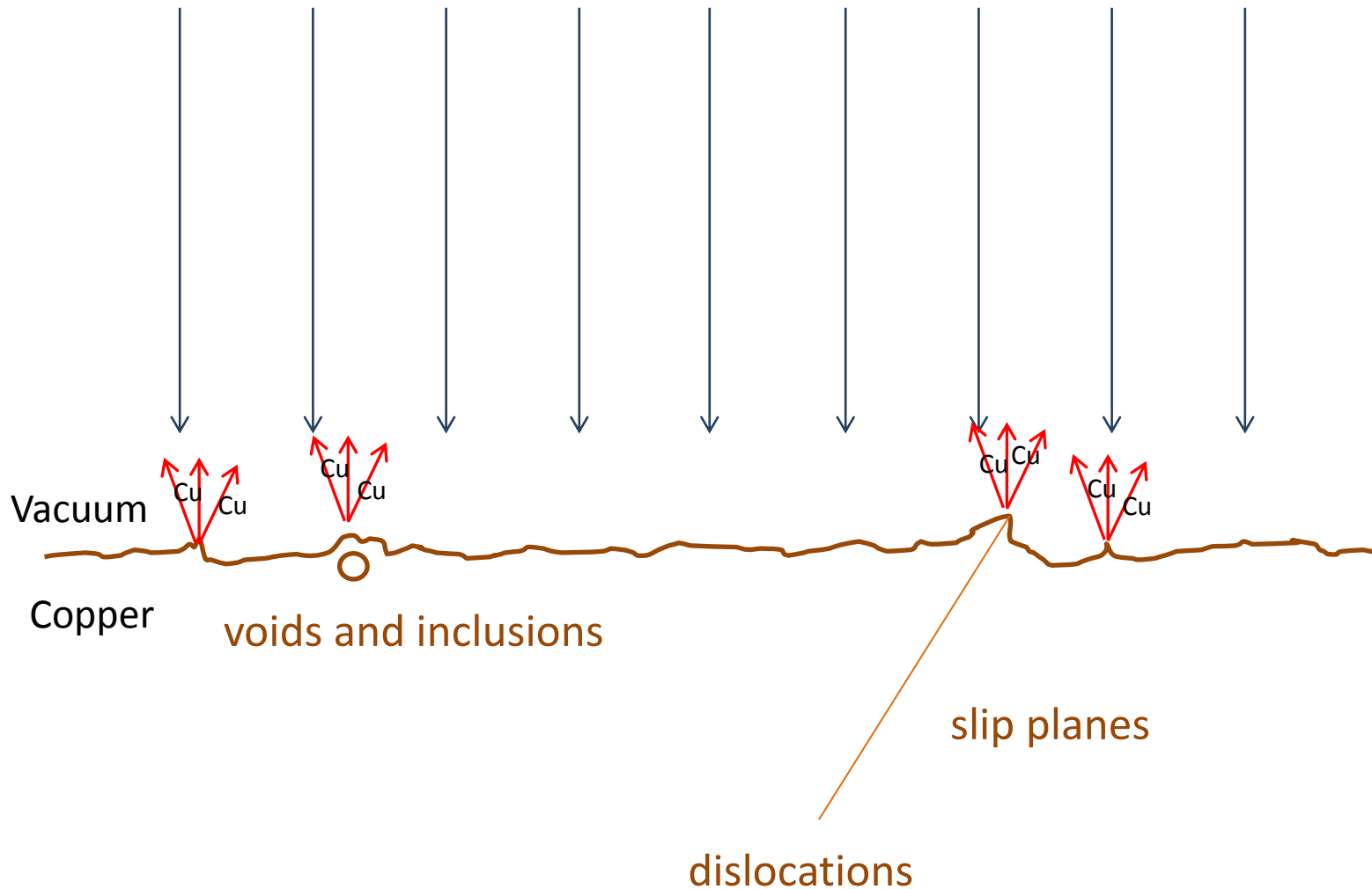
The external electric field causes a tensile stress and field emission current while still in the metal causes thermal induced stresses so the material imperfections and surface features evolve.



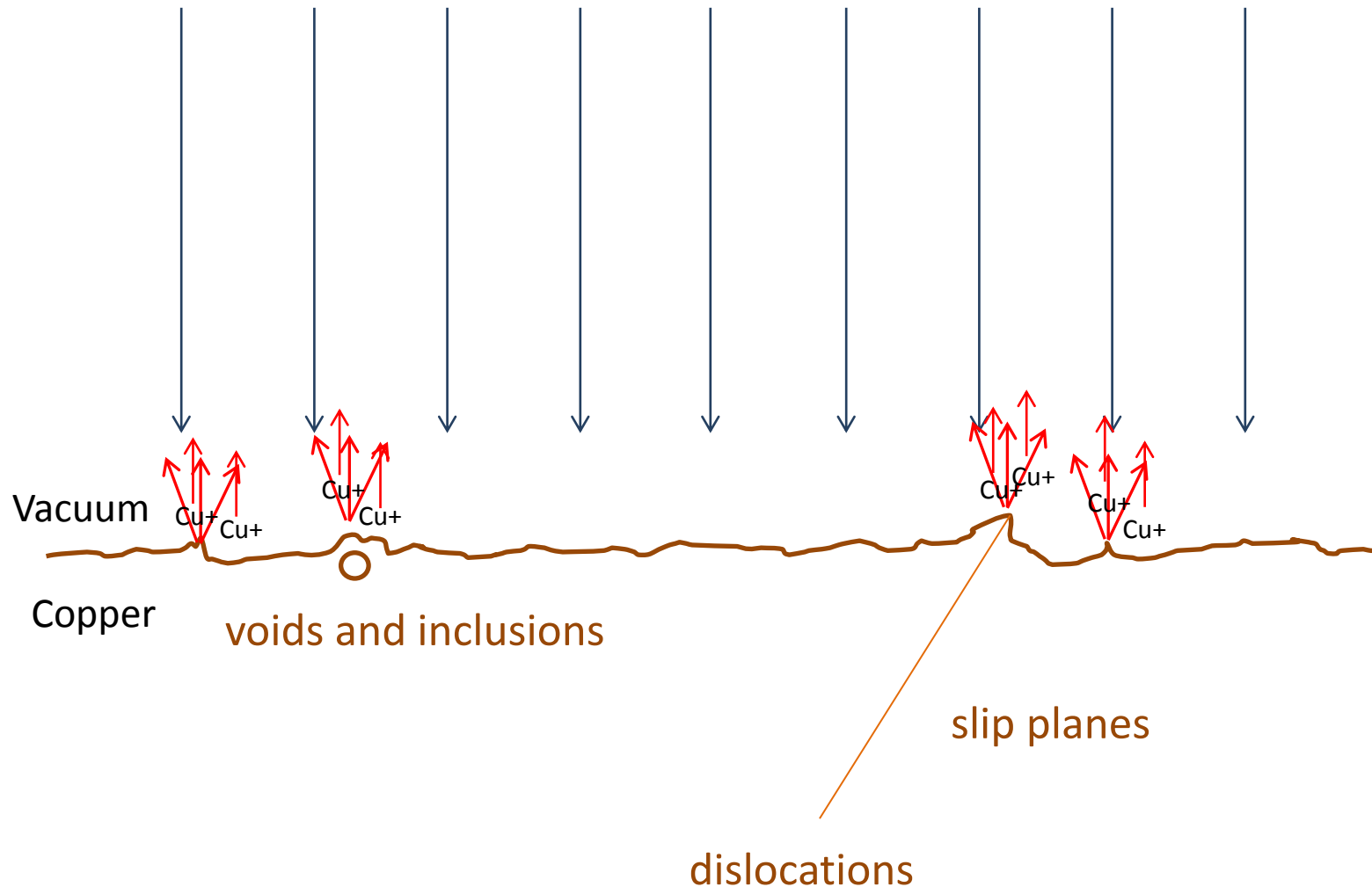
The external electric field causes a tensile stress and field emission current while still in the metal causes thermal induced stresses so the material imperfections and surface features evolve.



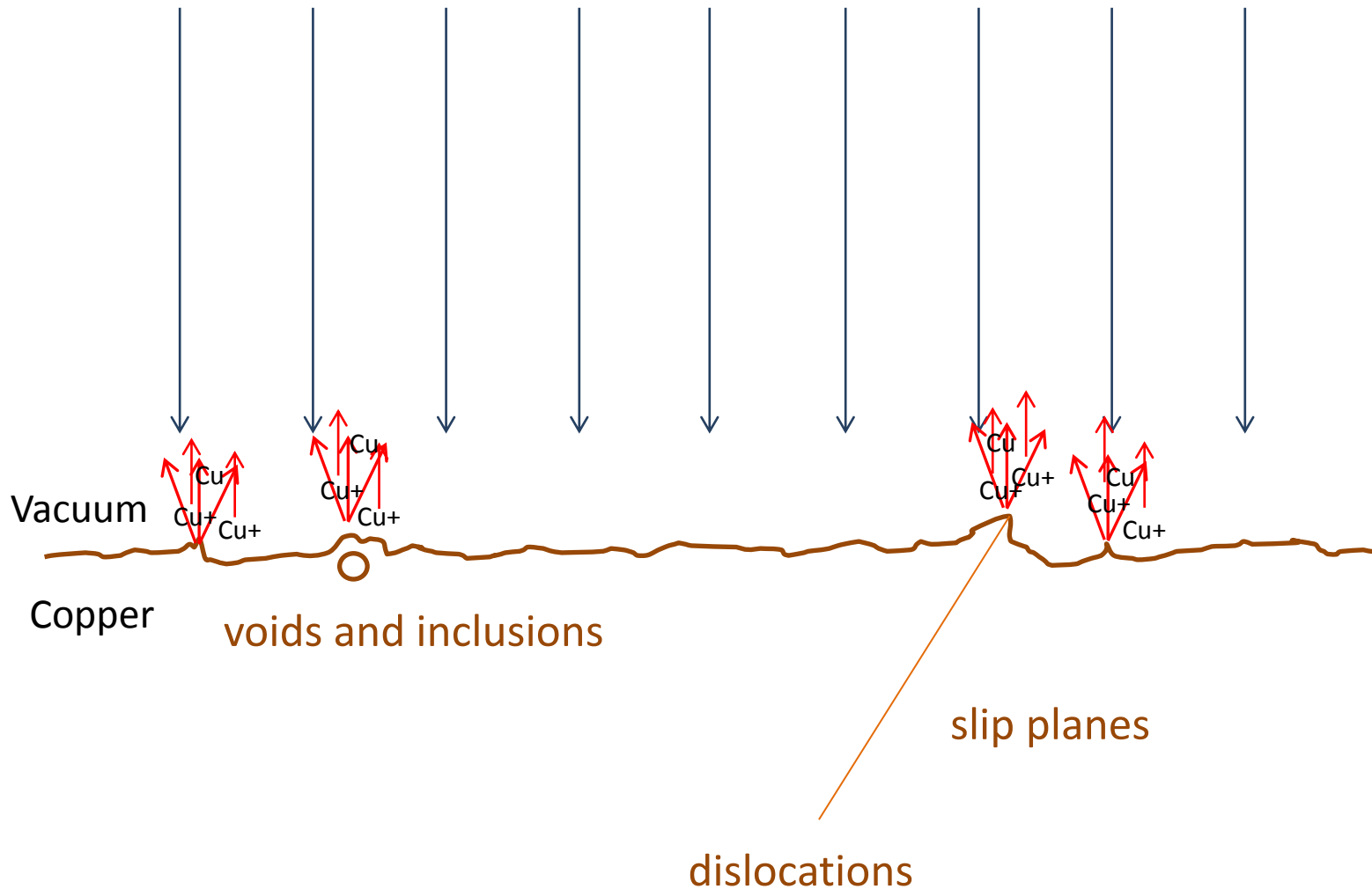
All the while, neutral copper atoms are coming off the surface field assisted evaporation.



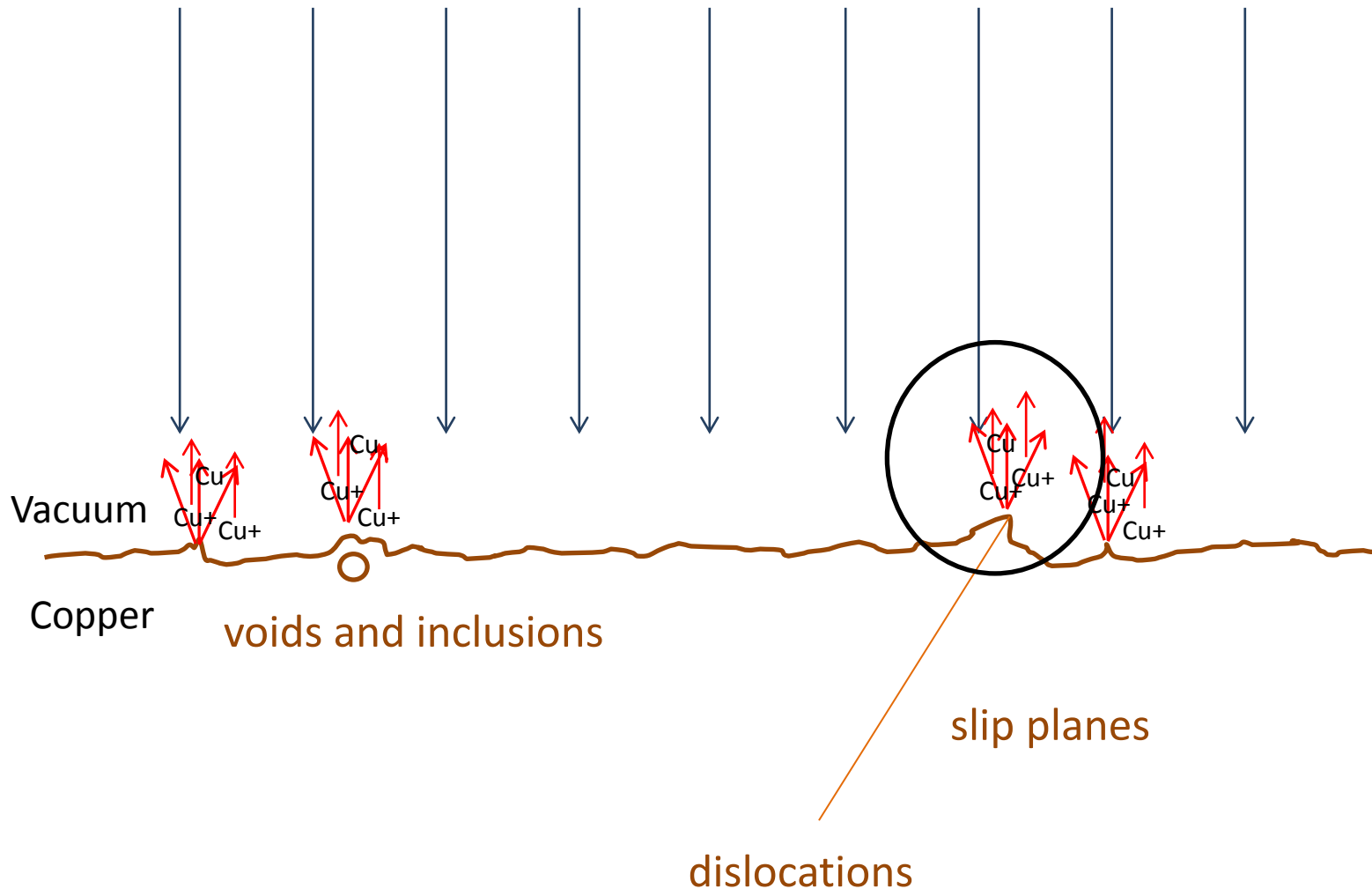
The copper atoms are ionized by the field emission current. the positively charged ions head to the surface and the electrons add to the emission current.



The copper ions hit the surface and sputter more copper in addition to that produced at by the original emission process.

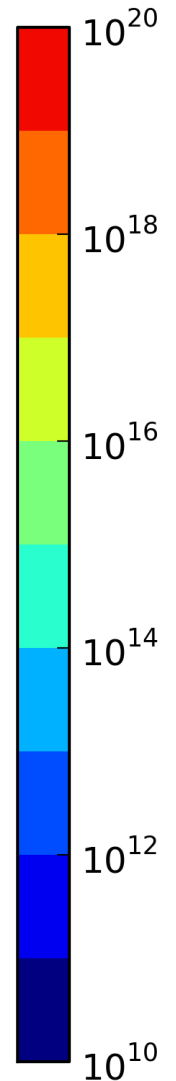
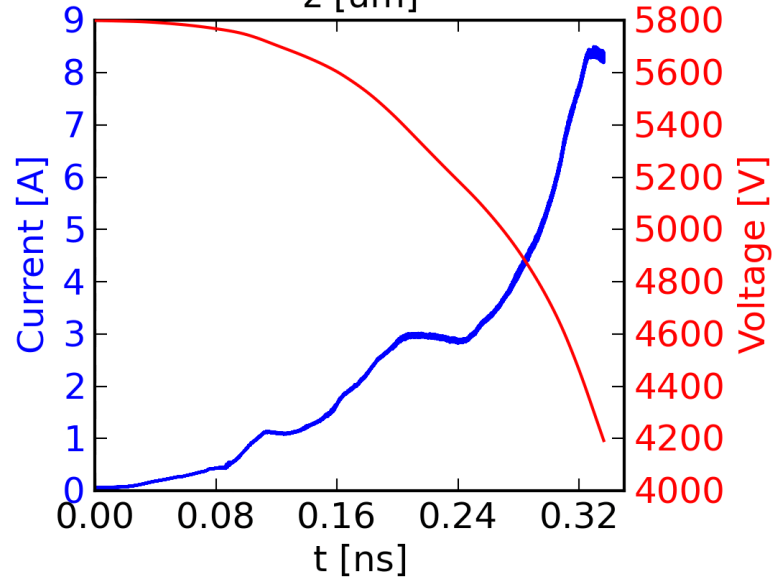
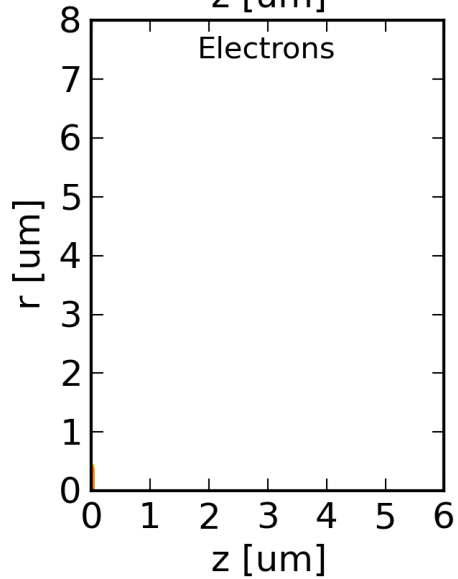
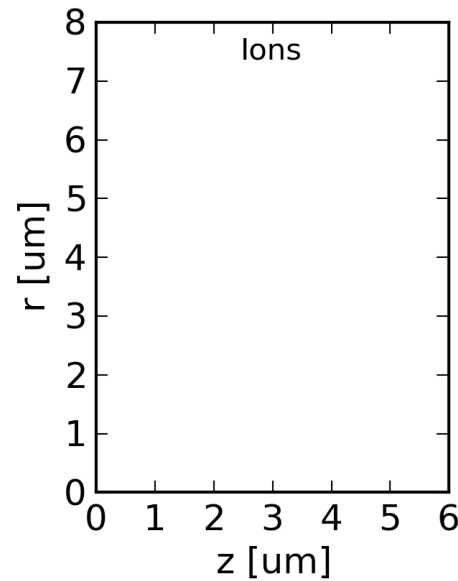
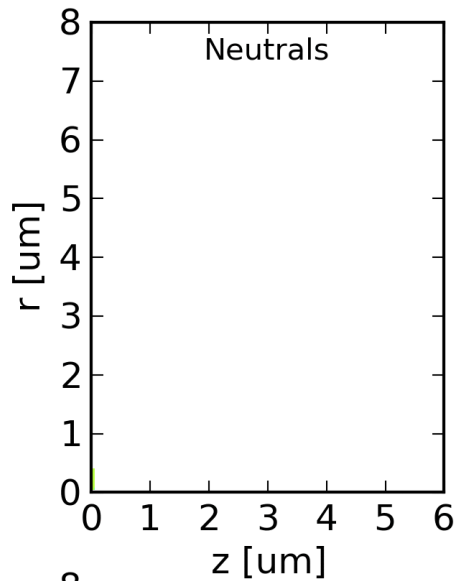


One of these emission points, on some rf or dc pulse, at some point passes a threshold and the process runs away. We will now switch to a computer simulation of the run-away process.



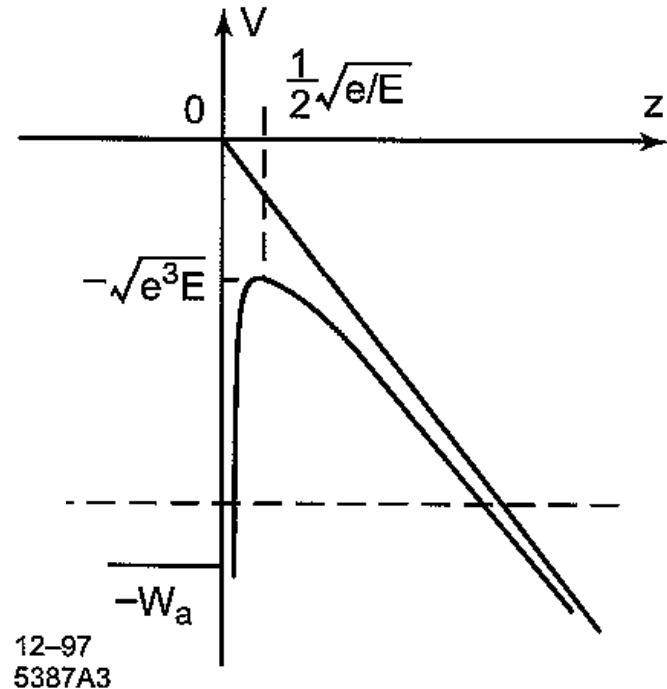
ArcPIC animation of breakdown turn-on by Kyrre Sjobaek

Densities, time = 0.000 [ns]



The surface potential used for solving the Fowler-Nordheim equation

$$V(z) = \begin{cases} -W_a & \text{for } z < 0 \\ -eEz - e^2/4z & \text{for } z > 0 \end{cases}$$



The Fowler-Nordheim equation (approximate, practical form)

$$I = A_e \frac{1.54 \times 10^6 \beta^2 E^2}{\varphi} e^{10.41 \varphi^{-1/2}} \times e^{-6.53 \times 10^3 \times \varphi^{3/2} / \beta E}$$
$$= \xi E^2 e^{-6.53 \times 10^3 \varphi^{3/2} / \beta E}$$

Units: $[I]=\text{A}$, $[E]=\text{MV/m}$, $[A_e]=\text{m}^2$, $[\varphi]=\text{eV}$ and $[\beta]=\text{dimensionless}$

Values: $\varphi = 4.5 \text{ eV}$ for copper

The Fowler-Nordheim equation

Analyzing real data

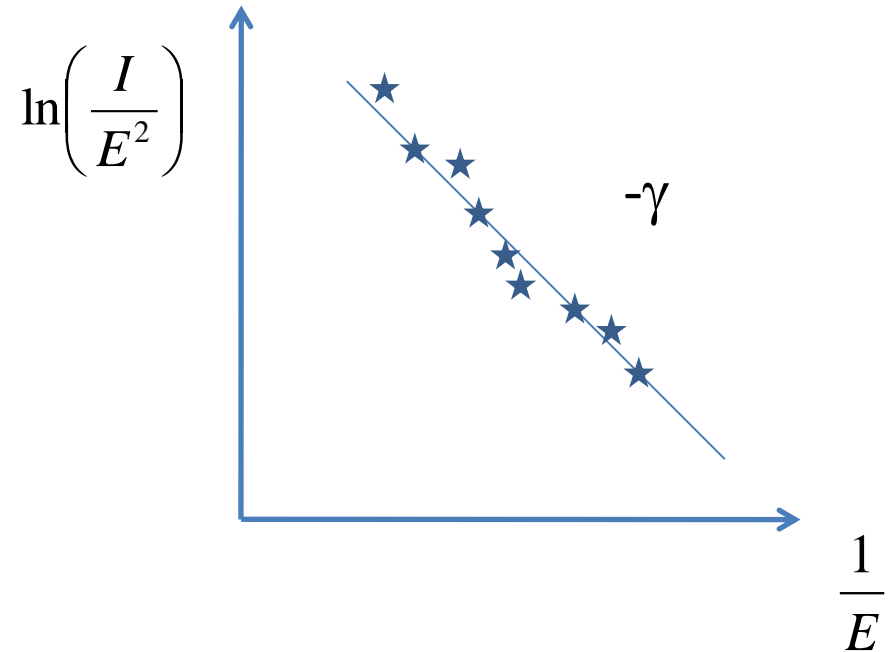
$$I = \xi E^2 e^{-\gamma/E}$$



$$\ln\left(\frac{I}{E^2}\right) = \ln(\xi) - \frac{\gamma}{E}$$

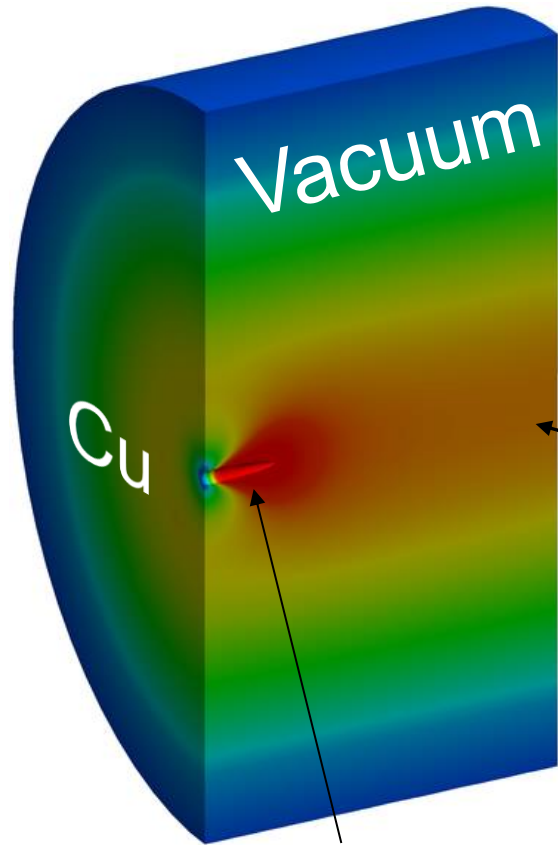
$$\beta = \frac{6.53 \times 10^3 \varphi^{3/2}}{\gamma}$$

$$\xi = A_e \frac{1.54 \cdot 10^6 \beta^2}{\varphi} \exp(10.41 \cdot \varphi^{-1/2})$$



You will have the opportunity to analyze a real set of data tonight for homework!

Effective Fowler-Nordheim Field Emission



Self-consistent effective FN field emission in RF and space charge fields using Pic3P

RF surface field map computed with Omega3P
(then driven at $f=12$ GHz)

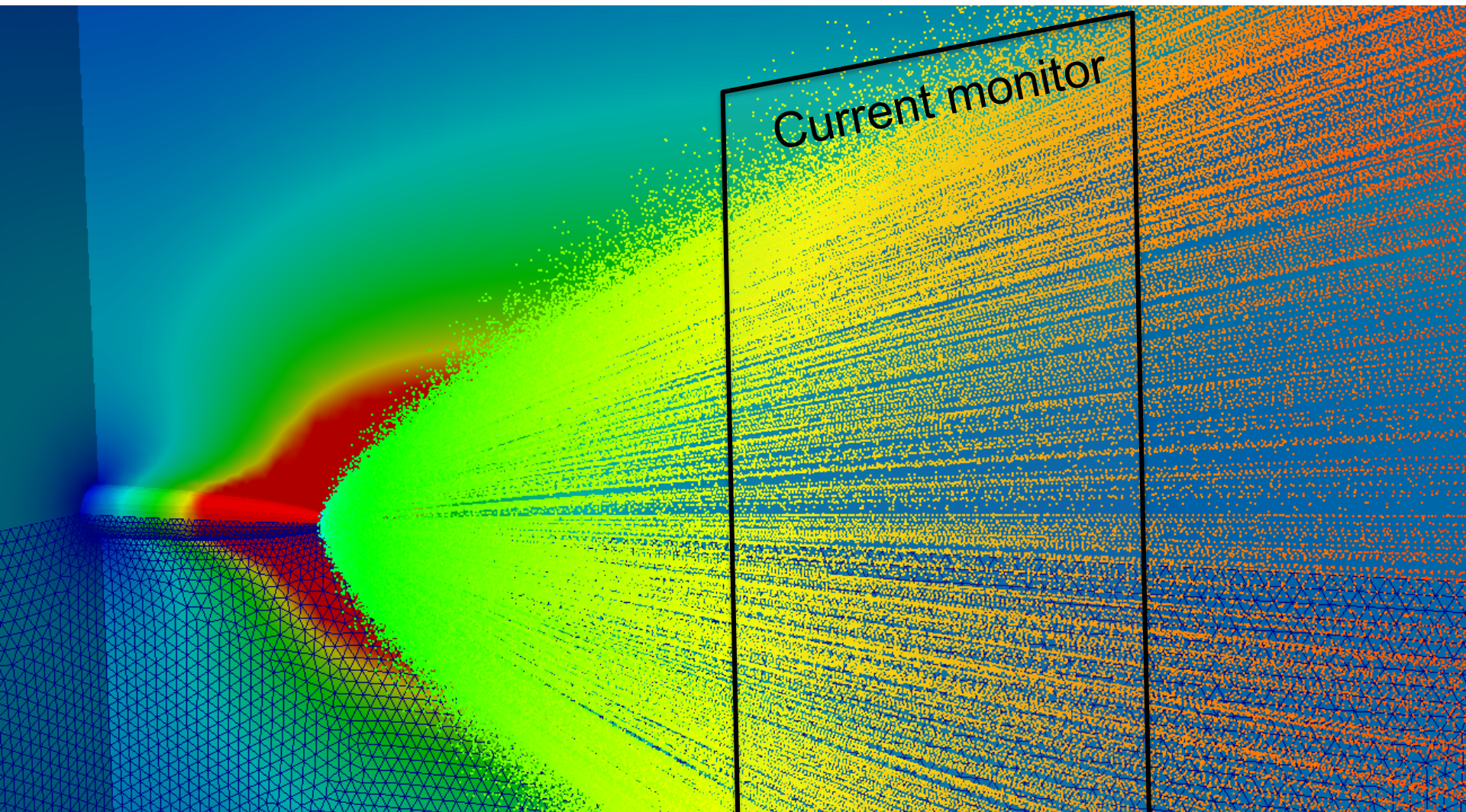
Assumptions:

- 200 MV/m surface fields ($E_{acc}=100$ MV/m)
- Tip does not change (fixed $\beta=50$)
- No transport phenomena
- No heating effects
- Particles emitted without energy spread

Single microscopic Cu tip protruding from surface of RF structure, RF field shown ($|E|$)

maximum emission current can be limited to simulate “self-healing” of sharp protrusions (realistic?)

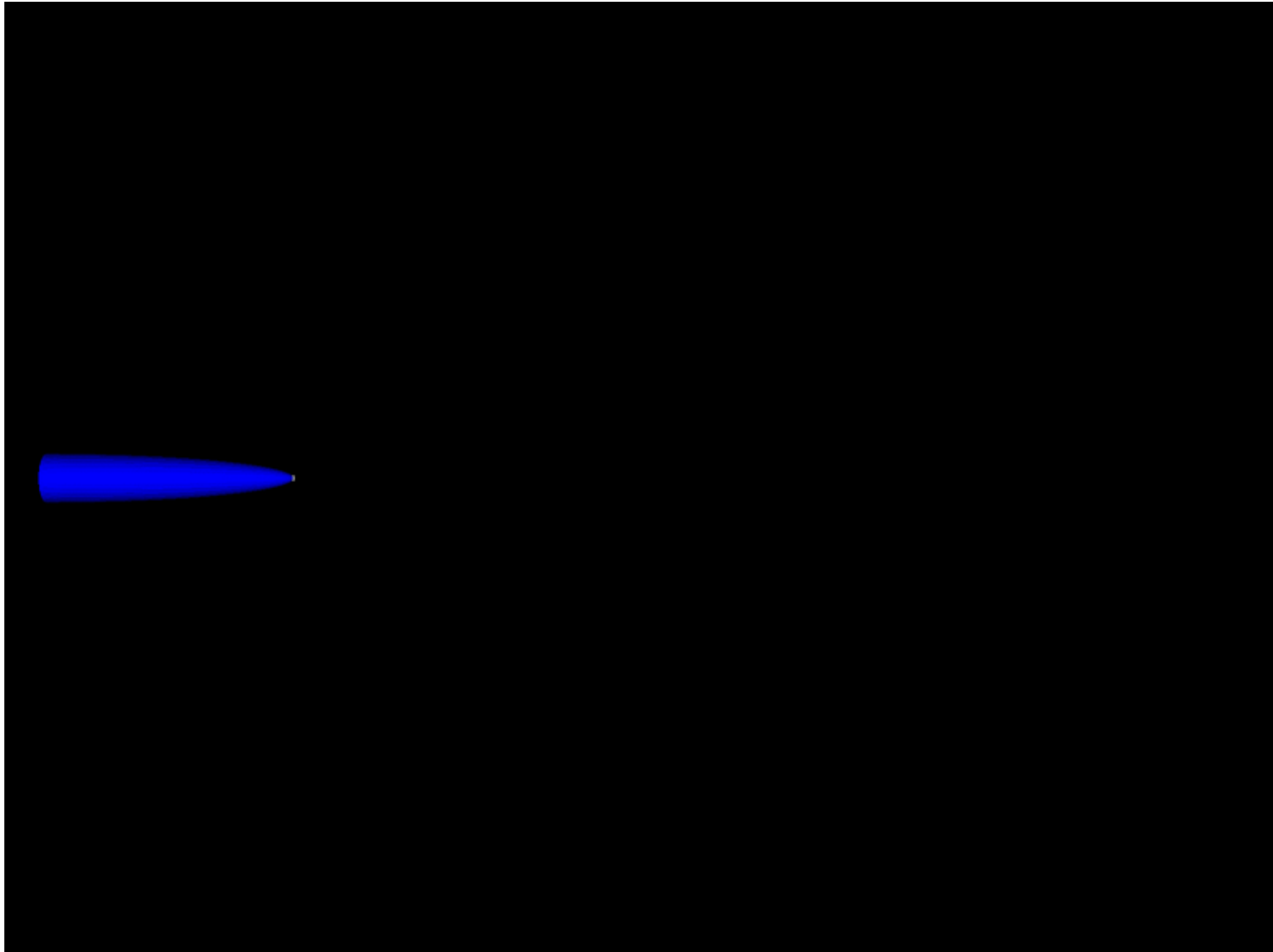
Pic3P Field Emitter Space-Charge Modeling



space-charge field $|E|$ in vertical symmetry plane
electrons colored by momentum

Space-Charge Fields (Contours of $|E|=\text{const}$)

(Case 2)



red: $|E| > 1$ MV/m, max: ~ 2.5 GV/m



Field emitter observed in Chamonix, France. MeVArc mini-school on rf acceleration.

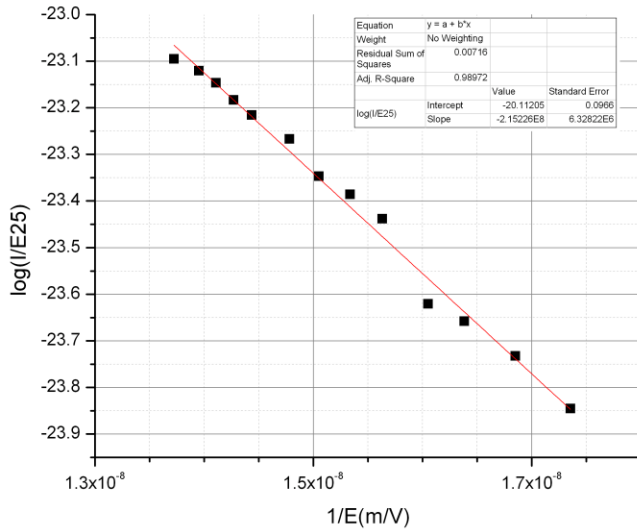
Electron emission

Fowler Nordheim Law (RF fields):

$$I_{\text{FN}}(\beta, \phi_0, A_e, E_0)$$

$$\bar{I} = \frac{5.79 \times 10^{-12} \exp(9.35 \phi_0^{-0.5}) A_e (\beta E_0)^{2.5}}{\phi_0^{1.75}} \exp\left(\frac{-6.53 \times 10^9 \phi_0^{1.5}}{\beta E_0}\right)$$

1. High field enhancements (β) can field emission.
2. Low work function (ϕ_0) in small areas can cause field emission.



typical picture →
geometric perturbations (β)

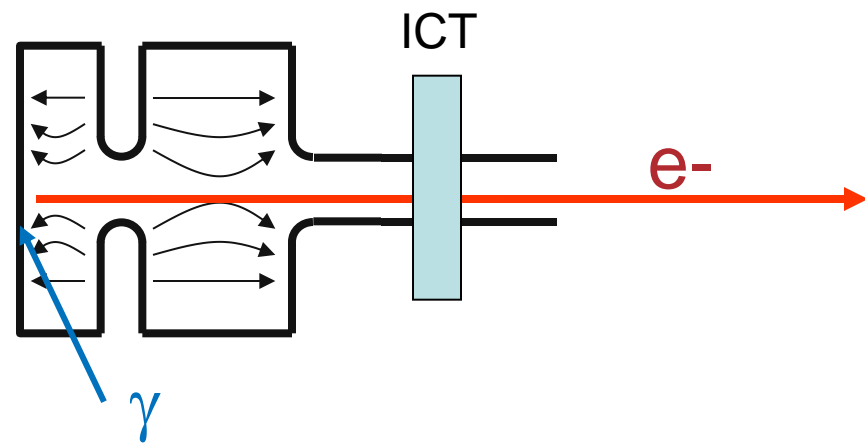
alternate picture →
material perturbations (ϕ_0)



(suggested by Wuensch and colleagues)

Schottky Enabled Photo-electron Emission Measurements

Data 2010-10-04
First results
from Tsinghua



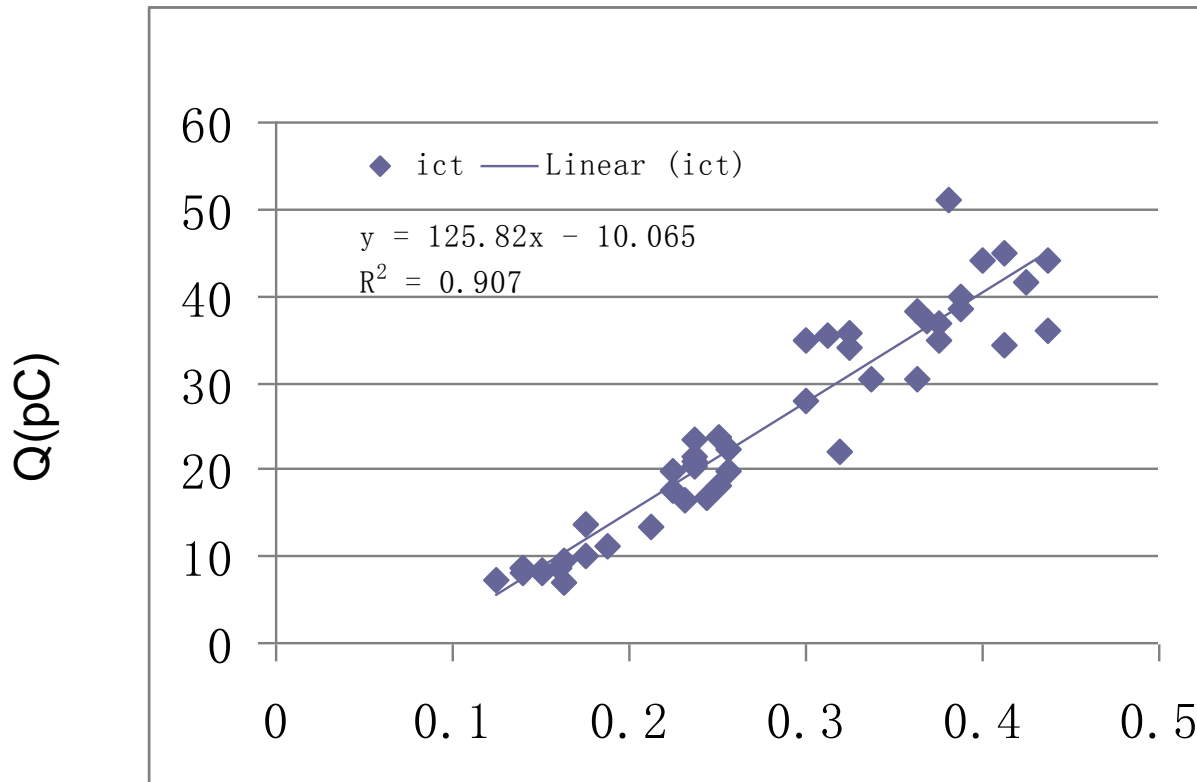
■ Experimental parameters

- work function of copper = $\phi_0 = 4.65$ eV
- energy of $\lambda=400\text{nm}$ photon = $h\nu = 3.1$ eV
- Laser pulse length
 - Long = 3 ps
 - Short = 0.1 ps
- Laser energy ~1 mJ (measured before laser input window)
- Field (55 – 70 MV/m)

Should not get photoemission

→ Long Laser Pulse (~ 3ps)

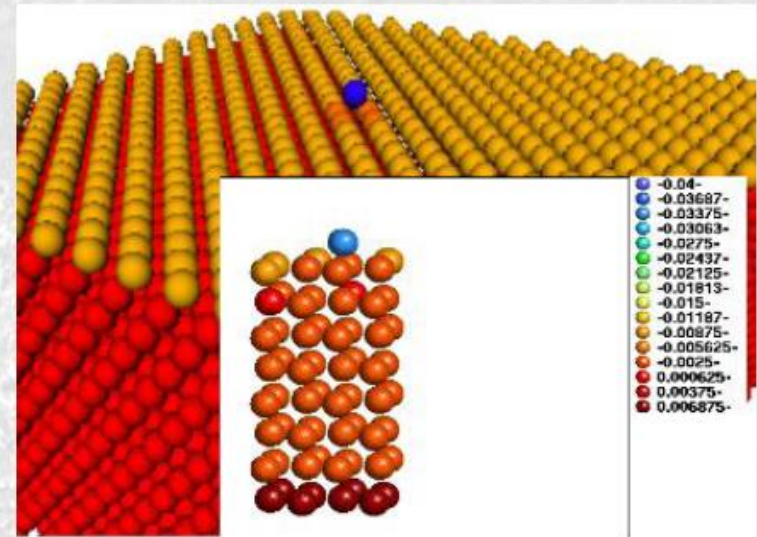
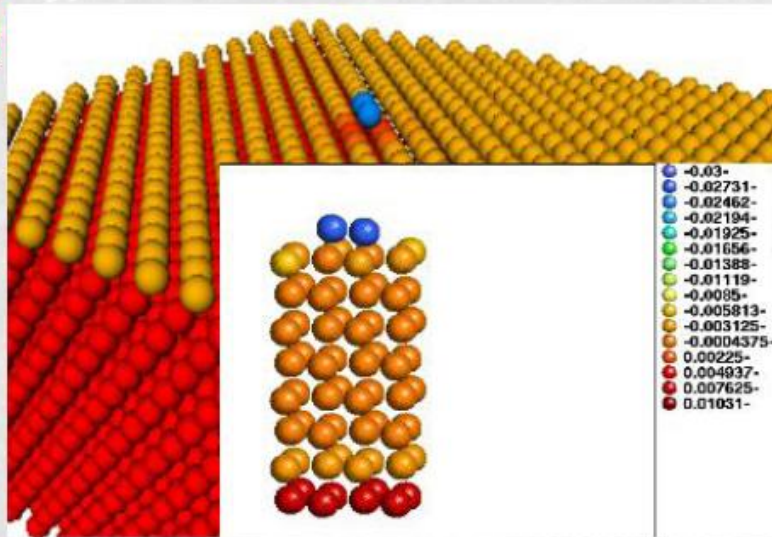
→ $E=55 \text{ MV/m}$ @ injection phase=80 → $55\sin(80)=54$



$Q \propto I$
single photon emission

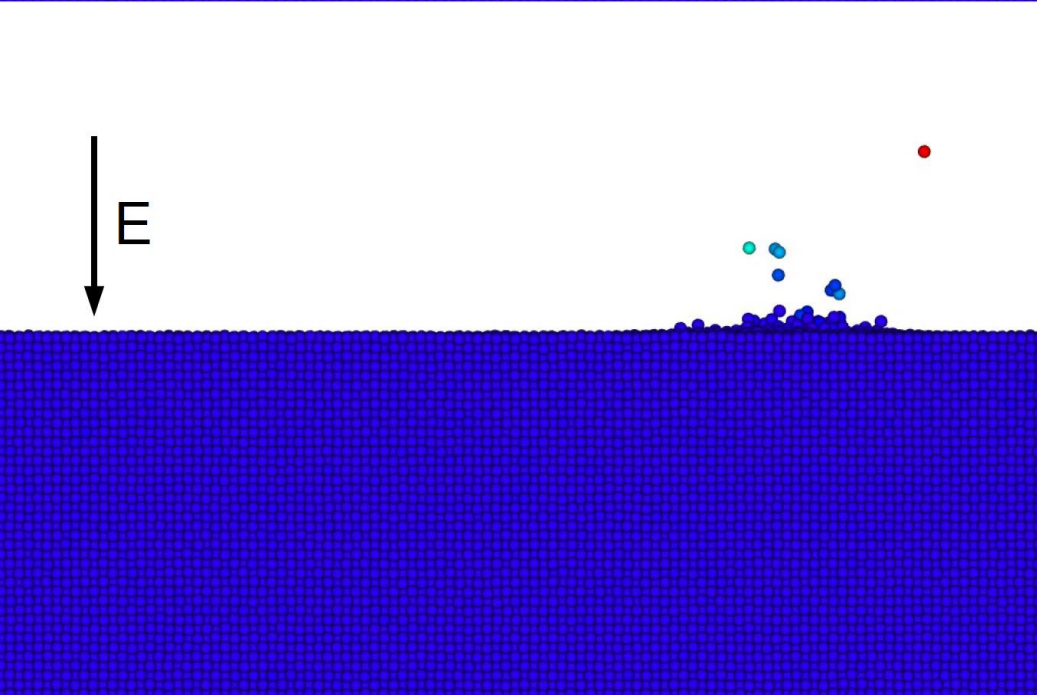
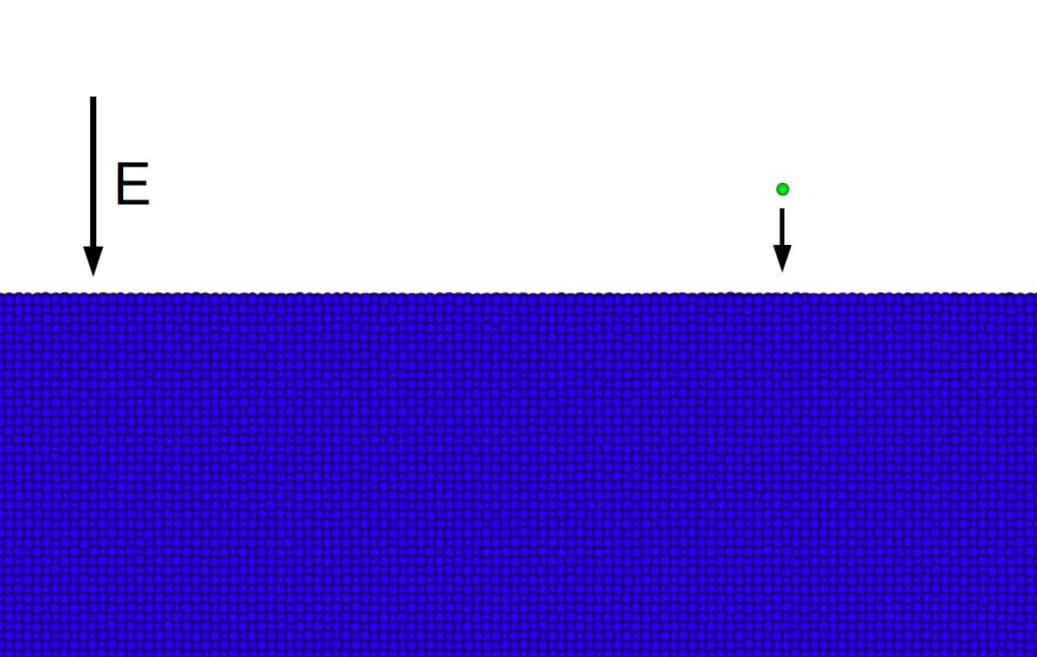
laser energy (mJ)
photocathode input window

Results of the recent work



	Single adatom		Two adatoms	
	DFT	ED-MD	DFT	ED-MD
Partial Charge, q_e	-0.032	-0.0215	-0.025	-0.0177

	Flat surface		Surface with one adatom
	present DFT	experiment [16]	
Work function, eV	4.61	4.46 ± 0.03	4.30



Molecular Dynamics Simulations of Ion Irradiation of a Surface under an Electric Field

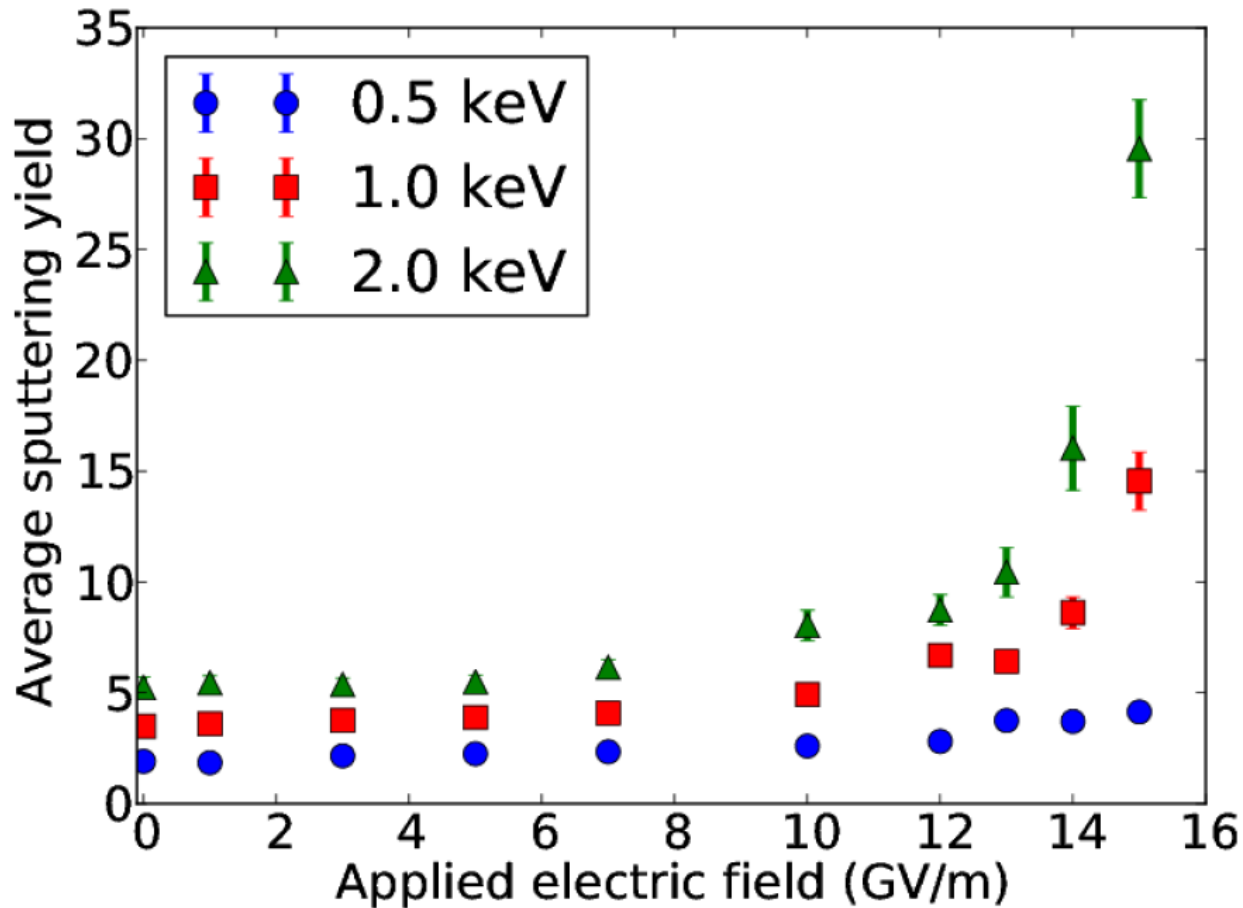
S. Parviainen, F. Djurabekova

HELSINGIN YLIOPISTO
HELSINGFORS UNIVERSITET
UNIVERSITY OF HELSINKI

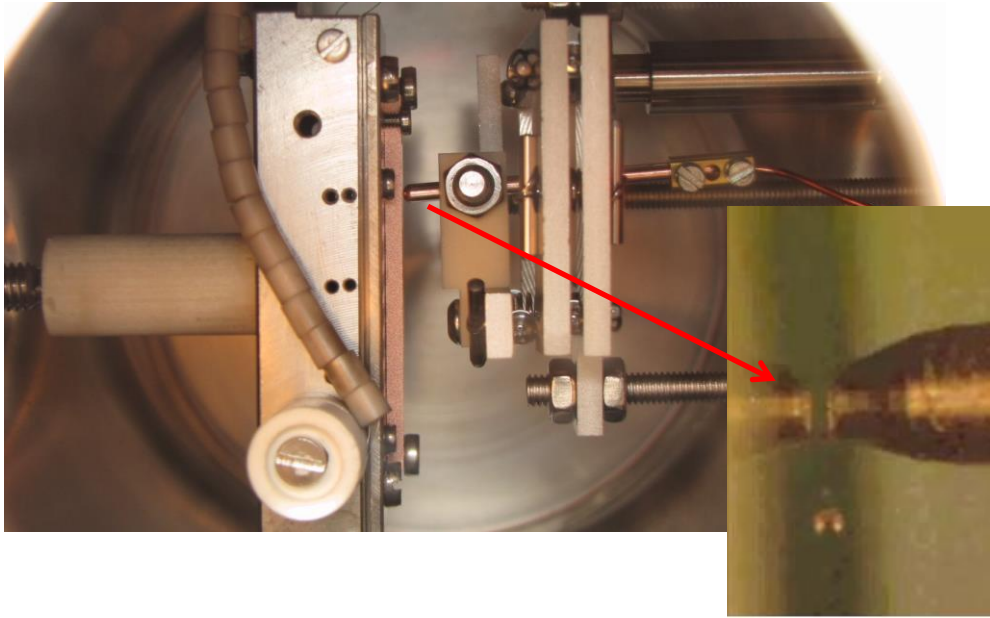
www.helsinki.fi/yliopisto



Sputtering yield vs. field



What are the CERN DC spark systems?



The CERN DC spark systems consist of an anode and cathode in a rod-plane geometry in ultrahigh vacuum. I will be talking about system I which is powered by the High-Rep-Rate circuit.

The gap size can be varied from 0-100 μ m by using a stepper motor. It is possible to monitor and actively control the gap with an accuracy of \sim 1.5 μ m.

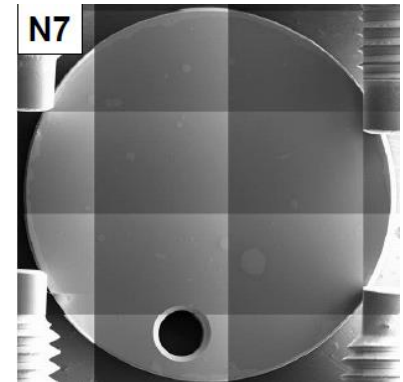
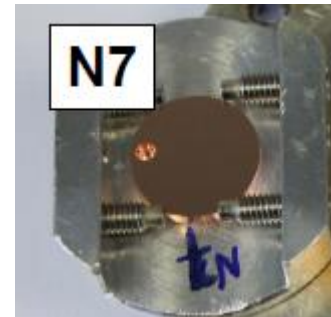
The diameter of the anode is 2.3mm and has a hemispherical tip.

High voltage is applied across the electrodes and the resulting current and voltage waveforms are analysed (largely automatically) and recorded.

The cathodes have a good surface quality.

From these we can tell whether a BD occurred and measure several properties of the BD such as the turn on time, the position of the BD within the pulse, the burning voltage and even the gap distance!

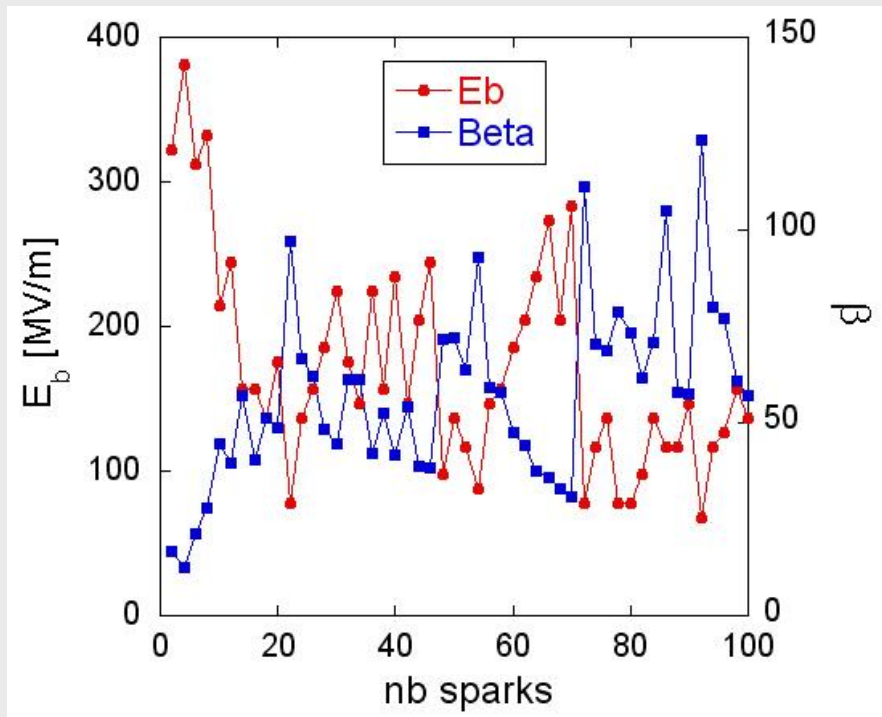
We are not currently able to measure the field enhancement factor β , with this setup however.



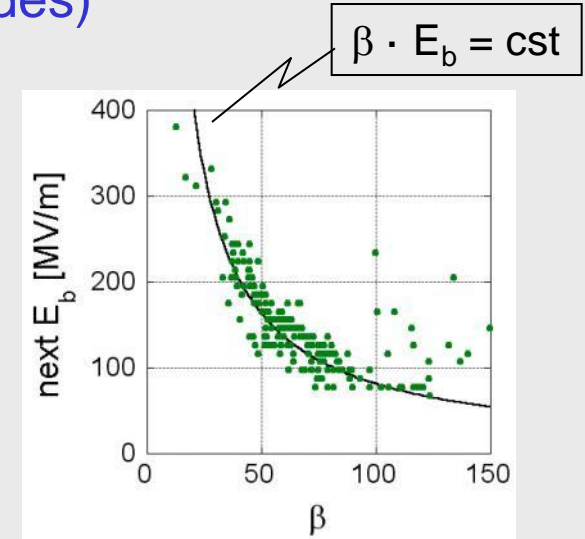
N. Shipman

Evolution of β & E_b during conditioning experiments

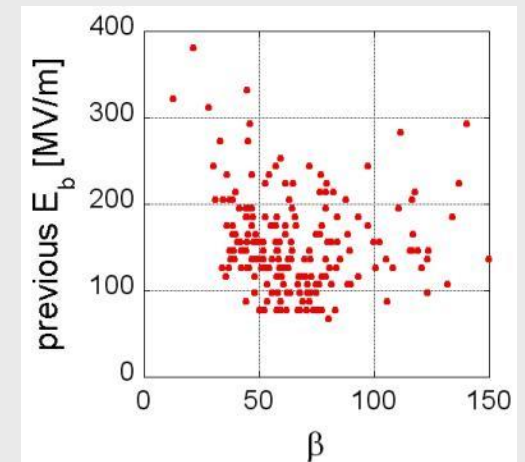
- Measurements of β after each sparks (Cu electrodes)



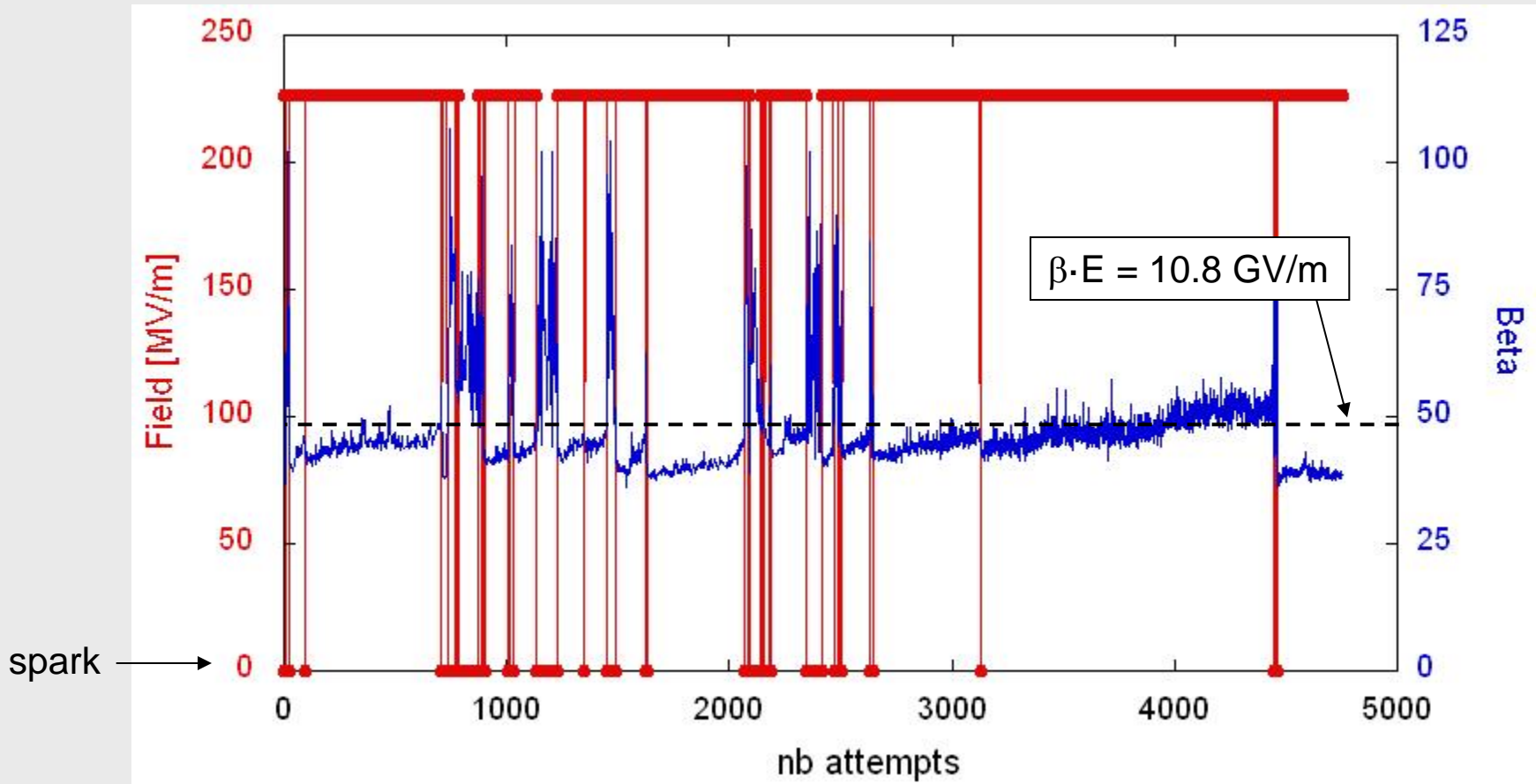
$\beta \leftrightarrow$ next E_b
correlation



$\beta \leftrightarrow$ previous E_b
no correlation



Evolution of β during BDR measurements (Cu)



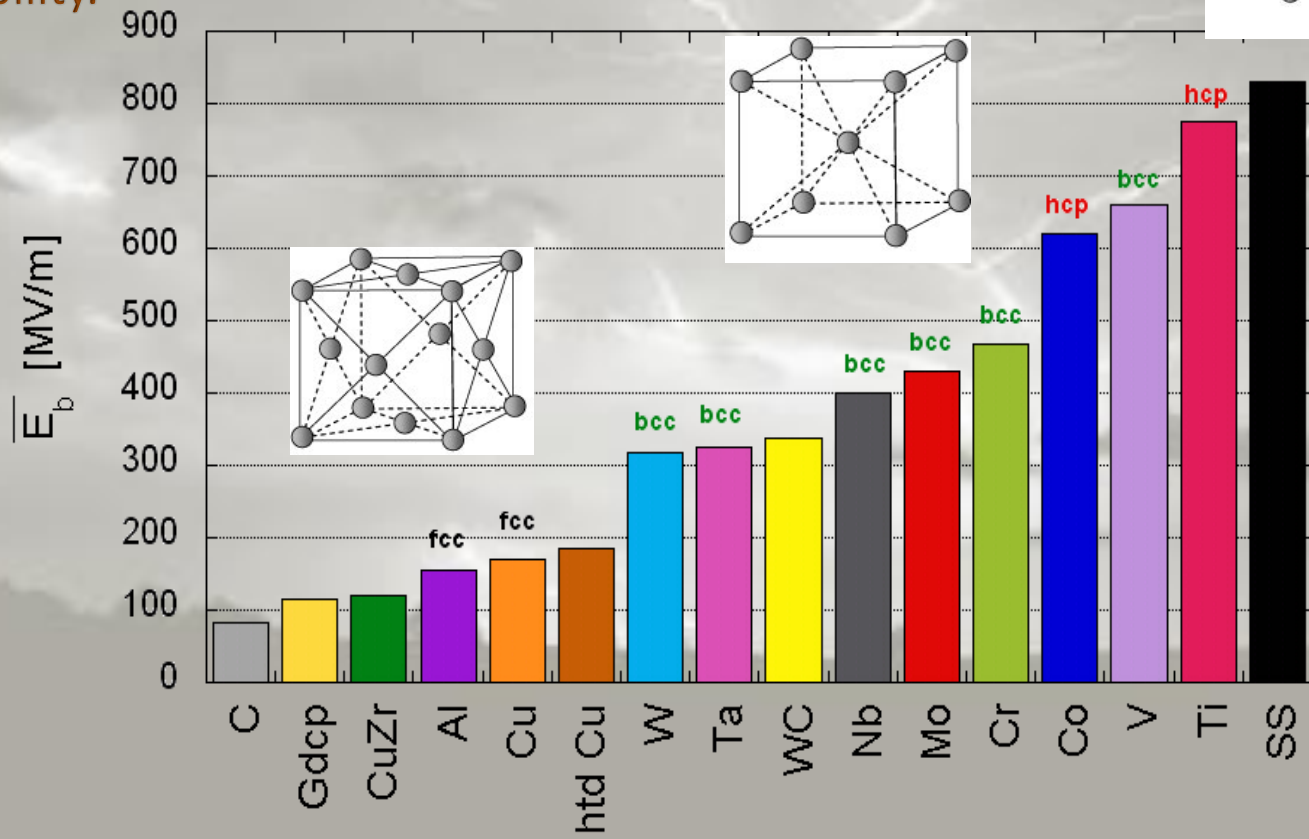
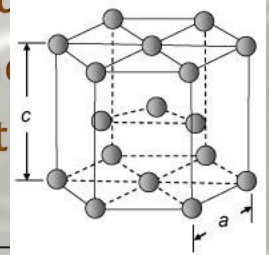
- breakdown as soon as $\beta > 48$ ($\leftrightarrow \beta \cdot 225 \text{ MV/m} > 10.8 \text{ GV/m}$)
- consecutive breakdowns as long as $\beta > \beta_{\text{threshold}}$

→ length and occurrence of breakdown clusters \leftrightarrow evolution of β

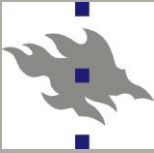


What are the field emitters? Why do we look for dislocations?

- The dislocation motion is strongly bound to the atomic structure of metals. In FCC (face-centered cubic) the dislocation are the most mobile and HCP (hexagonal close-packed) are the hardest for dislocation mobility.



A. Descoeur, F. Djurabekova, and K. Nordlund, DC Breakdown experiments with cobalt electrodes, CLIC-Note XXX, 1 (2010).



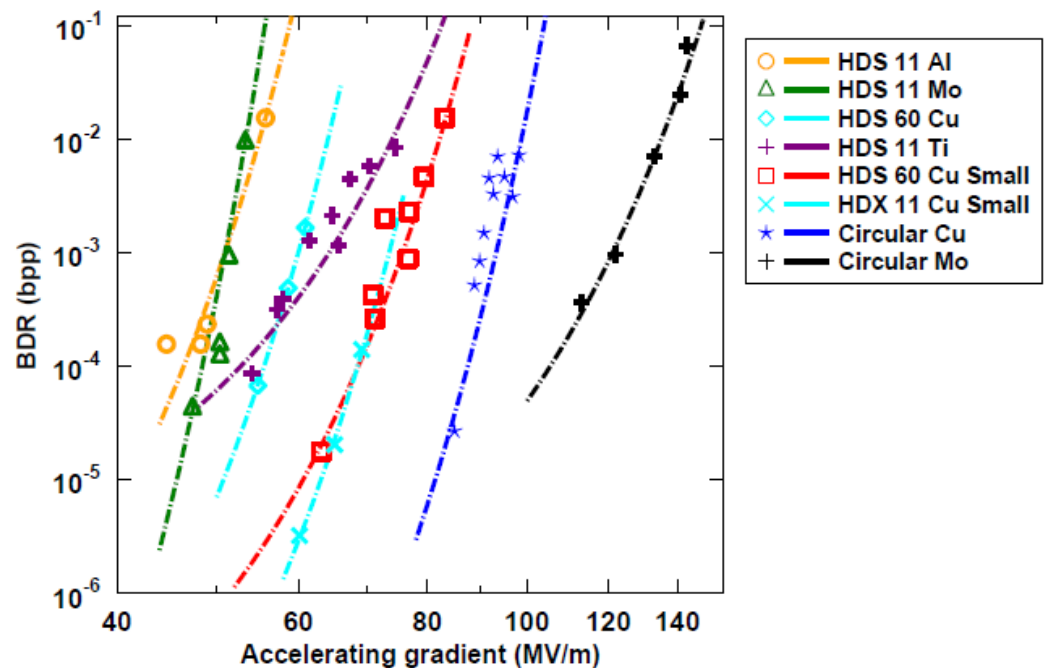
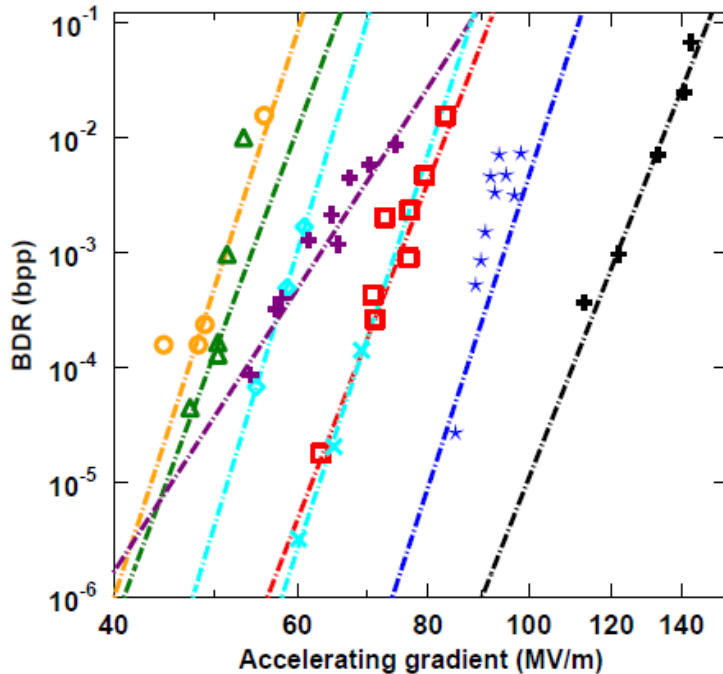
Dislocation-based model for electric field dependence

- Now to test the relevance of this, we fit the experimental data
- The result is:

$$BDR \propto BDR_0 e^{-\frac{(E^f - \epsilon_0 E^2 \Delta V)}{kT}} = A e^{-\frac{(E^f - \epsilon_0 E^2 \Delta V)}{kT}} = c_0 e^{-E^f / kT} e^{\epsilon_0 E^2 \Delta V / kT}$$

Power law fit

Stress model fit



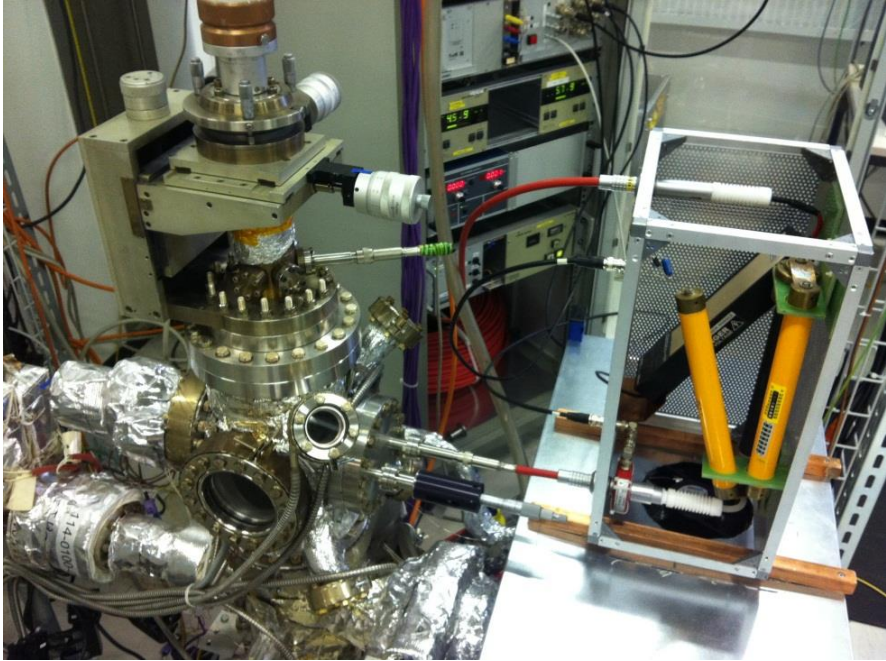
[W. Wuensch, public presentation at the CTF3, available online at <http://indico.cern.ch/conferenceDisplay.py?confId=8831.>] with the model.]

Summary of turn on times

Test	Frequency	Measurement	Result
Simulation dc spark			5-10 ns
New DC System	DC	Voltage Fall Time	7 ns
Swiss FEL (C-Band)	5.7GHz	Transmitted Power Fall Time	110 - 140ns
KEK T24 (X-Band)	12GHz	Transmitted Power Fall Time	20-40ns
CTF/TBTS TD24 (X-Band)	12GHz	Transmitted Power Fall Time	20-40ns
CTF SICA (S-Band)	3GHz	Transmitted Power	60-140ns

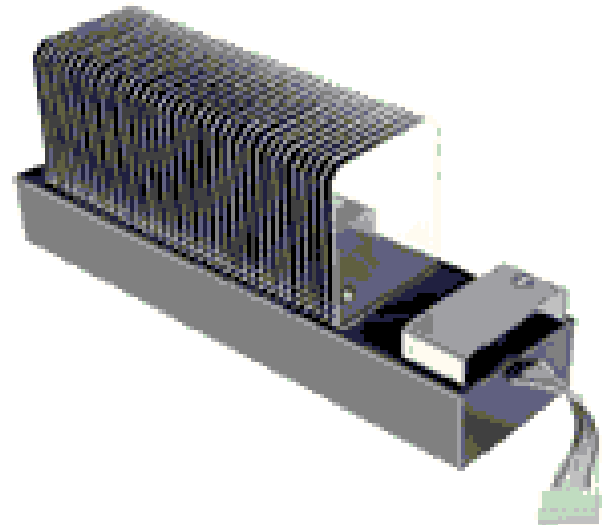
The turn on time could be related to the bandwidth of the structures or possibly the intrinsic size.

What is the High Rep Rate Circuit?



The picture above shows the HRR circuit. The metal box housing the switch is placed as close as possible to the vacuum chamber to minimise stray capacitance.

The HRR circuit uses a solid state switch to supply high voltage pulses (up to 10kV) at a rep rate of up to 1kHz. The energy is stored on a 200m/1us long coaxial cable.



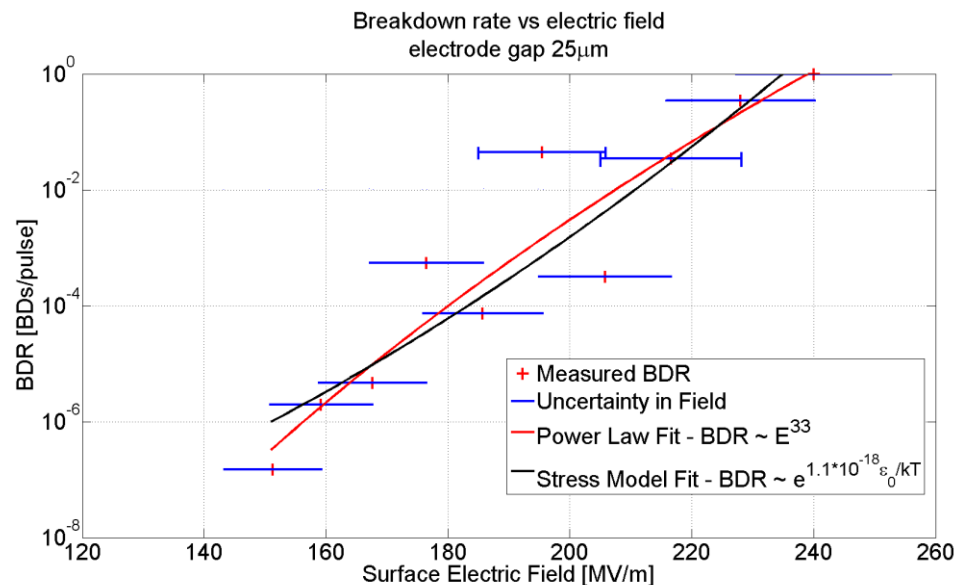
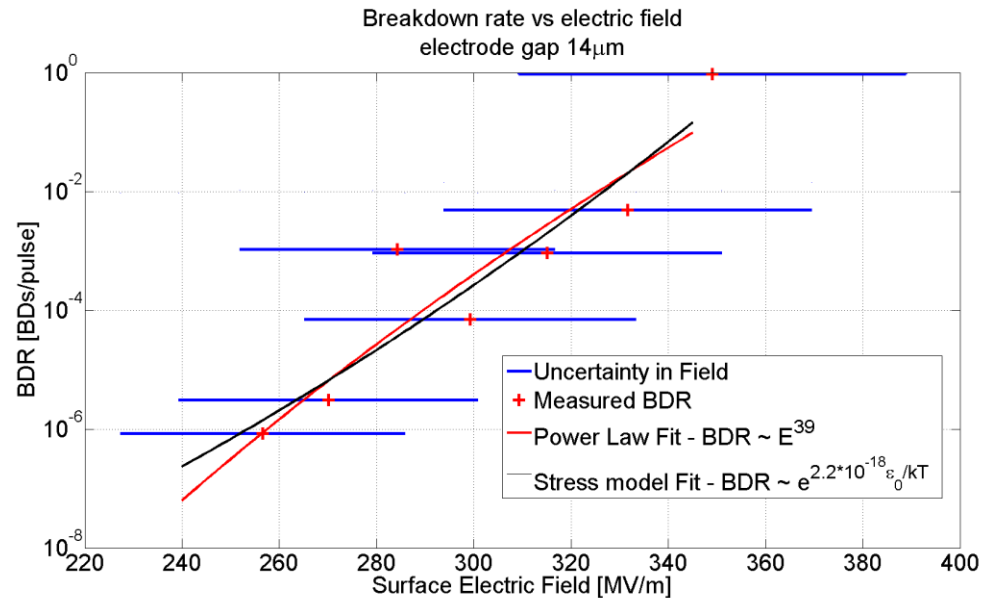
BDR vs E 14μm and 25μm gap

For each experiment the gap is first set to the required distance. Then the voltage is set at the highest value and the HRR circuit begins pulsing at 1000Hz.

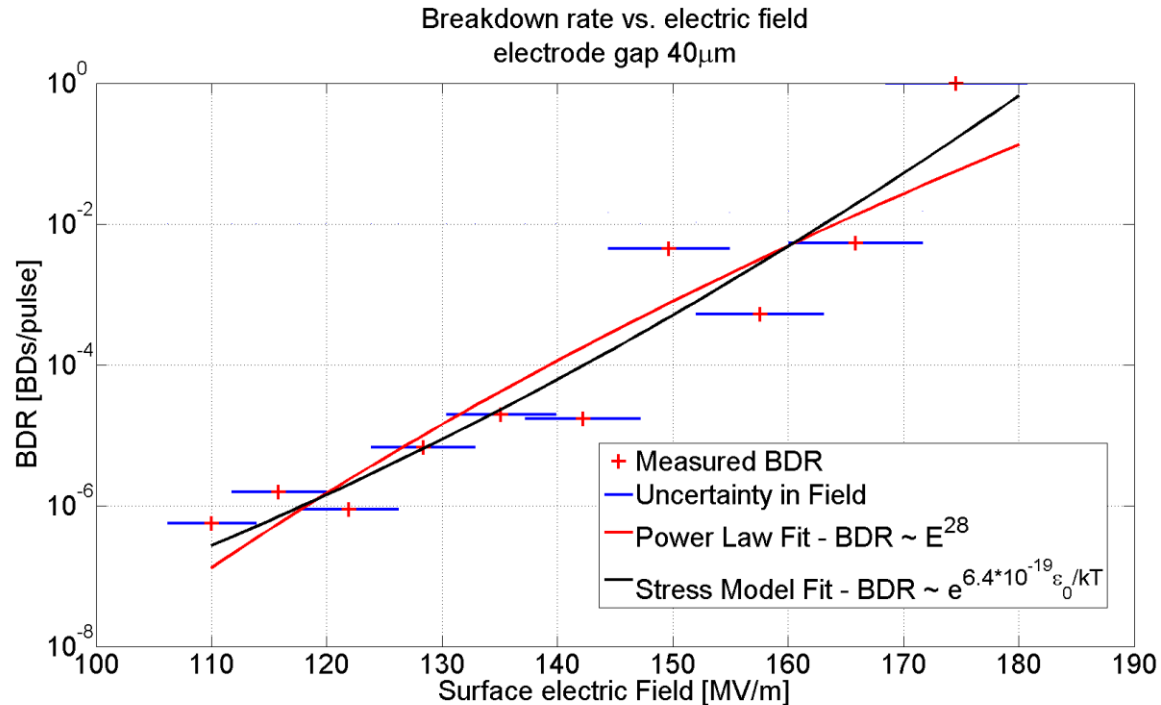
After 100BDs have been recorded or 10^7 pulses and at least 10BDs the voltage is reduced by 5%.

Every 10mins if no BD has occurred the HRR circuit is made to pulse at a predetermined voltage too low for a BD to occur, so the gap can be measured and automatically corrected.

As the uncertainty in the gap is always around 2μm the error in the field is much larger at smaller gap sizes.



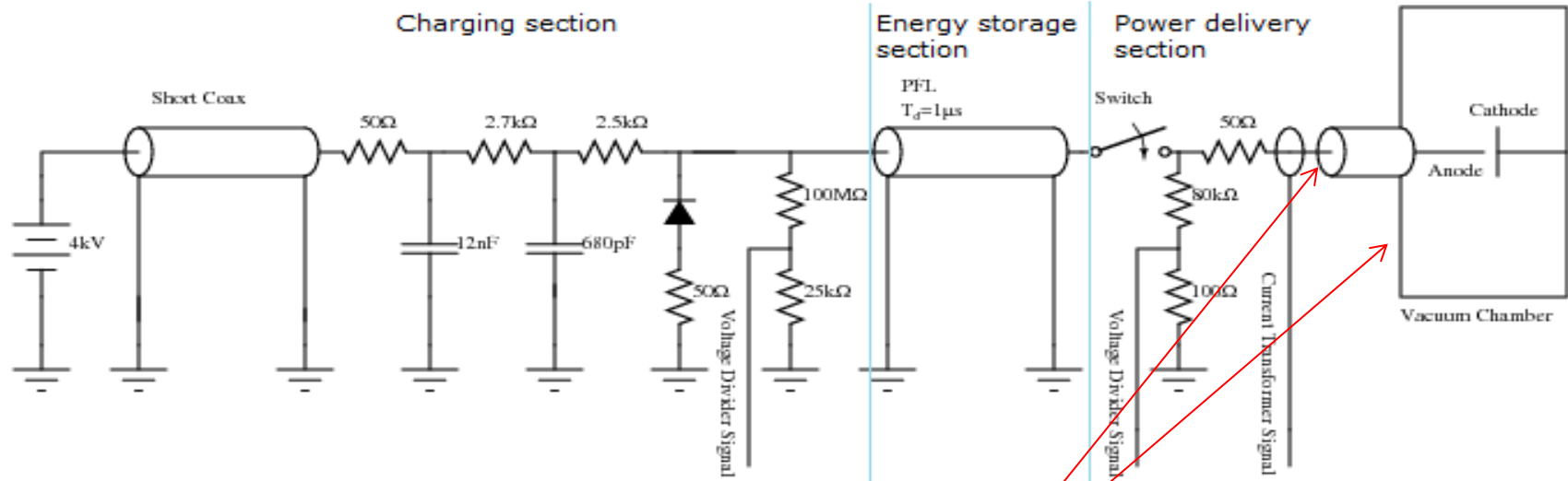
BDR vs E 40μm gap



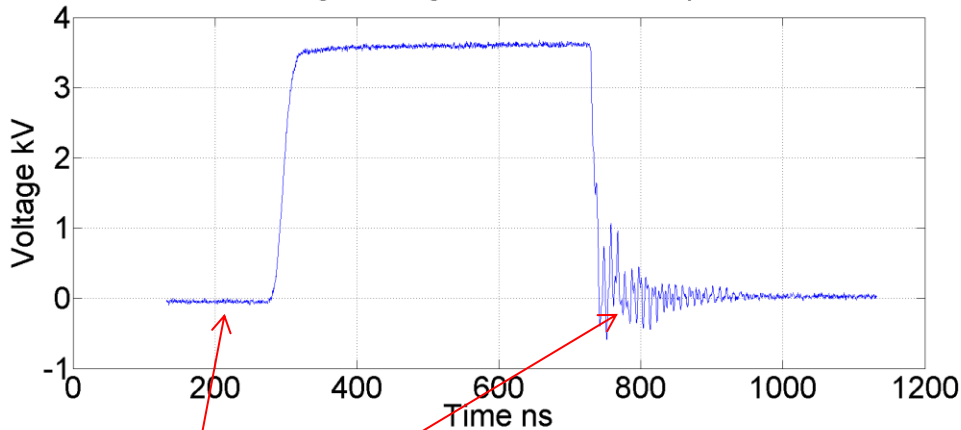
Both the power law model and the stress model fit the data well. Going to a lower BDR in the future should help distinguish between them. The exponents obtained for the power law model are very similar to those obtained in high power RF tests of accelerating cavities.

The fitted exponent tends to decrease for a larger gap.

Measured Burning Voltages



Voltage during breakdown example 1

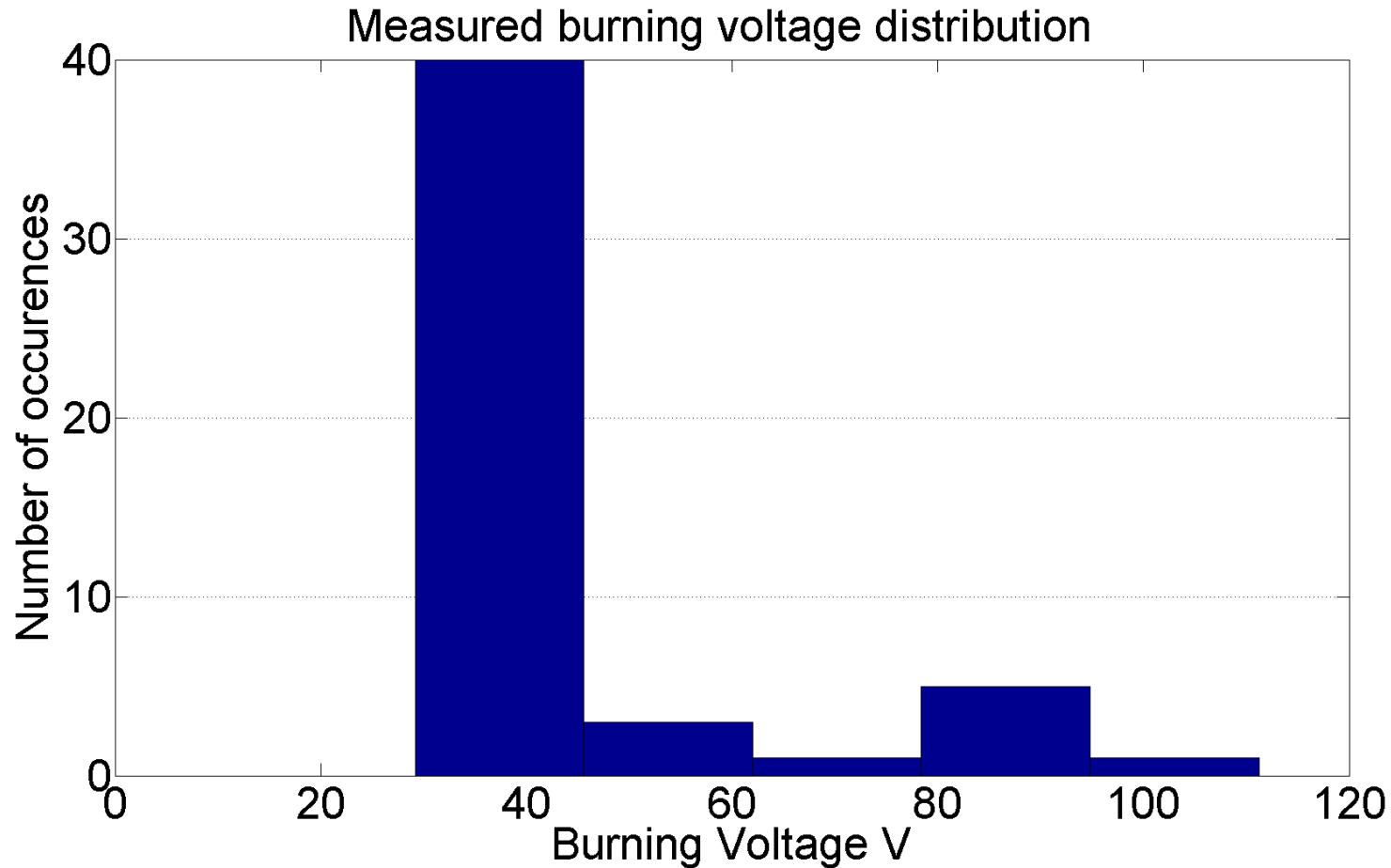


The burning voltage was measured across here.

It is the “steady state” voltage across the plasma of a spark during a breakdown at which point most of the voltage is dropped across the 50 Ohm resistor. It is a property of the material.

Subtract average voltage with switch closed from Average voltage during breakdown after initial voltage fall.

Measured Burning Voltages

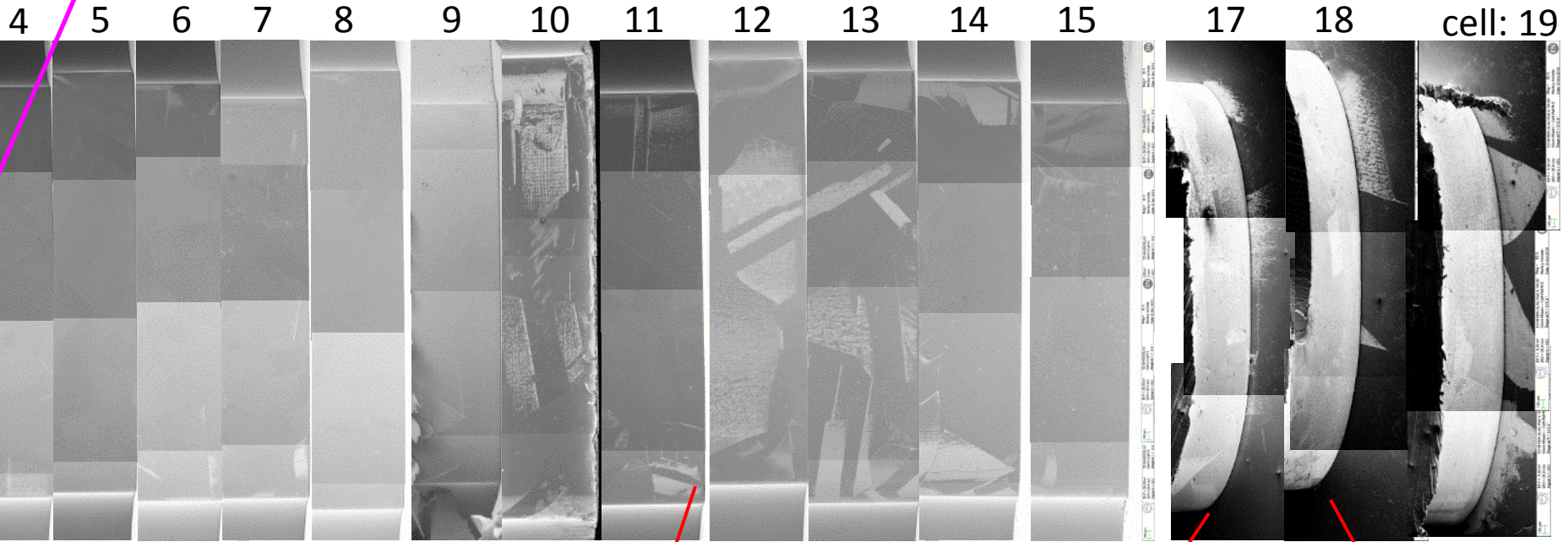


The literature gives a value for the burning voltage of clean copper of $\sim 23\text{V}$. This is lower than what I have measured so far in the DC spark system. But I have not measured or corrected for the short circuit resistance of cables etc.

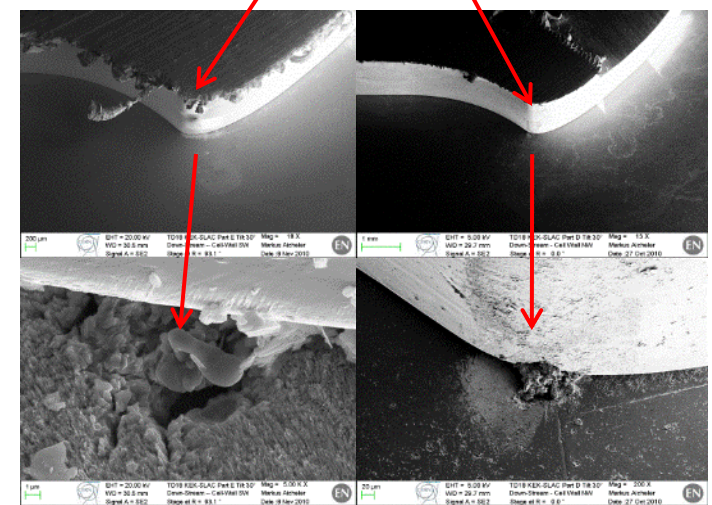
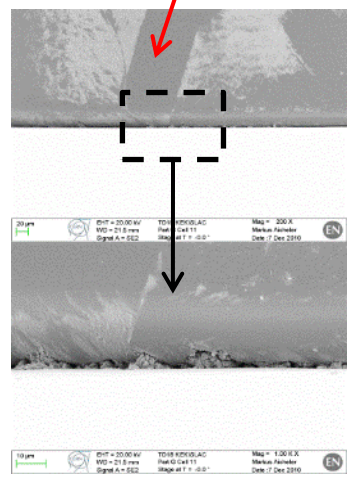
TD24 Pulsed surface heating limit

Last regular cell: 19

Cell # (cell #1 is a input matching cell):



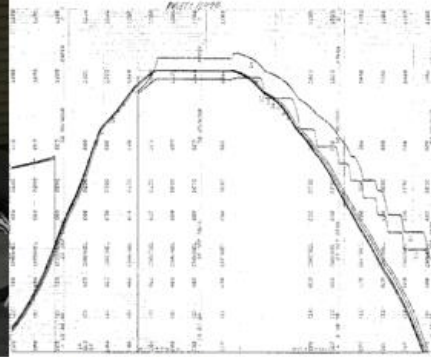
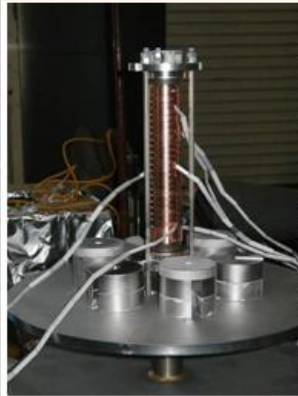
It seems that cell #10 (regular cell #9 ~ **middle cell**) exhibits the level of damage which could be considered as a **limit**.



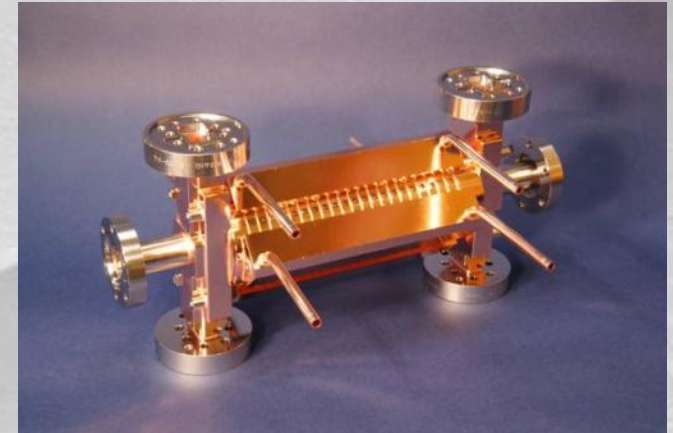
A. Grudiev

Images courtesy of M. Aicheler: <http://indico.cern.ch/getFile.py/access?contribId=0&resId=1&materialId=slides&confId=106251>

Diffusion Bonding of T18_vg2.4_DISC



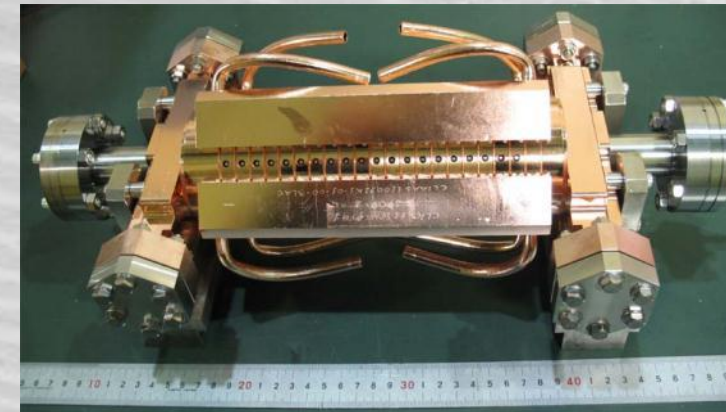
Pressure: 60 PSI (60 LB for this structure disks)
Holding for 1 hour at 1020°C



Vacuum Baking of T18_vg2.4_DISC



650°C
10 days



Stacking disks

Structures ready for test

Temperature treatment for high-gradient

Walter Wuensch

10 October 2011



The End



More information:

CLIC: <http://clic-study.org/>

CLIC workshop: <http://indico.cern.ch/conferenceDisplay.py?confId=275412>

Breakdown physics: <https://indico.cern.ch/conferenceDisplay.py?confId=246618>

High-gradient structures:

<http://indico.cern.ch/conferenceDisplay.py?confId=231116>

Further applications:

<https://indico.desy.de/conferenceDisplay.py?confId=6537>